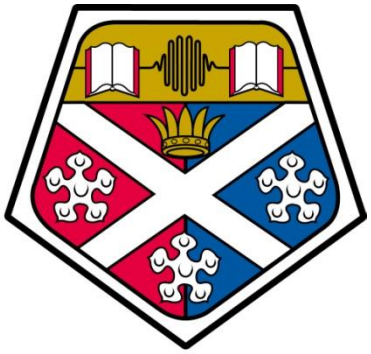

University of Strathclyde Glasgow

An investigation of Insulin-like Growth Factor Binding Protein-5 (IGFBP-5) as a Biomarker for the Detection of Early Liver Disease

By

Emma Margaret Large

May 2015

This thesis is in partial fulfilment for the degree of
Doctor of Engineering

Department of Biomedical Engineering
Wolfson Centre
106 Rottenrow East
University of Strathclyde
Glasgow G4 0NW

Declaration of Authenticity and Author's Rights

This thesis is the result of the author's original research. It has been composed by the author and has not been previously submitted for examination which has led to the award of a degree.

Signed:

Date:

Acknowledgements

I would like to express my gratitude to both my supervisors, Prof. M Helen Grant and Prof. David Flint, for their efforts and guidance throughout my EngD studies. Without their continued support, a completed thesis would not be in existence today!

I would also like to thank Mrs. Katie Henderson and Mrs Elizabeth Goldie for their technical support throughout my years in the lab. I am sincerely indebted to Mrs Katie Henderson. Your constant help and support is very much appreciated. Without it, my time in the lab might have been a lot more turbulent.

And finally, my family and friends; thank you for always being available with a listening ear and words of encouragement.

Abstract

With mortality rates of both men and women increasing considerably over the last decade from liver disease, along with the number of patients on the active liver transplant list in the UK on the increase, new diagnostic tools would be welcomed by hepatologists. This trend is possibly mirroring the increase in patient numbers with alcoholic liver disease (ALD), and non-alcoholic fatty liver disease (NALFD). The aim of this project was to find a suitable biomarker for the early detection of liver disease. One such biomarker that was proposed was insulin-like growth factor-binding protein-5 (IGFBP-5). IGFBP-5 is known to be involved in the wound healing response in epithelial tissues, and its expression is switched on in fibrosis of the lung. IGFBP-5 induces epithelial cell senescence, an important component in the failure to resolve healing which results in a compensatory fibrotic response. IGFBP-5 has also been identified as a tumour marker gene of interhepatic cholangiocarcinoma, a type of cancer of the bile ducts in the liver. This project aims to determine whether IGFBP-5 could be used as a biomarker for detecting liver damage and fibrosis.

Several models of liver disease were developed to determine if IGFBP-5 could potentially be a suitable biomarker using monolayers of primary rat hepatocytes cultured on collagen I coated tissue culture plastic dishes. Firstly, IGFBP-5 release into the culture medium from primary rat hepatocytes cultured over time was investigated along with models of oxidative stress, alcoholic liver disease (ALD), and non-alcoholic liver disease (NALFD). It was determined that the expression of IGFBP-5 over time in culture was increased, suggesting that it may have potential as a biomarker of dedifferentiation. Treatments with menadione, hydrogen peroxide, or ethanol and its primary metabolite acetaldehyde were used to unravel the story on oxidative stress. However, IGFBP-5 was undetectable in the culture medium after chronic treatment with each of the compounds listed. An in vitro model of NALFD was developed at the University of Edinburgh. The model was developed with the ability to induce either enhanced or minimal ROS formation. The in vitro study showed promising results, demonstrating that, with time in culture, in both models, an increase in IGFBP-5 expression was detected. Following on from the in vitro study, a patient study was undertaken to determine if patients with various types of liver disease had any changes

in their circulating IGFBP-5 levels. After extensive work, IGFBP-5 could not be detected in human serum using a commercially available kit. This was thought to be due to the human serum interfering with the assay kits ability to detect IGFBP-5.

IGFBP-5 does have potential as a biomarker of early liver disease, showing promising results from two models; de-differentiation and NAFLD. Further work into its involvement in liver injury or recovery mechanisms could determine it as useful biomaker in the hepatology clinic.

List of Abbreviations

ADH - alcohol dehydrogenase

AFP - alpha feto protein

ALD - alcoholic liver disease

ALDH - acetaldehyde dehydrogenase

ALT - Alanine aminotransferase

ANOVA - analysis of variance

APS - Ammonium persulphate

AST - Asparatate aminotransferase

BSA - Bovine serum albumin

BSO - buthionine sulfoximine

CPT - carnitine palmitoyl transferase

CT - computed tomography

CV - crystal violet

CYP - cytochromes P450

dH_2O - distilled water

DMEM - Dulbecco's minimum Essential Medium

dPBS - Dulbeccos' phosphate buffered saline

DMSO - dimethylsulfoxide

ECM - extracellular matrix

EGF - epithelial growth factor

EGTA - Ethylene glycol tetraacetic acid

EHS - Engelbreth-Holm-Swarm

ELISA - enzyme-linked immunosorbent assay

$FADH_2$ - flavin adenine dinucloetide

FCS - Foetal calf serum

FFA - free fatty acid

GAG - glycosaminoglycan

GGT - gamma-glutamyl transpeptidase

GSH - reduced glutathione

GST - glutathione S-transferase

HBV - hepatitis B virus

HEPES - 4-(2-hydroxyethyl)-1-piperazineethanesulfonic acid

HGF - hepatocyte growth factor

HIV - Human Immunodeficieny Virus

HRP - horseradish peroxidase

HSC - hepatic stellate cell

IGF - insulin-like growth factor

IPF - idiopathic pulmonary fibrosis

IGFBP-5 - Insulin-like growth factor binding protein-5

IR -insulin resistance

IRS-2 - insulin receptor substrate-2

JNK - c-Jun N-terminal kinases

LDH - lactate dehydrogenase

LOD - limit of detection

LPON - Lactate, Pyruvate, Octanoate and Ammonia

MAPK - mitogen-activated kinase

MEME - minimum essential medium Eagle

MEOS – microsomal ethanol oxidising system

MMP - matrix metalloproteinase

MOI - Multiplicity of infection

MS - metabolic syndrome

MTT - 3-(4,5-dimethylthiazol-2-yl)-2,5-diphenyltetrazolium bromide

NAFLD - Non-alcoholic fatty liver disease

NaPi - Sodium Phosphate

NASH - non-alcoholic steatohepatitis

NEAA - non-essential amino acids

NPC – non-parenchymal cell

NR – Neutral red

OPT - o-phthaldehyde

PBS - phosphate buffered saline

PFA - paraformaldehyde (PFA

PPARα - peroxisome proliferator-activated receptor alpha

RIA - radioimmunoassay

ROS - reactive oxygen species

SDS-PAGE - Sodium dodecyl sulfate polyacrylamide gel electrophoresis

SOD - superoxide dismutase

SREBP-1c - sterol regulatory element binding protein-1c

SSc - systemic sclerosis

TBS - Tris buffered saline

TCA - trichloroacetic acid

TEMED - Tetramethylethylenediamine

TGF-β -Transforming growth factor-β

TNF-α - tumour necrosis factor-α

TTBS - Tween Tris Buffered Saline

WT - wild-type (WT)

αSMA - alpha smooth muscle actin

List of Tables

List of Figures

Table of Contents

Chapter 1 Introduction

This thesis plans to investigate the functionality of hepatocytes in culture over a 9 day period of time and to correlate the Insulin-like growth factor binding protein (IGFBP) -5 release into the medium with dedifferentiation. Currently there is a lack of diagnostic tools for hepatologists to detect early liver disease in patients. Battler and Brenner (2005) have discussed the importance of developing a simple and non-invasive marker of hepatic fibrosis. IGFBP-5 has been proposed as a marker of early liver disease. IGFBP-5 is a member of a family of six IGFBPs that bind insulin-like growth factor (IGF) (Beattie et al., 2006). In vivo expression has been shown to induce skin fibrosis in mice (Yasuoka et al., 2006a). Its expression has been shown to be increased in human lung tissue of patients with Idiopathic Pulmonary Fibrosis (Pilewski et al., 2005) and it has been identified as a tumour marker for intrahepatic cholangiocarcinoma (Nishino et al., 2008). Expression of IGFBP-5 has also been shown to enhance the survival of hepatic stellate cells and myofibroblasts and the expression of profibrotic genes (Sokolovic et al., 2010).

1.1 The Liver

The liver is one of the major organs in the body and has a wide range of functions. It is involved in protein synthesis, detoxification, and production of necessary biochemicals for digestion.

Major cells types in the liver are as follows:

- Hepatocytes
- Kupffer cells
- Liver sinusoidal endothelial cells
- Hepatic stellate cells (HSCs)

The cells within the liver can be divided into two categories, parenchymal and non-parenchymal (NPC). The parenchymal fraction consists of hepatocytes, making up

almost 60 % of the total cellular population in the liver (See Figure 1.1). The NPC fraction comprises all the remaining cells within the liver (Martini et al., 2007).

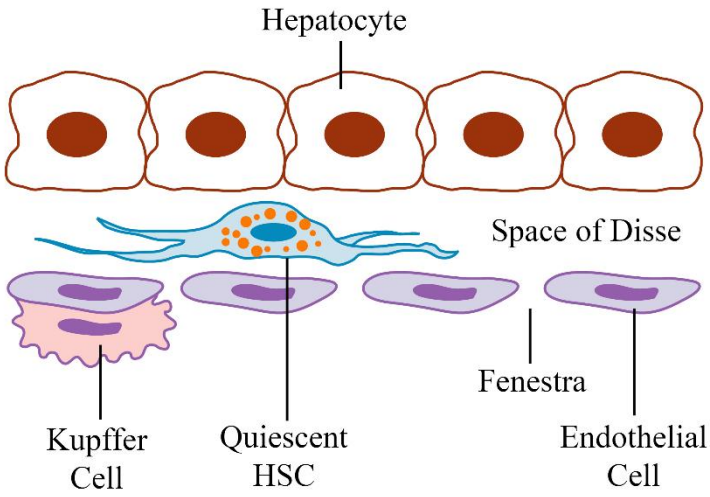

Figure 1-1 Schematic representation of a liver sinusoid

Liver sinusoid has hepatocytes in a cuboidal form, with endothelial cells lining the wall of the blood vessel. Liver resident macrophages reside on the luminal side of the endothelial cells with hepatic stellate cells (HSC) residing in the Space of Disse.

1.1.1 Hepatocytes

Hepatocytes are highly differentiated cells that perform the majority of the physiological functions associated with the liver. Hepatocytes are involved in protein, steroid, and fat metabolism along with vitamin, sugar and iron storage. They also exhibit morphologic, functional and biochemical heterogeneity based on their location across the liver acinus. Periportal zone 1 hepatocytes are highly oxygenated and involved in oxidative metabolism and ureagenesis while pericentral zone 3 is less oxygenated and involved in xenobiotic metabolism and liponeogenesis (LeCluyse et al., 2012).

Under healthy normal liver conditions, a size increase in cells is exhibited between zone 1 and 3, with cells in zone 1 being smaller than those in zone 3. Along with size variations between zones, hepatocytes exhibit morphological changes between zones

also, including glycogen storage, mitochondria and lipid vesicles (Ferri et al., 2005). Hepatocytes are cuboidal in shape and are highly polarised with distinct sinusoidal and canalicular domains that are separated by junctional complexes. Both membrane domains exhibit ultrastructural, compositional and functional differences, essential for heaptocyte's role in uptake, metabolism and biliary elimination of both endogenous and exogenous substances (Meijer et al., 1990, LeCluyse et al., 2012).

1.1.2 Kupffer cells

Kupffer cells are the resident macrophages in the liver with endocytic and phagocytic capacity. They can be located in the perisinusoidal space of Disse on the endothelial side. Kupffer cells exhibit long cytoplasmic extensions that facilitate direct hepatocyte to Kupffer cell contact (LeCluyse et al., 2012). In vitro, this has been demonstrated as key to demonstrating inflammatory mediated heptotoxicity (Hoebe et al., 2001). These macrophages are responsible for eliminating waste products and cellular debris i.e. endotoxins and bacterial products (Roberts et al., 2007).

1.1.3 Liver sinusoidal endothelial cells

Liver sinusoidal endothelial cells line the walls of the sinusoids, separating hepatocytes from the sinusoidal blood flow (De Leeuw et al., 1990). These cells differ from other endothelial cells due to the presence of fenestrae. It has been reported that the presence of fenestrae allow for the exchange of solutes, particles and fluids to be exchanged from the sinusoidal lumen to the hepatocytes. Liver sinusoidal endothelial cells also have a high endocytotic capacity and effectively uptake a wide variety of substances from the blood by receptor-mediated endocytosis (Braet and Wisse, 2002).

There is growing evidence that LSECs play a role in drug response and are targets for some chemical-induced hepatotoxicities. LSEC Phase I enzymes are not well characterised but it is evident that they contribute to metabolism, clearance and bioactivation of endogenous and exogenous substances. LSECs, in the absence of hepatocytes, are susceptible to acetaminophen toxicity, suggesting that they can metabolise the drug to its reactive metabolite, causing cytotoxic effects (Xie et al.,

2010). Xie et al., (2010) also demonstrated zonation effects on LSECs. Periportal LSECs expressed CD45 highly, while it was expressed low in midlobular and absent from centrilobular LSECs.

LSECs suffer from rapid loss of phenotype after culture in vitro. March et al., (2009) demonstrated the effects of extracellular matrix on the maintenance of function of LSECs in micro patterned cultures. Mixtures of collagen I and III and the addition of fibronectin had lower numbers of apoptotic cells per culture. Also, the addition of 3T3 fibroblasts and hepatocytes maintained high SE-1 expression and low levels PECAM-1, for up to 2 weeks in culture.

1.1.4 Hepatic stellate cells

In the normal liver, hepatic stellate cells contribute almost 5 % of the total cells within the liver, and are typically located in the space of Disse (Martini et al., 2007). In their quiescent state, stellate cells exhibit a large lipid droplet, used in the storage of vitamin A. Along with this, stellate cells play a role in the maintenance of basement matrix proteins i.e. collagen VI (Moreira, 2007). Upon activation or transdifferentiation to more fibroblastic-like cells triggered by hepatocyte injury e.g. viral hepatitis or hepatotoxicity, an activated stellate cell undergoes morphological changes and exhibits non-phenotypic characteristics. Enhanced cell migration and adhesion, increases in α-SMA and acquisition of fibrogenic capacity are exhibited. Activated stellate cells show upregulated gene expression of ECM components, matrix degrading enzymes and their inhibitors, which leads to the deposition of ECM at sites of increased activated stellate cells (De Minicis et al., 2007). Stellate cells produce important cytokines (Transforming growth factor-β (TGF-β)) and growth factors e.g. HGF and EGF for intracellular communication in normal and injured liver. The growth factors listed are potent factors for hepatocyte proliferation and regeneration after injury (Asahina et al., 2009).

1.2 Liver disease

1.2.1 Alcoholic Liver Disease (ALD)

Recent findings by the members of the Independent Scientific Committee on Drugs found that alcohol was overall the most harmful drug, ahead of heroin (Nutt et al., 2010). Alcohol was found to have the greatest effect by both harming users (i.e. drug specific mortality, dependence and loss of relationships) and harming others (i.e. crime, environmental damage and economic cost). A report by WHO (2009) also ranked alcohol as the third leading cause of global risk for disease. A study carried out by NHS Health Scotland (2010) demonstrated that Scottish people over the age of 18 drank 12.2 L of pure alcohol each year on average. These figures are 25 % higher than that consumed in England and Wales (9.7 L). A Scottish Government (2008) report also states that alcohol misuse in Scotland costs the Scottish economy an estimated £2.5 billion each year. Also, recent projections for the next 20 years for alcohol associated deaths demonstrated that if deaths increased at the same gradient as that over the last 10 years then a peak of between 160,000 and 250,000 deaths could occur in England and Wales (Sheron et al., 2011). Despite the high death rates and costs of alcohol misuse, hepatologists still lack a relevant biomarker for the detection of early liver disease. The liver is known to have an enormous capacity for regeneration and wound healing following an insult, however, early diagnosis is essential (Michalopoulos, 2014, Taub, 2004).

CYP2E1 plays an important role in the metabolism of toxicologically relevant molecules including ethanol. Chronic alcohol consumption has been shown to result in the induction of CYP2E1 (Chen et al., 1997). Oneta et al (2002) showed that moderate alcohol consumption (40 g ethanol per day taken over one week) led to a significant induction of CYP2E1 in man with no signs of liver damage assessed by markers of liver health: aspartate aminotransferase, alanine aminotransferase and gamma glutamyltranspeptidase. As CYP2E1 is so closely associated with the pathogenesis and severity of alcoholic liver disease, it is worrying that in the liver of a moderate drinker CYP2E1 is being induced. CYP2E1 generation of tissue damaging ROS is another principle mechanism that is thought to be responsible for alcohol

induced liver damage (Knockaert et al., 2011, Chen et al., 1997). The formation of acetaldehyde by CYP2E1 and acetate by aldehyde dehydrogenase (ALDH) both produce NADH when alcohol is consumed, thus increasing the cytostolic and mitochondrial NADH and reactive oxygen species (ROS) formation (see Equation 1).

$$Ethanol + NADPH + H^+ + O2 \xrightarrow{CYP2E1} Acetaldehyde + NADP^+ + 2\,H_2O$$

Equation 1-1. Oxidative pathway of Ethanol involving CYP2E1

CYP2E1 is involved in the oxidative pathway of ethanol at elevated concentrations (2 – 10 mM) in comparison with ADH. ADH is involved in the oxidative pathway at much lower concentrations (0.2 – 2.0 mM) (Bullock, 1990, Nassir and Ibdah, 2014). Acetaldehyde is a highly reactive and toxic metabolite that causes tissue damage. Damage is caused by the DNA and protein adducts that promote glutathione depletion, lipid peroxidation and mitochondrial damage (Nassir and Ibdah, 2014, Caro and Cederbaum, 2004, Yu et al., 2010).

1.2.2 NAFLD

Non-alcoholic fatty liver disease (NAFLD) was first described in 1980 (Ludwig et al., 1980). NAFLD is the most common form of liver disease in the developed world, affecting between 20 and 30% of the population in the USA and Western Countries (Bedogni et al., 2005). This is mirroring the global epidemic of Type II diabetes and obesity. There is a spectrum of severity of NAFLD which ranges from steatosis to liver failure. Firstly, NAFLD manifests as simple steatosis with no inflammation, which is followed by non-alcoholic steatohepatitis (NASH; steatosis with inflammation and hepatocyte injury). NASH leads to more severe forms of NAFLD such as fibrosis, cirrhosis, hepatocellular carcinoma or liver failure (Krawczyk et al., 2010).

Steatosis, the abnormal accumulation of triglycerides in the liver, also plays a role in Alcoholic Liver Disease (ALD) (Ferré and Foufelle, 2010). The accumulation of lipids in the liver in this case is in part due to the transcription factor peroxisome proliferator-activated receptor alpha (PPARα). PPARα is a receptor of free fatty acids, and is

known to induce genes involved in transport, oxidation and export of free fatty acids (Vanden Heuvel, 1999). Free fatty acids also act as ligands for PPARα, leading to the activation of PPARα, and hence the induction of peroxisomal β-oxidation, mitochondrial β-oxidation and microsomal fatty acid hydroxylation which restore normal levels of fatty acids. Fatty acid levels are elevated during ethanol consumption and ethanol metabolism inhibits PPARα capacity to bind DNA and induce reporter genes (Mello et al., 2008, Nanji et al., 2004).

It is widely accepted that NAFLD is strongly associated with the features of metabolic syndrome (MS). The underlying factors of MS include visceral obesity, dyslipidaemia, hyperglycaemia, and hypertension (Kim and Younossi, 2008). NAFLD is most commonly found in morbidly obese people (BMI $\geq$ 40 kg/m^2) (Adams et al., 2009). It is currently accepted that insulin resistance (IR) leads to obesity, however, obesity exacerbates insulin resistance (IR). IR occurs when a given concentration of insulin does not produce the expected biological response. This could be attributed to reduced glucose transport due to free fatty acids inhibiting the proximal insulin signalling steps, including tyrosine phosphorylation of insulin receptor substrates (Tarantino et al., 2010). The insulin receptor is a tyrosine kinase receptor that utilises the peptide sequences of the insulin receptor as substrates i.e. Shc and Gab-1, to mediate signalling. Many pathways are activated when insulin receptor substrates undergo phosphorylation, including PI3K-Akt pathway (controlling metabolic actions of insulin), the mitogen-activated kinase (MAPK) pathway (controlling cellular effects, such as growth and differentiation), and signal transduction through CAP/cbl/Tc10 pathway (controls glucose transport via GLUT-2) (Leclercq and Horsmans, 2008, Tilg and Moschen, 2008). This all leads to an increase in hepatic glucose output and a reduction in uptake by peripheral tissues.

Increases in plasma glucose and/or insulin levels induce hepatic free fatty acid (FFA) synthesis and trigger steatosis. The increase in FFA production can be attributed to the over expression of sterol regulatory element binding protein-1c (SREBP-1c) which

increases the expression of all lipogenic enzymes and thus increasing FFA synthesis (Pessayre, 2007). Several cycles involving hepatic mitochondrial dysfunction and reactive oxygen species (ROS) can play a role in the evolution of steatosis into NASH in some patients. It has been proposed that the release of cytochrome c from the mitochondria partially blocks the electron flow in the respiratory chain, along with the accumulation of NADH and decreases in formation of flavin adenine dinucloetide ($FADH_2$), that cause the formation of several ROS including hydrogen peroxide, superoxide anion radical and the hydroxyl radical (Pessayre and Fromenty, 2005). Excessive levels of ROS not only damage cells by oxidising DNA, but also activate a variety of stress-sensitive intracellular signalling pathways such as nuclear factor (NF) -kB, p38 MAPK, JNK/SAPK and hexosamine (Newsholme et al., 2007) leading to disruption to the insulin signalling cascade, and hence contributing to insulin resistance. Also, a novel model of steatosis showed that hepatocytes with lipid accumulation were sensitive to tumour necrosis factor-α (TNF-α) induced apoptosis via the ASK1-JNK signalling pathway (Zhang et al., 2010).

ROS and the activation of stress-sensitive intracellular signalling pathways have been implicated in the progression of steatosis to liver fibrosis. Pro-fibrotic IGFBP-5 could be involved in the development of hepatic fibrosis in NAFLD.

1.2.3 Fibrosis

Fibrosis occurs during chronic damage to the liver and results in the accumulation of extracellular matrix (ECM) proteins, such as collagen I and fibronectin. There are several main causes of fibrosis including the progression of NAFLD to fibrosis, with fibrosis leading to non-alcoholic steatohepatitis (NASH) (Bataller and Brenner, 2005). In particular, inflammation as a result of the release of proinflammatory cytokines and PPAR signalling and activity are thought to be the main contributors to hepatic fibrosis. Upon liver injury, hepatic stellate cells can become activated contributing to the progression of fibrosis through growth factor and cytokine production and increased production of ECM (Friedman, 2003).

TGF-β controls proliferation, cellular differentiation and other functions in most cell types. It has been identified as one of the major contributors to the fibrotic response in tissues as it induced myofibroblasts to synthesize and contract ECM. Studies have shown that patients with alcoholic liver disease have more TGF-β produced in their livers in comparison with patients with healthy livers suggesting that the development of alcohol-induced liver damage may be associated with TGF-β. It is also known for controlling liver size and does so in vivo and in vitro by inducing apoptosis. This occurs through the activation of a caspase-dependent mechanism which leads to cell death (Cain and Freathy, 2001). TGF-β is under investigation by many research groups as a possible therapeutic target as a treatment against scarring of tissue and hence fibrosis (Leask, 2007). TGF-β is the most potent factor in stimulating type I collagen gene transcription. It also regulates expression of matrix metalloproteinases (MMPs) and their inhibitors, and modulates inflammatory reactions by influencing T cell functions. Therefore, TGF-β is considered to be a major factor accelerating the progression of organ fibrosis (Inagaki and Okazaki, 2007).

1.3 Current in vitro hepatocyte models

In vitro techniques, specifically hepatocyte-based in vitro systems are currently widely used to address a variety of pharmacological and toxicological issues. Hepatocyte-based cultured systems remain a vital part of the developmental stages of new potential drugs (Soars et al., 2007), for the prediction of in vivo clearance and drug-drug interactions. Currently, in vitro hepatocyte systems are seen as advantageous over whole animal studies, which are no longer ethically or economically acceptable. Animal models poorly predict what will happen in the human scenario, but a currently required by regulatory bodies to be conducted before any drugs enter clinical trials. A classic case in 1992, Fialuridine, a HBV therapy, passed through animal studies demonstrating no toxicity. However, when the drug was used in clinical trials, 7 out of 15 patients receiving treatment experienced server toxicity (Colacino, 1996). Human hepatocytes contain a complete complement of enzymes that a drug would encounter during liver metabolism, and aid in the early metabolism studies of new drugs.

However, there is still a lack of an ideal primary hepatocyte culture system despite years of research into developing one. Current hepatocyte culture systems are limited in use due to the rapid de-differentiation of the cells in culture. The cytochromes P450 (CYP) function is a major loss seen after just 48-72 hr in culture (Elaut et al., 2006, Paine et al., 1982, Stefan G. Hübscher, 2005). CYP play a major role in the metabolism of a large range of xenobiotics. Approximately 90% of oxidative drug metabolism can be attributed to CYP 1A2, 2C9, 2C19, 2D6, and 3A4. Also, freshly isolated hepatocytes cultured on a collagen film exhibit a flattened morphology, depolarise and lose many surface characteristics of normal hepatocytes in vivo. This occurs, at least partly, due to the disaggregation of the hepatocytes during the isolation process resulting in the loss of tight and gap junctions (Luttringer et al., 2002).

1.4 Current biomarkers for the detection of liver disease

Currently a series of liver function tests are carried out to determine if liver injury is present. These comprise of alanine aminotransferase (ALT), asparatate aminotransferase (AST), bilirubin and albumin levels. Scans, including ultrasound, computerised tomography (Ip et al., 2002) and elastography can also be used. While ALT remains the gold standard in clinical chemistry, biopsy remains the gold standard in diagnosing liver disease. Normal ranges for clinical biochemistry tests are detailed in Table 1.1. In many cases an invasive liver biopsy is required to confirm the presence or absence of liver damage after liver enzymes are assessed. Liver biopsy is a painful procedure that must be carried out under general anaesthetic. Histopathology is also the only definitive way to determine the accumulation of intracellular triglycerides in NAFLD.

Liver Blood Test	Normal ranges in healthy individuals
ALT	7 – 56 U/l
AST	5 – 40 U/l
Bilirubin	3 – 22 µmol/l
Albumin	39 – 50 g/l

Table 1-1 Liver blood tests

Normal healthy patient serum levels of common liver biomarkers. Adapted from (Purkins et al., 2004)

1.4.1 ALT

Serum ALT is the current biochemistry standard in a clinical setting as an indicator of hepatotoxic effects, however, some false negative and false positive of liver injury occur, and it is not ideal for a gold standard metric. Despite this, serum ALT has an exceptional track record in a clinical setting, but this does not translate well in a preclinical setting (Ozer et al., 2008). ALT plays a role in amino acid metabolism and gluconeogenesis. It catalyses the reductive transfer of an amino acid group from alanine to alpha-ketoglutarate to yield glutamate and pyruvate. Damaged hepatocytes release their contents into the extracellular space, leading to accumulation of enzymes, including ALT, in the circulation and hence its utility as a biomarker of hepatoxicity (Ozer et al., 2008). Normal ranges of ALT are 7 - 56 U/l (Purkins et al., 2004). Organ specificity is critical to the success of any biomarker. ALT is primarily located in the liver, however, lower levels of ALT enzymatic activity are found in the heart and skeletal muscle. Intense exercise, like a run or weightlifting for example can lead to increases in liver enzymes (Giboney, 2005). Pettersson et al. (2008) demonstrated increased blood levels of ALT in healthy individuals that underwent moderate exercise including weightlifting. Elevations for ALT were seen for up to and beyond 7 days post exercise. As well as exercise, diet has been implicated as a cause of elevated ALT. Purkins et al (2004) carried out a study with healthy male individuals whose diets included high carbohydrate/high calorie diet, high fat/high calorie diet or a balanced normal diet. Rises in blood transaminases were caused by the high carbohydrate content of the diet and not specifically the calorie content.

1.4.2 AST

Serum AST is a less specific liver biomarker in comparison with ALT. It is expressed in liver, brain, heart and skeletal muscle. Similarly with ALT, AST catalyses the reductive transfer of an amino acid group from aspartate to alpha-ketoglutarate to yield glutamate and pyruvate. Upon injury, it is released from heaptocytes, but also from other cell types such as myocytes. AST, used as part of a ratio with ALT, can aid physicians to differentiate liver injury from different organ injury (Ozer et al., 2008). AST can also be elevated by exercise and diet, as seen with ALT. After a high carbohydrate/high calorie diet, serum AST levels were elevated to 56.8 ± 30.2 U/l (Purkins et al., 2004). Normal ranges for AST are 5 – 40 U/l.

1.4.3 Bilirubin

Total bilirubin is a composite of hepatic and non-hepatic bilirubin. This degradation product of haemoglobin is used as a marker of hepatobiliary toxicity, particularly cholestasis (drug induced cholestasis can be caused by a range of drugs including nevirapine, a non-nucleoside reverse transcriptase inhibitor used for the treatment of Human Immunodeficieny Virus (HIV)) (Padda et al., 2011). Bilirubin has been identified to be a more specific marker for identifying the severity of hepatotoxicity than aminotransferases (Dufour et al., 2000). There are some drawbacks in relation to bilirubin also. Elevations in total bilirubin can be associated with hemolysis.

1.4.4 Novel Biomarkers

ALT is currently the front runner in predicting hepatotoxicity, however, there are drawbacks, mainly its non-specificity to the liver. Much research is currently being undertaken in the field to identify novel markers of hepatotoxicity and liver disease. Table 1.2 lists some novel biomarkers along with ALT. Ideally a biomarker specific and non-invasive to the liver is required (Lockman et al., 2012, Bataller and Brenner, 2005). This would reduce the need for invasive biopsy to confirm progression of liver disease state and aid preclinical and clinical drug studies. Two potential highly liver-specific novel biomarkers for the detection of liver injury are miR122 and arginase-1.

MicroRNAs are small (~22 nucleotides long) noncoding RNAs that are involved in post transcriptional gene regulation (Bartel, 2004). They play important regulatory roles in animals and plants by targeting mRNAs for cleavage inducing translational repression. Some roles include viral infections (Jopling, 2008), cell differentiation and cardiotoxicity (Sandhu and Maddock, 2014) and carcinogenesis (Lewis and Mohanty, 2010). MicroRNAs are popular in biomarker research as they are abundant in a wide range of tissues including blood (Bartel, 2004, Starkey Lewis et al., 2012, Shifeng et al., 2013, Kia et al., 2015, Hornby et al., 2014). An in vivo mouse study evaluating the use of microRNA for liver specific acetaminophen toxicity highlighted two microRNAs as having potential as novel hepatotoxicity biomarkers. Upon exposure to a single bolus dose of acetaminophen, miR122 expression was decreased in the liver and a subsequent upregulation in the blood. The study also demonstrated the liver specificity of miR122, and its sensitivity to hepatotoxicity (Gao et al., 2012). Indeed, miR122 demonstrated toxicity earlier and at lower doses than that seen with ALT. Further to this, Zhang et al (2010) carried out a patient study to determine if miR122 was a suitable biomarker for liver disease, other than drug–induced liver injury. To determine if the microRNA was specific to the liver, patients with skeletal muscle disease were included (Zhang et al., 2010). Patients with chronic hepatitis B virus (HBV) had significant increases in miR122 in comparison with controls. With increasing ALT levels, increases in miR122 were also evident, for patient samples with the lowest ALT levels (5-50 U/l), miR122 was increased 3.43-fold. The mean fold increases for patients with muscle injury were 1.08 and 7.8 for miR122 and ALT respectively. Concentrations of miR122 were also not significantly different between the control group and the muscle injury group. All the evidence so far points to miR122 being a useful liver specific marker. Starkey-Lewis et al (2011) demonstrated the relevance of miR122 as a biomarker for the detection of acetaminophen-induced toxicity. There was a highly significant increase in miR122 in patients with acute liver injury post acetaminophen ingestion. miR122 increases were also highly correlated with serum ALT activity. Kia et al (2015) demonstrated that miR122 in vitro was highly correlated with LDH release after dosing with diclofenac and acetaminophen over a 24 h period. However, with diclofenac dosing miR122 in the medium did not

accumulate earlier than LDH indicating that miR122 would not be suitable to detect early indications of toxicity. Kia et al (2015) also demonstrated that miR122 levels in vitro are highly correlated with the differentiated state of the cell type used in the model, with primary human hepatocytes exhibiting the highest levels. Suitability of the marker in an in vitro setting would have to take cell type used in to consideration.

miR122 has also been identified as a potential marker of cholestasis-induced liver injury using bile duct ligation mice and patients with biliary calculi as models of cholestatic liver injury (Shifeng et al., 2013). In this study, miR122 levels exhibited similar time-course as ALT, the classic liver biomarker. Despite the similar trends with ALT, the changes in concentration were greater in miR122 than ALT. This results was translated to the clinic with patients with biliary calculi exhibiting elevated levels of miR122 relative to control patients (Shifeng et al., 2013).

Despite the published relevance of miR122 as a potential biomarker for the detection of liver disease, a clinically suitable assay is not yet available (Hornby et al., 2014). Sample preparation is currently required with much of the published work carried out on serum or cell culture medium. Reverse transcription-quantitative PCR (RT-qPCR) is currently the most widely used method of detection and can exhibit assay variation, from RNA isolation and normalisation controls. Inter-individual variation would also have to be considered, not yet considered in any of the published work.

Arginase-1, also a more liver specific biomarker is currently being investigated. It is a hydrolase enzyme that catalyses the hydrolysis of arginine to urea and ornithine. Arginase-1 is highly liver specific, making it a popular novel liver biomarker choice. After transplantation, arginase-1 was monitored with a peak after 1 day post-transplant (Ashamiss et al., 2004). Arginase-1 was shown to decrease more rapidly than other liver function tests. This study also highlighted that detection of arginase-1 was more sensitive in the bile. However, bile is only accessible during hospitalisation post transplantation. Biomarker studies of arginase-1 are limited and due to it being a more

sensitive marker measured from bile, it remains unlikely without significant study and validation that it will be used in the clinic.

Given the large body of research in this area, no novel biomarker has been adopted in the clinic. There still remains a need for further research into novel biomarkers that are easily measured and sensitive to early liver damage.

Marker	What does it detect?	Tissue location	Liver localisation	Function	Clinical/preclinical
Alanine Aminotransferase	Injury	liver, skeletal muscle	Hepatocytes	Glucose - alanine cycle	Clinical
Glutamate Dehydrogenase	Injury	liver, kidney, muscle, intestine	Hepatocytes	amino acid production urea production	Clinical
Malate Dehydrogenase	Injury	muscle, kidney, brain, intestine	Hepatocytes	TCA cycle	Preclinical
Glutathione S Transferase-α	Injury	liver, adrenal, ovary, stomach, kidney, testes	Hepatocytes	glutathione transferase	Pre-clinical
Purine Nucleoside Phosphorylase	Injury	bone marrow, liver, intestine, spleen	Hepatocytes, endothelial, Kupffer cells	purine pathway	Pre-clinical
Arginase-1	Injury	Liver	Hepatocytes	urea cycle	Clinical
Paraoxonase-1	Function	liver, diaphragm	Hepatocytes	esterase, protects lipoproteins from lipid peroxidation	Pre-clinical
miR122	Injury	Liver	Hepatocytes	small non-coding RNAs repress translation	Pre-clinical

Table 1-2 Liver biomarkers, both current and novel and their applicability to liver

Adapted from (Ozer et al., 2008)

1.4.5 Non-invasive Elastography

Imaging tools allow investigation of the structure of the liver without biopsy. Common techniques include computed tomography (CT) and ultrasound. A novel technique, transient elastography, is a recently developed non-invasive technique for the assessment of hepatic fibrosis. FibroScan®, a commercially available medical device from EchoSens, France, measures the liver stiffness which enables the assessment of liver disease severity. This method utilises a 1-dimensional ultrasound transducer (5 MHz) and receiver mounted alongside a vibrator producing a low-frequency pulse or shear wave (50 Hz). To assess liver stiffness, the probe is placed on the skin between the ribs above the liver. The rate of progression of the shear wave is monitored. Progression of the wave is dependent on the elasticity of the tissue. A series of waves can detect deformations in the tissue as the waves progress through it. To calculate the elasticity of the liver, the velocity of the waves approximate to the Young's modulus, E. Deformations are plotted as a function of time and depth to create a 2-dimensional elastograph. The slope of the graph (speed of propagation) is the liver stiffness expressed as kPa. Due to its ease of use, adoption in clinics has occurred (Cobbold et al., 2007). Sandrin and team (2003) assessed FibroScan®, for both intra and interoperator reproducibility as well as its ability to diagnose fibrosis versus liver biopsy. The elasticity of patients' livers with varying degrees of fibrosis, as measured by FibroScan, correlated with biopsy. It differentiated between patients with cirrhosis and advanced fibrosis, highlighting its use in identifying patients in need of treatment to prevent advancement to a cirrhotic state. A review of healthy livers determined that age and sex did not impact on the liver stiffness (Kim and Younossi, 2008). A study conducted on 69 healthy patients concluded a mean liver stiffness measurement of 4.5 ± 0.4 kPa using FibroScan® (Kim and Younossi, 2008). A study conducted with 135 patients with confirmed ALD was carried out to determine if elastography was a usefool tool in its prediction in comparison with other tools used for the diagnosis of fibrosis and cirrhosis (Fernandez et al., 2015). Elastography outperformed other tools and demonstrated a positive correlation with AST values concluding that elastography was currently the most accurate method of identifying fibrosis in patients with ALD. A review of 50 literature papers concluded in favour of transient elastography stating that it had excellent diagnostic accuracy (Friedrich-Rust et al., 2008). However, 5.5 % of the patients recruited to the Sandrin study did not yield results due to narrow

intercostal spaces or being overweight. Operator compliance was also acceptable (Sandrin et al., 2003). However, the low frequency waves are attenuated by fatty tissue, hence measurements in obese patients is not an option for diagnosis of liver fibrosis. As, many patients with obesity have NAFLD, which can lead to the development of fibrosis, these are a cohort of patients that could not use elastography despite needing routine assessment to prevent the onset of advanced fibrosis and subsequent cirrhosis. As well as this, the levels of steatosis and its effect of liver stiffness measurements taken from transient elastography has not been well researched. Petta et al (2015) have carried out a study to assess the impact of the severity of steatosis of liver stiffness in patients with NAFLD. This study demonstrated that the greater the severity of steatosis the higher the liver stiffness measurement. Subsequently, caution should be taken with liver stiffness measurements from patients with histologically identified NAFLD.

1.5 IGFBP-5 as a biomarker of liver disease

Mounting evidence in the literature links insulin-like growth factor binding protein-5 (IGFBP-5) to fibrosis and hence its study in this thesis. In vitro models of liver disease using primary rat hepatocytes were developed and assessed for the secretion of IGFBP-5 as a function of time in culture and as a result of chronic insult (treatment of up to 9 days in culture) from oxidative toxins and the accumulation of triglycerides in hepatocytes.

IGFBP-5 is a member of the insulin-like growth factor (IGF) axis. The IGF axis plays a crucial role in regulating cellular growth, differentiation and apoptosis. It comprises two peptide growth factors (IGF-I and IGFB-II), cell surface IGF-I and IGF-II receptors (IGF-IR and IGF-IIR) and six soluble IGF binding proteins (IGFBP-1-6) as well as a family of IGFBP proteases which as increasingly well-defined (Beattie et al., 2006). The liver is the main source of IGF-I and its hepatic expression is under the control of pituitary growth hormone. IGF-I and -II a as well as the receptors IGF-IR and –IIR are expressed in a wide variety of tissues.

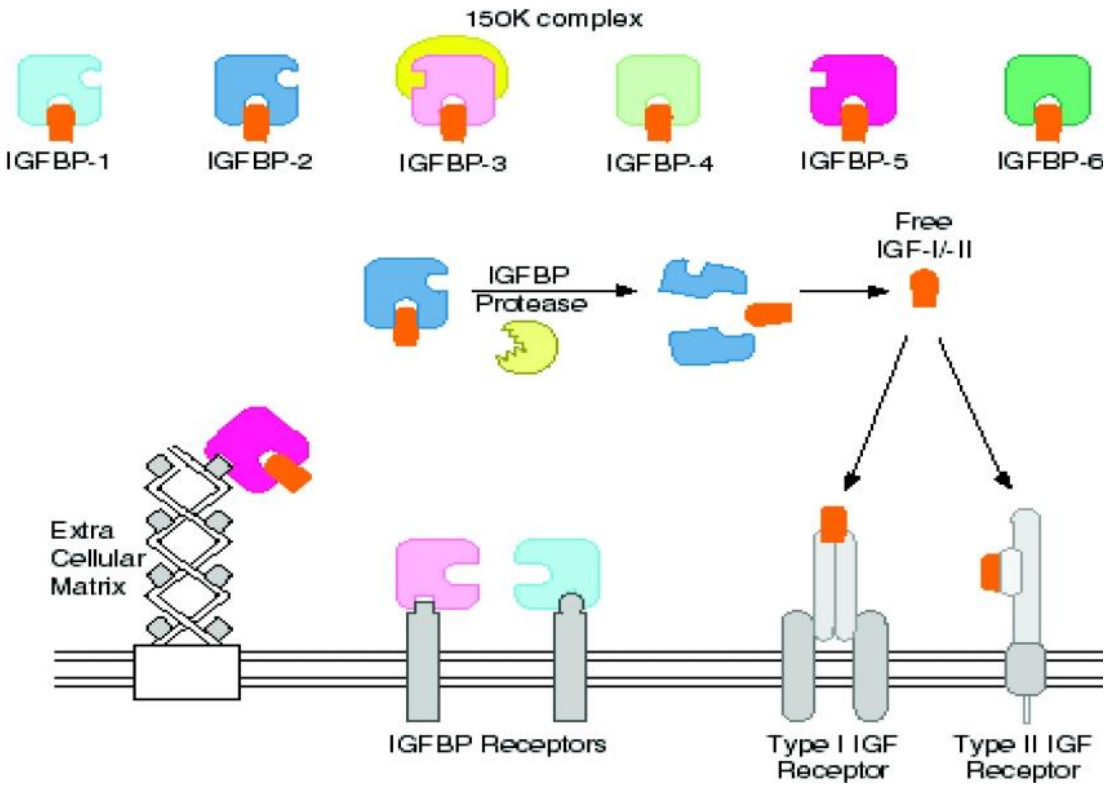

Figure 1-2 Schematic of the IGF axis.

The IGF axis consists of IGF-I and –II (Note IGF-I and –II are orange in colour). IGF-I and –II bind all IGFBPs. IGFBP-5 (pink) also has a high affinity to bind extracellular matrix. IGFBP proteases act to hydrolyse IGFBPs releasing IGF-I and –II to bind IGF-IR and –IIR. (Beattie et al., 2006)

IGFBPs are important members of the IGF axis, and IGFBP 1 - 6 have been cloned and vary in length from 201 – 289 residues, with a molecular weight of between 24 and 44 kDa. They are secreted by many cell types and bind with high affinity to IGF. Almost 95 % of circulating IGFs in serum and other biological fluids are bound to IGFBPs (Beattie et al., 2006). IGFs have a higher affinity to bind with IGFBPs over cell surface receptors; hence IGFs bound to IGFBPs are restricted from accessing the cell surface IGF-IR (see Figure 1.2). Additionally, some IGFBPs can bind to the extracellular matrix (ECM) (Arai et al., 1994).

Species	Human	Mouse	Rat
Expression sites	Testes Trabecular meshwork Bone Lung Uterus and placenta Ovary	Limbs Kidney Lung Ovary Spinal cord Skeletal muscle Mammary glands	Pancreas Kidney Ovary Lung Kidney Forebrain Eyes Liver Pituitary

Table 1-3 Major expression sites of IGFBP-5 in human, mouse and rat

Adapted from (Schneider et al., 2002).

IGFBP-5 is a 28.5 kDa protein (252 residues) and is slightly basic. It contains three important regions, the N-terminal, C-terminal and the core made up of intra-domain disulfide bonding of cysteine between the N-and C-terminals. The C-terminal contains a heparin binding sequence (long), important in ECM and other protein binding glycosaminoglycans (GAGs) and heparan sulphate. The central domain also contains a heparin binding sequence (short). The mid region has been proposed as a site for cleavage by phosphorylation, with the N-terminal being the site for IGF-I and –II binding. Neither the mid-region nor the C-terminal bind IGF-I or –II (Kalus et al., 1998). IGFBP-5 is expressed in many tissues and these are listed in Table 1.3.

It has been reported that IGFBP-5 may have a role in the progression of fibrosis. IGFBP-5 binds to collagen, fibronectin, and GAGs e.g. heparan sulfate, and by doing so decreases its affinity for binding to IGF. In turn, this increases the activity of IGF including its promotion of wound healing. IGFBP-5 has been implicated in the induction of both pulmonary and epithelial fibrosis (Sureshbabu et al., 2009b, Yasuoka et al., 2006a, Pilewski et al., 2005, Yasuoka et al., 2006a). It could also be implicated in the fibrotic response in the liver.

1.5.1 IGFBP-5 and Lung

Pilweski and team (2005g) demonstrated that IGFBP-5 expression could be the initiating event in ECM production in idiopathic pulmonary fibrosis (IPF). IPF fibroblasts in in vitro culture showed both increased expression of mRNA levels of IGFBP-5, as well as protein levels in culture supernatants compared with control cells. mRNA levels also increased 2-fold in comparison with normal fibroblasts. The team demonstrated that this effect was not a result of the increased number of fibroblasts in IPF tissue, but an increase in expression within each fibroblast in comparison with healthy fibroblasts. Protein levels of IGFBP-5 were on average 1000 times higher when compared with normal fibroblasts. Further to this, Pilweski and team demonstrated that IGFBP-5 could stimulate the production of ECM in normal fibroblasts. Infecting primary adult lung fibroblasts with adenovirus containing IGFBP-5 also increased the deposition of collagen type I and fibronectin (Pilewski et al., 2005b). Yasuoka et al (2006b) also demonstrated that over expression of IGFBP-5 in mice triggered mononuclear cellular infiltration in mouse lung tissues. Infiltration of macrophages upon IGFBP-5 over expression has also been observed.

1.5.2 IGFBP-5 and Skin

Patients with systemic sclerosis (SSc) were also identified to have an increased level of human IGFBP-5 mRNA in comparison with normal skin tissue (Feghali and Wright, 1999). Yasuoka et al (2006a) developed a murine model to demonstrate that subcutaneous injections of adenovirus IGFBP-5 would induce skin fibrosis. An increase in collagen deposition, dermal thickness and collagen bundle diameter were observed in IGFBP-5 overexpressing mice. In contrast to the implication of IGFBP-5 in the progression of SSc and fibrosis, Wang et al (2015) demonstrated that IGFBP-5 inhibits melanoma cell proliferation and suppresses tumour growth in vivo through inhibition of ERK 1/2 and P38-MAPK pathways. Further to this, IGFBP-5 was demonstrated to suppress epithelial to mesenchymal (Wang et al., 2015).

1.5.3 IGFBP-5 and Liver

Conversely, Sokolovic et al (2012) demonstrated a possible protective role of IGFBP-5 in fibrosis. The overexpression of IGFBP-5 in Abcb4$^{-/-}$ mice (in vivo mouse model for the study of chronic cholangiopathy) impaired the progression of liver fibrosis,

which was demonstrated by the reduction in ECM by hydroxyl proline content and by sirius red staining for connective tissue. Moreover, Sokolovic et al (2012), also demonstrated that the overexpression reduced inflammation and oxidative stress in the model. It has been suggested that IGFBP-5 blocks infiltrating inflammatory cells which normally act to enhance fibrosis through inflammatory cytokines, thus inducing collagen synthesis. A marker of infiltrating macrophages and the resident macrophages, the Kupffer cells, F4/80 mRNA, was significantly lower in IGFBP-5 overexpressing mice in comparison with control mice. Macrophages hold a relevant role in inflammation in fibrosis (Yasuoka et al., 2006b, Yasuoka et al., 2009).

1.5.4 IGFBP-5 and Breast Cancer

Further to this, Sureshbabu et al. (2012), investigated the role of IGFBP-5 in the survival of MCF-7 human breast cancer cells. Levels of IGFBP-5 were higher in all samples of breast cancer tissue in comparison with control tissue samples. High levels of IGFBP-5 has also been correlated with poor outcome of breast cancer, and overexpressed in breast tissue with positive auxillary lymph nodes (Li et al., 2007). Despite the link with patient outcome, no correlation was evident between tumour size or clinical grade and IGFBP-5 (Li et al., 2007).

Despite conflicting opinions on IGFBP-5's role in fibrosis in published literature, there is strong evidence to suggest that it could also play a role in the pathogenesis of liver injury and subsequent fibrosis.

1.6 Aims and Objectives of this thesis

This aim of this thesis was to investigate IGFBP-5 as a biomarker for the detection of liver disease using multiple in vitro models. The work aims to highlight IGFBP-5s involvement in the aging process of primary rat hepatocyte as well as its role in fibrosis. IGFBP-5 also enhances the responses to injurious agents such as menadione and hydrogen peroxide.

The objectives of the individual studies in this thesis are:

- To develop and characterise the in vitro model and correlate dedifferentiation with IGFBP-5.
- To investigate IGFBP-5 release upon oxidative stress via multiple dosing of menadione or hydrogen peroxide.
- To determine if IGFBP-5 plays a role in hepatocyte toxicity via ethanol and its major metabolite acetaldehyde.
- To transfect primary hepatocytes with IGFBP-5 and determine if this would alter the toxicity seen with menadione or hydrogen peroxide.
- To assess IGFBP-5 release upon triglyceride accumulation in hepatocytes (NAFLD model), and determine if IGFBP-5 initiates a fibrotic response with hepatic stellate cells.
- To investigate if IGFBP-5 in human serum samples is altered with various liver diseases i.e. diabetes and NASH.

Initially, an in vitro model of primary rat hepatocytes in monolayer was characterised. Their dedifferentiation was documented along with IGFBP-5 release into the medium. After determining that IGFBP-5 expression may be involved in some way in the aging/de-differentiation process, we investigated in Chapter 4 whether IGFBP-5 expression in hepatocytes could affect the way they deal with classic oxidative stress inducing toxins, menadione and hydrogen peroxide.

With alcohol misuse being highly prevalent in the UK and in Scotland in particular, the development of a biomarker for the detection of early liver disease would be

welcomed in hepatology clinics. Bataller and Brenner (2005) have discussed the importance of developing a simple and non-invasive marker of hepatic fibrosis. The first step in this process involves taking a known hepatotoxin and evaluating its effects on in vitro cell cultures. The objective of this chapter was to develop a model of oxidative stress without causing cell death and to investigate the effects of a range of concentrations of two classic hepatotoxins on HepG2 cells and primary rat hepatocytes. The toxic effects of exposure to ethanol and acetaldehyde with the viability and function of the cells were characterised by using crystal violet (CV), WST-1, lactate dehydrogenase (LDH), reduced glutathione (GSH) and Lowry assays as well as correlating the effect of ethanol and acetaldehyde with IGFBP-5 release into the culture medium.

In Chapter 5 data is presented and discussed on a range of concentrations of IGFBP-5 which were considered to determine a suitable concentration to transfect the cells with. The hepatocytes transfected with IGFBP-5 were then insulted with two well published and characterised oxidative toxins; Menadione and Hydrogen peroxide

Chapter 6 describes the details of a NAFLD model that was used to determine if IGFBP-5 was upregulated upon triglyceride accumulation in hepatocytes in vitro. Further to the simple NAFLD model, we investigated whether the conditioned medium from NAFLD model cultures induced a fibrotic response in culture of LX2 cells, a hepatic stellate cell line developed by Professor Scott Friedman at Mount Sinai School of Medicine in New York to study hepatic fibrosis and anti-fibrotic therapies (Xu et al., 2005). IGFBP-5 has already been shown to induce skin and lung fibrosis. A murine model for dermal fibrosis demonstrated that when mice received a subcutaneous injection of replication deficient serotype 5-adenovirus expressing IGFBP-5, this resulted in significant increases in dermal thickness and collagen bundle thickness in comparison on mice that had received adenovirus expressing IGFBP-3 or no complementary DNA (Yasuoka et al., 2006). In addition, normal lung fibroblasts incubated with recombinant IGFBP-5 for 48 h induced a 16-fold increase in fibronectin

levels (Pilewski et al., 2005). Could the IGFBP-5 secreted in the NAFLD model have the same effect on hepatic stellate cells?

Chapter 2 Materials and Methods

2.1 Preparation of hepatocyte perfusion solutions

Hank's Buffer (10 x)

NaCl	80 g	1.37 M
KCl	4 g	53.66 mM
$MgSO_4.7H_2O$	2 g	8.11 mM
$Na_2HPO_4.2H_2O$	0.6 g	4.22 mM
KH_2PO_4	0.6 g	4.41 mM

The above salts were dissolved in 1 L distilled water and stored at 4 °C.

Krebs - Henseleit Buffer (2 x)

Solution A

Distilled water	785 ml
16.09 % (w/v) NaCl	200 ml
1.1 % (w/v) KCl	150 ml
0.22 M KH_2PO_4	25 ml
2.74 % (w/v) $MgSO_4.7H_2O$	50 ml
0.12 M $CaCl_2.6H_2O$	100 ml

Solution B

$NaHCO_3$	9.71g / 1 L distilled water (115.58 mM)

The solutions for A were added to a brown 2 L glass bottle in the order shown above and 5 % CO_2/95 % O_2 was bubbled through the final solution for 10 min. Solution B was bubbled in the same gas mixture for 10 min, and this was then added to solution A while still bubbling the gas through.

Hank's I Buffer

$NaHCO_3$	1.05 g	24.99 mM
4-(2-hydroxyethyl)-1-piperazineethanesulfonic acid (Hepes)	1.5 g	12.58 mM
Bovine serum albumin (BSA)	3.33 g	
Ethylene glycol tetraacetic acid (EGTA)	114 mg	0.6 mM
Distilled water	450 ml	
Hank's Buffer (10 x)	50 ml	

Hank's II Buffer

$NaHCO_3$	1.05 g	24.99 mM
Hepes	1.5 g	12.58 mM
$CaCl_2.2H2O$	147 mg	2.0 mM
Distilled water	450 ml	
Hank's Buffer (10 x)	50 ml	

Krebs Albumin Buffer

Hepes	1.5 g	12.58 mM
BSA	5 g	
Distilled water	250 ml	
Krebs-Henseleit Buffer (2 x)	250 ml	

Krebs - Hepes Buffer

Hepes	1.5 g	12.58 mM
Distilled water	250 ml	
Krebs-Henseleit Buffer (2 x)	250 ml	

These solutions were pH adjusted to pH 7.4 with 5 M NaOH and then filter-sterilised through a 0.22 µm filter into sterile bottles.

2.2 Isolation of primary rat hepatocytes

The perfusion of the rat liver was conducted under sterile conditions in a laminar flow hood with all equipment sterilised using a solution of 70 % v/v ethanol in water.

Hepatocytes were isolated by a modified collagenase perfusion method (Moldeus et al., 1978). The rats used for the perfusion were male Sprague-Dawley (180 – 220 g) and were obtained from the BPU at the University of Strathclyde. The surgery was carried out in accordance with the Home Office Project Licence. The rat was anaesthetised by an intraperitoneal injection of a solution of 57.4 mg/ml Phenobarbital sodium (Ceva Sante Animale; 0.2 ml). The rat was placed on its back and its abdomen was wiped with 70 % v/v ethanol. Incisions were then made by first cutting through the skin whilst lifting the skin with blunt forceps, followed by U-shaped incisions through the muscle layer. The intestine was carefully lifted aside thereby exposing the portal vein. Heparin (1000 U/ml in PBS; 0.1 ml) was injected into the inferior vena cava and was left to circulate for 1 minute. A small incision was then made into the portal vein and the cannula (stainless steel; internal and external dimensions were 1.75 m and 2.5 mm respectively) was immediately inserted approximately 1 cm into the vein. The final position of the cannula was just below the first venous branch into a liver lobe. A surgical clip was used to secure the cannula. Immediately after cannulation, the perfusion was initiated *in situ* with Hank's I buffer at a flow rate of approximately 5 ml/min (22 mm H_2O). The animal was sacrificed by piercing the diaphragm with the scissors. The liver was excised by dissecting the liver free from the diaphragm, intestines and stomach and finally, with the rat in a tilted position, by cutting the dorsal ligaments. The excised liver was transferred into a beaker of Hank's I buffer containing EGTA (0.6 mM: 114 mg/500 ml), which was re-circulated through the cannula for approximately 10 minutes. The liver was then transferred into a 250 ml beaker with Hank's II buffer containing collagenase (253 Units/mg; 78 mg; Type II lyophilised Collagenase prepared from Clostridium Histolyticum; Gibco, Invitrogen Corporation) and calcium chloride (2 mM: 147 mg/500 ml) to digest the extracellular matrix. Perfusion was performed under recirculation until the liver was soft and cells appeared to be dissociated. Flow was then stopped and the liver was transferred to a Petri dish containing Kreb's-Hepes buffer containing albumin and teased with a forceps to disperse the cells. The cell suspension was then passed through a sieve

(Sigma cell culture reagents, UK) with a 50 µm mesh to remove any clumps of cells and connective tissue. The cells were then allowed to settle under gravity on ice, the supernatant was removed and they were then washed twice with 50 ml Kreb's-Hepes buffer. Again the cells were allowed to settle under gravity on ice and the supernatant was removed.

2.3 Determination of hepatocyte viability and initial yield

Viability was checked using a haemocytometer and the Trypan blue exclusion test. A suspension of cells (10 µl) was added to 990 µl 0.1 % (w/v) Trypan blue in phosphate buffered saline (PBS) and loaded on the haemocytometer. Cells in all 9 areas were counted and an average was found. The viability was expressed as a ratio of cells excluding Trypan blue to the total number of cells. 10µl of the solution was loaded onto a haemocytometer and all 18 square areas were counted. The viability was calculated by expressing the cells excluding Trypan blue over the total number of cells. Only cell suspensions with viability greater than 75 % were used.

2.4 MTT Microplate Assay

The MTT is reduced in the mitochondria of the cells to form a purple formazan salt, a reaction which is dependent on co-factors and enzymes, and hence used as a marker of metabolic activity or viability. A solution of 10 mM MTT [3-(4,5-dimethylthiazol-2-yl)-2,5-diphenyltetrazolium bromide] was made up in PBS (0.414 g/100 ml) pH 6.75. The solution was then filtered through a 0.2 µm filter and stored at 4 °C. Once the cells in the 96 well plates were ready to undergo the assay, the medium was removed and 50 µl of MTT solution added to each well. The plates were then incubated at 37 °C for 4 hours. After the incubation time the MTT solution was removed and 200 µl of DMSO was added to each well to dissolve the formazan salt that had formed. The solution was mixed to form an even colour and the absorbance was read at 540 nm using a plate reader.

2.5 Neutral Red (NR) Assay

Neutral red is a vital stain that is taken into viable cells and accumulated in the lysosomes. This weak cationic dye readily penetrates the cell membranes and binds to anionic sites in the lysosomal matrix. NR (Borenfreund and Puerner, 1985) (5 mg) was dissolved in 100 ml PBS and incubated overnight at 37 °C. The solution was then filtered through a 0.2 µm filter and stored at 4 °C. Destain was made up using 50 ml ethanol, 1 ml glacial acetic acid and 49 ml distilled H_2O. Once cells in the 96 well plates were ready, medium was removed and NR solution (100 µl) was added to each well. The plates were then incubated at 37 °C for 3 hours. After incubation the NR solution was removed and destain (100 µl) was added to each well. The plate was then gently shaken for approximately 30 minutes until a homogenous colour was obtained in each well. The absorbance was then measured at 540 nm using a plate reader.

2.6 Determination of total protein

Solution A

1 % (w/v) Copper Sulfate	1 ml
2 % (w/v) Na-K tartrate	1 ml
2 % (w/v) Na_2CO_3	98 ml

Solution B

1:4 dilution of Folins (Ciocaltau) reagent in distilled water

Protein content of the samples was determined using a previously described method (Lowry et al., 1951) with BSA as a standard. Standards contained concentrations of between 0 and 200 µg/ml BSA in 0.5 M NaOH. To both the samples (50 µl) and standards (50 µl), 950 µl of 0.5 M NaOH and 5 ml of solution A was added and mixed thoroughly. These solutions were incubated for 10 minutes at room temperature after which 0.5 ml of solution B was added and the solutions were again mixed thoroughly. These were then incubated for between 30 and 90 minutes at room temperature. The absorbance of the reaction was measured against a water blank at 725 nm.

2.7 Sodium dodecyl sulfate polyacrylamide gel electrophoresis (SDS-PAGE)

At each time point, Petri dishes were placed on ice. Medium was removed and wells were washed 3 x with PBS pH 7.4. The cells were scraped into 1 ml 0.1 M NaPi buffer pH 7.5 and homogenised with 7 strokes of a motor driven pestle in a Teflon glass homogeniser. The homogenates were stored in Eppendorfs at -70 °C awaiting analysis. The protein content of the homogenates was measured as described in section 2.6. The samples were then prepared in Laemmli buffer at 1 mg/ml and boiled for 2 min in stoplock Eppendorfs to denature the proteins.

Stacking gel buffer 0.5 M Tris buffer pH 6.8

6.0 g Tris-HCl was dissolved in 40 ml distilled water and titrated to pH 6.8 with approximately 48 ml of 1 M HCl. The solution was made up to 100 ml with distilled water and stored at 4 °C.

Resolving gel buffer 1.5 M Tris buffer pH 8.8

36.33 g of Tris-HCl was dissolved in 48 ml of 1M HCl, made up to 200 ml with distilled water and stored at 4 °C.

1.5 % (w/v) Ammonium persulphate (APS)

APS (7.5 mg) was accurately weighed out and dissolved in 5 ml distilled water. The solution was made freshly before every use.

Electrophoresis buffer (10 x) 0.25 M Tris/1.92 M Glycine/1 % (w/v) SDS buffer pH 8.3

30.3 g Tris-HCl, 144 g Glycine, 10 g SDS were dissolved in distilled water. The pH was adjusted with 1 M HCl and the solution was made up to a final volume of 1 L with distilled water and stored at 4 °C.

The glass plates were cleaned with 70 % ethanol to ensure they were clean and assembled in the casting chamber. The gel solutions were prepared as described in Table 2.1.

Solutions	Stacking gel	10 % Resolving gel
Acrylamide/bis acrylamide (40% w/v)	1 ml	5.625 ml
Stacking gel buffer	2.5 ml	-
Resolving gel buffer	-	5.625 ml
1.5% APS	0.5 ml	1.125
Distilled water	6 ml	10.125 ml
Tetramethylethylenediamine (TEMED)	5 µl	17.25 µl

Table 2-1 Preparation of SDS-PAGE gels

The resolving gel was cast first and allowed to set for about 15 min. Once the resolving gel was set, the stacking gel was cast on top and the combs were inserted into the gel to prepare wells for the protein samples. Once the gels were set they were transferred into the electrophoresis tank and the upper chamber and tank were filled with 1 x electrophoresis buffer. The combs were removed and the wells were loaded with samples and a molecular weight marker standard. The gels were run at a current of 50 mA for 15 min then at 150 V until the samples had migrated to a few centimetres from the bottom of the gel.

2.8 Immunoblotting

Tris/Glycine buffer (10 x)

1.92 M Glycine	144 g/L
0.25 M Tris	30 g/L

The above solutions were dissolved in distilled water at pH 8.3.

Transfer buffer	
Distilled water	1400 ml
Methanol	400 ml
Tris/Glycine buffer (10 x)	200 ml

Tris buffered saline (TBS) 10 x	
200 mM Tris	24.22 g/L
5 M NaCl	292.2 g/L

Tween Tris Buffered Saline (TTBS)

This solution was made up by adding 0.5 ml Tween 20 to 1 L TBS (1 x).

The PVDF membranes were placed in methanol for 2 min prior to being placed in transfer buffer. The Scotchbrite pads, filter paper and gels were placed in transfer buffer also for 15 min to soak. Gels were then transferred onto the membrane and sandwiched between two pieces of filter paper and Scotchbrite pads in transfer cassettes (see Figure 2.1 for a diagram of assembly). These were then placed into the tank which was connected to the cooling unit and filled with transfer buffer. A current of 200 mA was then applied overnight.

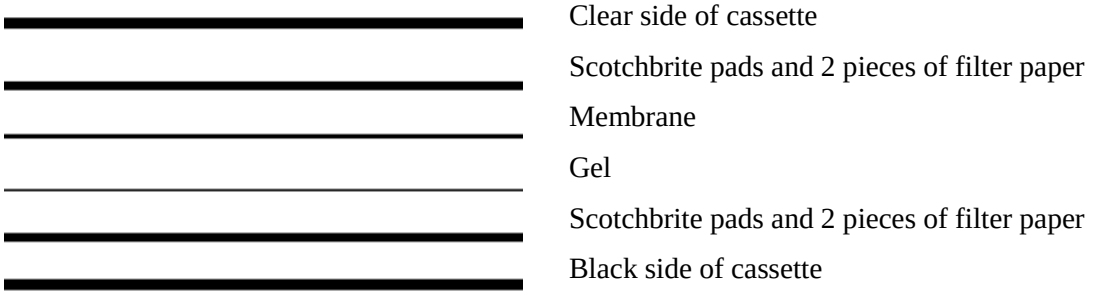

Figure 2-1 Assembly of cassettes with gel and membrane for immunoblotting

The membranes were then blocked in 3 % v/v gelatin in TTBS on a shaker at room temperature for 2 h. They were then washed (1 x) with TTBS, and placed on a shaker for 5 min. The primary antibody was diluted as directed in 1 % v/v gelatin in TTBS. The solution was added to the membranes and placed on a shaker for 2 h. The membranes were then washed (3 x) in TTBS and shaken for 5 min. The secondary antibody was diluted as directed in 1 % v/v gelatine in TTBS. The solution was added to the membranes and shaken for 2 h. The membranes were then washed (3 x) with TTBS for 5 min and then washed (1 x) with TBS for 5 min. A Bio-Rad alkaline phosphatase detection kit was used to visualise the bands in accordance with the manufacturer's instructions. A working solution was prepared by adding 1 ml of solution A and 1 ml of solution B to 98 ml of the development buffer. This was added to the membranes and placed on a shaker for 5 – 10 min. The membranes were then washed with distilled water and blotted between filter paper to dry. The membranes were scanned onto a computer and analysed using ImageJ (http://rsbweb.nih.gov/ij/; [date accessed 11.05.11]) to determine the intensity of the bands.

2.9 Measurement of IGFBP-5 by ELISA

The mouse IGFBP-5 enzyme-linked immunosorbent assay (ELISA) (R&D Systems, UK; DY578) was carried out as per the manufacturer's instructions.

Wash buffer

0.05 % Tween 20 in PBS (0.2 µ filtered), pH 7.2 - 7.4

Block buffer

5 % Tween 20 with 0.05 % NaN_3

Reagent diluent

5% Tween 20 in PBS (0.2 µ filtered) containing 2 % heat inactivated normal goat serum, pH 7.2 - 7.4

Substrate solution

1 : 1 mixture of solution A (H_2O_2) and solution B (tetramethylbenzidine)

Stop solution

1 M H_2SO_4

The capture antibody was diluted to a working solution of 0.4 µg/ml in PBS. The 96 well microplate was immediately coated with 100 µl of capture antibody, the plate was sealed and left at room temperature overnight. The wells were washed with wash buffer 3 x (400 µl). After the last wash the plate was inverted and blotted with absorbent tissue paper to remove any remaining wash buffer. The plate was then blocked by adding 300 µl block buffer to each well and then incubated at room temperature for 1 h. The wash steps were repeated and 100 µl of medium samples and standards were added. Standards were diluted in Williams' E medium with the top concentration of 16 ng/ml. The plate was sealed and incubated at room temperature for 2 h. The wash steps were repeated. The detection antibody was diluted to a working concentration of 200 ng/ml in reagent diluent. 100 µl of detection antibody was added to each well and incubated at room temperature for 2 h. The wash steps were repeated. A working dilution of streptavidin-horseradish peroxidase (HRP) (1 : 200) in reagent diluent without 2 % heat inactivated normal goat serum was prepared. 100 µl was added to each well and incubated at room temperature for 20 min in the dark. The wash steps were repeated. 100 µl of substrate solution was added to each well and incubated at room temperature for 20 min in the dark. After 20 min 50 µl of stop solution was added to each well and the absorbance was read at a wavelength of 450 nm. The limit of detection for the assay is 0.125 ng/ml.

2.10 HepG2 Culture

Hep G2 human hepatoma cells were obtained from the Centre for Drug Safety Science, University of Liverpool. Cells were routinely grown in 75 cm^2 flasks as mono-/multi layer cultures in a humidified atmosphere of 5 % CO_2 in air until confluent (3 days). To passage the cells, the growth medium, (Dulbecco's Minimum Essential Medium

(DMEM) containing 10 % v/v foetal calf serum (FCS), penicillin G (50 units/ml) and streptomycin sulphate (50 µg/ml)), was removed and the culture was washed with 2 x 10 ml versene buffer in order to remove any FCS that would otherwise inhibit the activity of the trypsin. The wash medium was replaced with a small quantity (1-2 ml) of a solution of trypsin (0.05 % w/v) in versene buffer. After 3-6 minutes incubation time at room temperature, the cells were detached from the flask surface by tapping with the palm of the hand against the side of the flask. The cell suspension was diluted with a small quantity of the DMEM growth medium. Cells were maintained at a split ratio of 1:3.

2.11 Measurement of lactate dehydrogenase (LDH) activity

Solutions

0.1 M Sodium Phosphate (NaPi) buffer pH 7.6

0.2 M Na_2HPO_4 was prepared by adding 14.2 g to 500 ml distilled H_2O and 0.2 M NaH_2PO_4 was prepared by adding 2.4 g to 100 ml distilled H_2O. For pH 7.6, 87 ml of 0.2 M Na_2HPO_4 was added to 13 ml 0.2 M Na_2HPO_4. The pH was checked and adjusted with the appropriate solution.

A pyruvate/NADH solution was prepared by dissolving 3 mg pyruvic acid and 3 mg NADH in 1 ml NaPi buffer.

Assay

The cell viability was assessed by LDH leakage through the membrane into the medium. LDH activity was measured using a published method (Bergemeyer *et al*., 1963). For the assay, 0.86 ml of the phosphate buffer and 40 µl of the pyruvic acid/NADH solution were mixed in a 2.5 ml UV-cuvette. 100 µl of the medium removed from the cells after incubation with the toxin were added to start the reaction. The solution was mixed by inverting the cuvette twice and the absorbance was measured at 340 nm continuously for 60 seconds. The enzyme activity was defined as:

(change in absorbance/min)/E = µmol/ml^{-1} min^{-1} of LDH activity, where E is the molar extinction coefficient for NADH (6.22 mM^{-1}cm^{-1}).

2.12 Determination of reduced glutathione (GSH) by fluorimetry

Solutions

Phosphate buffer pH 8.0

Solution 1 was prepared by dissolving 17.8 mg Na_2PO_4 (0.25 Mm) and 0.93 g EDTA (6.6 mM) in 500 ml d.H_2O. Solution 2 was prepared by dissolving 5.33 g NaH_2PO_4 (0.45 M) and 0.186g EDTA (6.36 mM) in 100 ml d.H_2O. The pH of solution 1 was adjusted to 8.0 using solution 2.

Standards were prepared in the range of 0 to 100 µM GSH using 10 % v/v trichloroacetic acid (TCA).

Assay

The intracellular GSH was measured using a previously reported method (Hissin & Hilf, 1976). Aliquots of 25 µl of standards and samples were added to a 12 ml test tube and to that 2.3 ml of pH 8.0 phosphate buffer was added. 100 µl of 1 mg/ml o-phthaldehyde (OPT) in methanol was added to each sample and standard. The samples and standards were then incubated for 15 minutes in the dark and fluorescence was measured on a Shimadzu RF-5001 PC Spectrofluorometer (λ = 350 nm excitation; λ = 420 nm emission wavelengths). The concentrations of GSH were expressed as µM, with quantification being achieved using the standard solutions.

2.13 WST-1 Assay

For WST-1 (Roche Applied Science, Germany), a 10 % dilution of WST-1 (50 µl) was added to each well containing cell and medium and incubated for 1 h at 37 °C in a humidified atmosphere of 5 % CO_2 in air. After 1 h, plates were shaken thoroughly for 1 min prior to measuring the absorbance (450 nm) on a plate reader.

2.14 Crystal Violet (CV) assay

Cells were washed with PBS and 100 µl 4 % paraformaldehyde (PFA) was added for 30 min to fix the cells. After 30 min, PFA was removed and wells were washed with 100 µl PBS (2x) before adding 100 µl CV for 20 min. After 20 min, CV was removed and wells were washed with 200 µl PBS (3x). The stain was then solubilised overnight with 0.1 % Triton X-100 in PBS. Plates were shaken thoroughly prior to measuring the absorbance (540 nm) on a plate reader.

2.15 Human IGFBP-5 ELISA

The human IGFBP-5 ELISA (R&D Systems, UK) was carried out as per the manufacturer's instructions.

Wash buffer

0.05 % Tween 20 in PBS (0.2 µ filtered), pH 7.2 - 7.4

Blocking buffer

5 % Tween 20 with 0.05 % NaN_3

Reagent diluent

5% Tween 20 in PBS (0.2 µ filtered) containing 2 % heat inactivated normal goat serum, pH 7.2 - 7.4 prepared 1-2 h prior to use.

Substrate solution

1 : 1 mixture of solution A (H_2O_2) and solution B (tetramethylbenzidine)

Stop solution

1 M H_2SO_4

The capture antibody, mouse anti-human IGFBP-5 was diluted 180-fold to give a working solution of 0.4 µg/ml in PBS. The 96 well microplate was immediately coated with 100 µl of capture antibody, the plate was sealed and left at room temperature

overnight. The wells were washed with wash buffer 3 x (400 µl). After the last wash the plate was inverted and blotted with absorbent tissue paper to remove any remaining wash buffer. The plate was then blocked adding 300 µl block buffer to each well and then incubated at room temperature for 1 h. The wash steps were repeated and 100 µl of medium samples and standards were added. Standards were diluted in Williams' E medium with the top concentration of 40 ng/ml. The plate was sealed and incubated at room temperature for 2 h. The wash steps were repeated. The detection antibody, biotinylated goat anti-human IGFBP-5 was diluted 180 fold to a working concentration of 200 ng/ml in reagent diluent. 100 µl of detection antibody was added to each well and incubated at room temperature for 2 h. The wash steps were repeated. A working dilution of streptavidin-HRP (1 : 200) in reagent diluent without 2 % heat inactivated normal goat serum was prepared. 100 µl was added to each well and incubated at room temperature for 20 min in the dark. The wash steps were repeated. 100 µl of substrate solution was added to each well and incubated at room temperature for 20 min in the dark. After 20 min 50 µl of stop solution was added to each well and the absorbance was read at a wavelength of 450 nm.

Chapter 3 De-differentiation of Primary Rat Hepatocytes in Culture

3.1 Introduction

To investigate Phase I CYP-mediated biotransformations in cultured rat hepatocytes over a period of 9 days in culture, CYP-mediated hydroxylation of testosterone was undertaken. This reaction involves a variety of members of the CYP superfamily of enzymes present in both human and rat. Phase II, glutathione S-transferase (GST) isoenzymes, are also a widely used marker of de-differentiation, hence GSTP1 expression was measured over 9 days in culture also.

3.1.1 GSTP1 Expression

The Glutathione S-transferases (GST) are a family of multi-functional proteins which catalyse the conjugation of GSH electrophiles, the reduction of organic hydroperoxides and certain GSH-dependent isomerisations (Ketterer, 1988). They are binding proteins for a number of lipophiles, such as bilirubin, haem and hormones (Mannervik et al., 1988). Phase II GST activity is altered from in vivo levels when hepatocytes are isolated (Vandenberghe et al., 1988). GSTs are enzymes involved in the detoxification of many chemicals, including lipids, drugs and DNA hydroperoxides. They catalyse the conjugation of the of reduced glutathione (GSH) with electrophile (Ketterer, 1988), and are also involved in the hepatic uptake of bilirubin and the intracellular transport of haem and steroid hormones. There are a number of isoforms that have been identified, which include alpha, mu and pi. GSTA and GSTM are abundant in normal rat liver. GSTM plays a major role in the detoxification of many carcinogens (Nakamura et al., 2009). GSTA is more readily decreased than GSTM (Tee et al., 1992). GSTA and GSTM are abundant in normal rat liver unlike GSTP1. GSTP1 appears to be developmentally regulated. The GSTP1 form has been shown to be most abundant in foetal liver but is almost absent postnatally (Tee et al., 1992). It has been shown to have a specific developmental pattern in the foetal liver and is abundant in an 18 day old foetal liver, however, it has also been shown that GSTP1 is present in an adult liver during hepatocarcinogenesis (Tee et al., 1992). GSTP1 is often referred to as a marker of de-differentiation, and is not present in normal rat liver in vivo or in freshly isolated cells; however, expression

is induced within 24 h in hepatocyte culture (Lockman et al., 2012). Expression of the total GST activity after isolation has been shown to be reduced by 50% after 24 h in culture in comparison to levels in freshly isolated hepatocytes (Daniel, 1993). It has been suggested that alterations in GSTP1 expression in primary cultures could be attributed to the presence of hormones and growth factors present in serum with which media are often supplemented (Hatayama et al., 1991).

3.1.2 Testosterone hydroxylation

Testosterone hydroxylation is a commonly used marker of de-differentiation and this is widely published (Kern et al., 1997). Several biotransformations can be investigated at once with this substrate, hence, testosterone is often favoured as a probe substrate to provide a fingerprint of CYP activity in the rat. There are many reported metabolites of testosterone. Formation of 7α-, 6β-, 16α- and 2α- hydroxytestosterone is indicative of CYP2A, CYP3A, CYP2C and CYP2C11 activity respectively (Wortelboer et al., 1990). CYP2C11 is the major expressed isoenzyme in the male rat liver and is particularly susceptible to changes in hepatic environment, hence making it a sensitive measurement of cell phenotype (Chovan et al., 2007, Chen et al., 1997). Padgham and Paine (1993) demonstrated that among a group of CYPs, CYP2C11 decreased by 50% after isolation, in comparison to a 2-3 fold increase in other CYPs investigated, CYP1A1, 2B1/2, 3A1/2 and 4A1. Androstenedione formation involves CYP2C11, CYP2B1, CYP2B2 and a cytosolic steroid dehydrogenase (Swales et al., 1996). The reduction in the formation of testosterone metabolites can be correlated to the decline in Phase I metabolic function of primary rat hepatocytes in culture.

The aim of the chapter is to develop and characterise an in vitro model of primary rat hepatocytes, and to determine if IGFBP-5, the potential biomarker of interest, is present or upregulated with time in culture.

3.2 Methods

3.2.1 Development and optimisation of the in vitro culture system

A range of plastics were investigated to see if they caused any differences when culturing primary rat hepatocytes on them (Iwaki® 24 and 96 well tissue culture plates, Sterilin, UK; TPP 96 well tissue culture treated plates, Switzerland; Greiner bio-one Cellstar® 24 and 96 well tissue culture plates, Belgium; Costar® 96 well tissue culture treated plates, BD Falcon™ 24 and 96 well tissue culture treated plates, BD Biosciences, UK).

The effects of collagen vs. no collagen coating were investigated along with different cell attachment times (2, 4 and 24 h).

Parameters being investigated:

- Various tissue culture plastics (Iwaki, Sterilin, TPP, Greiner bio-one Cellstar, Costar and BD Falcon)
- Collagen source (commercially sourced and in-house prepared)
- Attachment times (2, 4 and 24 h)
- Medium volume (0.5, 0.7 and 1.0 ml)

For all experiments, cells were seeded on rat tail tendon collagen (30 µg/cm^2). Collagen (in-house prepared unless otherwise stated) was diluted in sterile distilled water (dH_2O) to the desired concentration (see Table 3.1). Collagen was allowed to dry overnight. Wells were then washed once with dPBS and were then ready for seeding. Cells were seeded on coated plates (BD Falcon™ 24 and 96 well tissue culture treated plates, BD Biosciences, UK, unless otherwise stated) in 1.0 ml or 200 µl medium, respectively (Williams' E medium (Life Technologies, UK) containing 5 % v/v foetal calf serum (FCS), L-glutamine (2 mM), penicillin G (50 units/ml), streptomycin sulphate (50 µg/ml) and fungizone (250 µg/ml)) respectively for 4 h (unless otherwise stated) to allow for attachment in a humidified atmosphere of 5 %

CO_2 in air at 37 °C. After 4 h, the medium was removed, cells were washed with Dulbeccos' phosphate buffered saline (dPBS) (2x) and medium was replaced for a total of 24 and 48 h, unless otherwise stated. MTT and NR (Borenfreund and Puerner, 1985) were used to assess viability.

Culture plastic	**Collagen coating**	**Coating volume of dH_2O**
96-well plate	9.6 µg	150 µl
24-well plate	60 µg	25 µl
60 mm petri dish	625 µg	1.5 ml

Table 3-1 Collagen coating of various tissue culture plastics

Different sources and batches of collagen were investigated to determine any adverse effects on viability. Commercially sourced collagen was assessed in comparison with in-house prepared rat tail tendon collagen. Devro Medicals' (Glasgow, UK) Apcoll pepsin-solubilised collagen or Apcoll acid-solubilised collagen and 4 different batches of in-house prepared rat tail collagen were used for culture of primary rat hepatocytes. Cells were seeded at 3 x 10^6 cells per 60 mm dish in 2 ml medium for 4 h. After 4 h plates were washed once with serum free complete medium and replaced with fresh medium. Medium was changed at 24 h. At 48 h medium was removed, plates were washed with dPBS (2x) and cells were fixed with 10 % buffered formalin.

Varying attachment times (2, 4 and 24 h) were investigated to determine their effects on cell attachment times. Attachment times refer to the period of time for which the freshly seeded hepatocytes were left to adhere to the culture surface prior to the first medium change. At this point the unattached cells were removed from the plate.

Varying medium volume on a 24 well plate (0.5, 0.7 and 1.0 ml) was also investigated.

3.2.2 Cell staining and Microscopic Evaluation of Viability

The cells were stained with acridine orange (100 µg/ml in PBS). Live cells are stained by cell-permeable acridine orange, which has an emission maximum at 525 nm (green). Analysis was performed using a Zeiss AxioImager ZI microscope with 20x/0.5 PH2 water lens by Mrs Elizabeth Goldie.

3.2.3 Seeding of cells and preparation of samples for monitoring dedifferentiation

60 mm petri dishes (BD Falcon™, BD Biosciences, UK) were collagen coated (30 µg/cm^2) and seeded with primary rat hepatocytes at a density of 1.5 x 10^5 cells/cm^2 in 2 ml of medium (Williams' E containing 5 % v/v Foetal Calf Serum (FCS), L-glutamine (2 mM), penicillin G (50 units/ml), streptomycin sulphate (50 µg/ml) and fungizone (250 µg/ml)). Plates were incubated at 37 °C for 2 h after which time medium was removed. All plates were washed twice with Dulbecco's PBS (Lonza, Switzerland). Medium was replaced (3 ml) and plates were incubated up to 3, 6 and 9 days at 37 °C. Plates incubated up to 3 and 6 days did not have a medium change to allow for the accumulation of secreted proteins and the measurement of IGFBP-5. Plates incubated up to 9 days had a medium change at 3 and 6 days in culture. Medium that was removed was stored in Eppendorfs, centrifuged at 1000 rpm and placed at -70 °C awaiting analysis for IGFBP-5 secretion. Cells were homogenised in a 5 ml homogenisation tube in 7 up and down strokes of a motor driven homogeniser.

3.2.4 Immunoblotting for GSTP1

See Chapter 2 Section 2. The primary antibody (GSTP1, subunit Y_f) was diluted 1/10000 in 1 % v/v gelatin in TTBS. The secondary antibody (anti-rabbit IgG) was diluted 1/10000 in 1 % v/v gelatine in TTBS. No housekeeping protein was run as expression over 9 days was unlikely to be constant.

3.2.5 Testosterone Hydroxylation

A stock solution of 200 mM testosterone was prepared in methanol and stored at 4 °C. At each time point, medium was removed from each Petri dish containing a monolayer of primary rat hepatocytes. The monolayers of cells were washed 2 x with 5 ml Hank's II buffer. A working solution of testosterone (100 µM) was prepared in Hank's II buffer and 6 ml was added to each Petri dish. They were then incubated at 37 °C for 60 min. To stop the reaction, the Petri dishes were placed on ice, the solution was removed and immediately placed at -70 °C awaiting further analysis.

3.2.6 Analysis of testosterone hydroxylation by HPLC

A stock solution (2 mM) of testosterone and its metabolites was prepared in methanol. The stock solution was diluted in 30 % methanol to give 20 and 200 µM mixtures. All stock solutions were stored at 4 °C. Prior to analysis, standards containing 0.25, 0.5, 1, 2.5, 5, 10 and 20 nmol of testosterone and its metabolites were prepared using the 20 and 200 µM stock solutions. 50 µl of internal standard (11α-hydroxyprogesterone; 20 mg/ml in methanol) was added to each standard and made up to 150 µl. Standards were vortexed for 30 s and placed in HPLC vials.

Thawed samples (3 ml) were transferred into polypropylene centrifuge tubes, 50 µl of the internal standard was added prior to extraction in 6 ml dichloromethane. Samples were vortexed for 1 min and then centrifuged for 10 min at 2000 g. The top aqueous layer was transferred to a clean polypropylene centrifuge tube and extraction was carried out again in 3 ml dichloromethane. Samples were vortexed for 1 min and centrifuged for 10 min at 2000g. The top aqueous layers were then discarded and both organic layer containing testosterone and its metabolites were combined and washed with 3 ml of 0.02 M NaOH. Samples were vortexed and centrifuged again, and the aqueous layer discarded. The washing step was repeated with distilled water (3ml). The aqueous layer was removed and the remaining organic phase was placed in Gyrovap (rotary evaporation system) at 65 °C to evaporate the solvent. Samples were then stored at -20 °C awaiting analysis.

The samples were reconstituted in 150 µl filtered methanol (30 %), vortexed for 30 s and placed in HPLC vials.

Standards and samples (10 µl) were injected onto an Eclipse XD8-C18 (3 µm particle size; 3 x 100 mm i.d.) column and the analytes resolved. The mobile phase, consisting of distilled water (solvent A), methanol (solvent B) and acetonitrile (solvent C) was delivered at a flow rate of 0.4 ml/min using the following gradient conditions (see Table 3.2)

Time (min)	**Solvent A/Solvent B/Solvent C (% v/v/v)**
0	65/34.6/0.4 %v/v/v
18.5	54.8/44.4/0.8 %v/v/v
25	47/51.9/1.1 %v/v/v
38	30/68.5/1.5 % v/v/v
39	65/34.6/0.4 % v/v/v
42	65/34.6/0.4 % v/v/v

Table 3-2 Gradient conditions used in HPLC

3.3 Results

3.3.1 Development and optimisation of in vitro culture system

3.3.1.1 The effects of various collagen substrata on the morphology of cultured primary rat hepatocytes in vitro

Primary rat hepatocytes cultured on various sources of collagen, including in-house prepared collagen and commercially available (Devro Medical, UK) collagen, was used to determine a suitable substratum. Hepatocytes cultured on each substratum displayed similar morphology. Each image in Figure 3.1 displays a good monolayer of hepatocytes with intact membranes and also exhibited some hepatocytes containing 2 nuclei. Different collagens were assessed via microscopy in this experiment, as different substratum could have an impact on cell morphology.

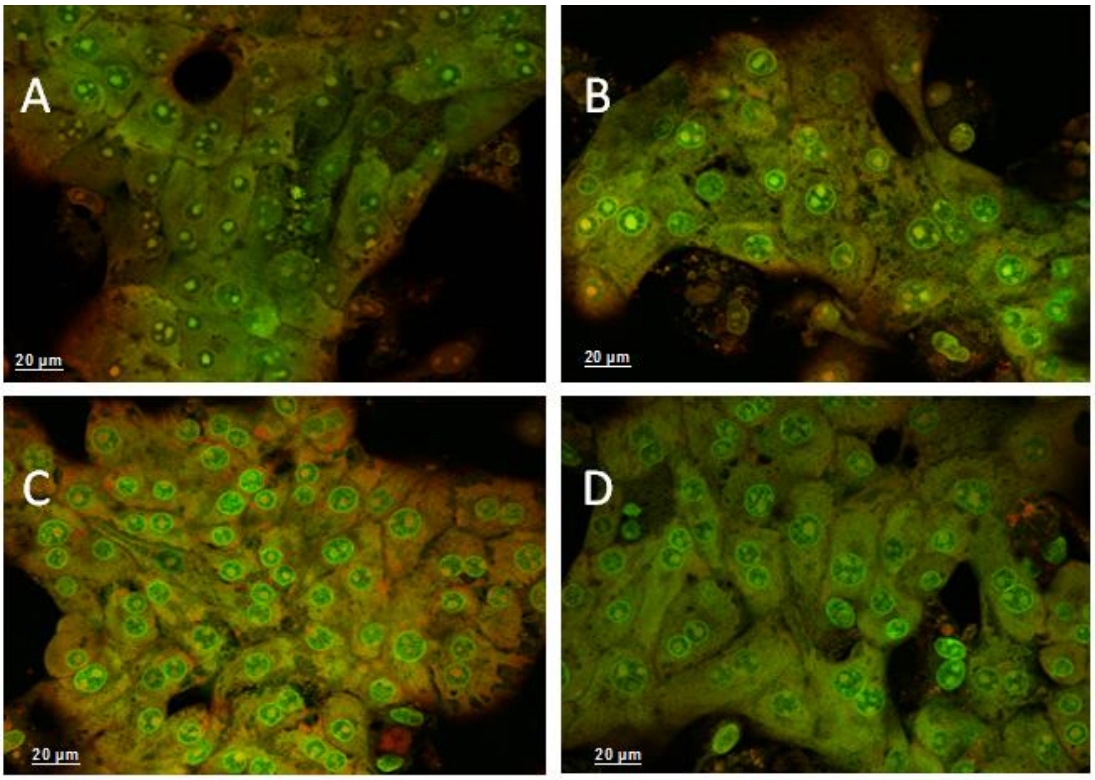

Figure 3-1 Microscopy images of primary rat hepatocytes on various collagens.

Images include some commercially available collagen after 48 hr in culture (A = Devro Apcoll acid soluble collagen; B = Devro Apcoll pepsin soluble collagen; C = Rat tail collagen; D = Rat tail collagen) stained with Acridine orange (green). Analysis was performed using a Zeiss AxioImager ZI microscope with 20x water lens.

3.3.1.2 The effects of various plastic culture dishes on cultured primary rat hepatocytes in vitro

Figure 3.2 and 3.3 show MTT assay results after culturing primary rat hepatocytes on tissue culture plastics (24- and 96-well plates) from various companies. There was no statistical difference between the MTT reduction values of cells cultured on any of the plastics. To aid with adherence of hepatocytes, tissue culture plastics must be coated with ECM such as collagen. To investigate the effects of various plastics, they must also be coated with collagen. Higher MTT absorbance values were observed in 24-well plate cultures in comparison with 96-well plate cultures.

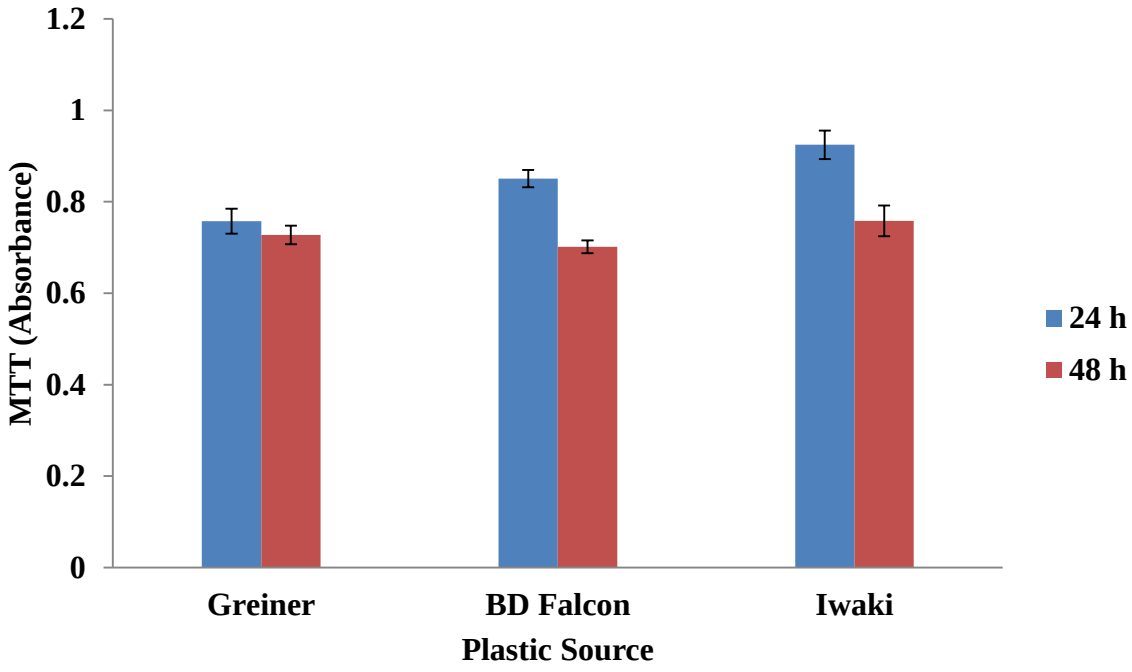

Figure 3-2 MTT assay results and different plastic sources.

Primary rat hepatocytes cultured on collagen (in-house prepared) coated 24 well plates from various sources after 24 and 48 h in culture.Results are Mean ± SEM, n = 3. No statistical difference was observed by ANOVA followed by Fischer's individual error rate

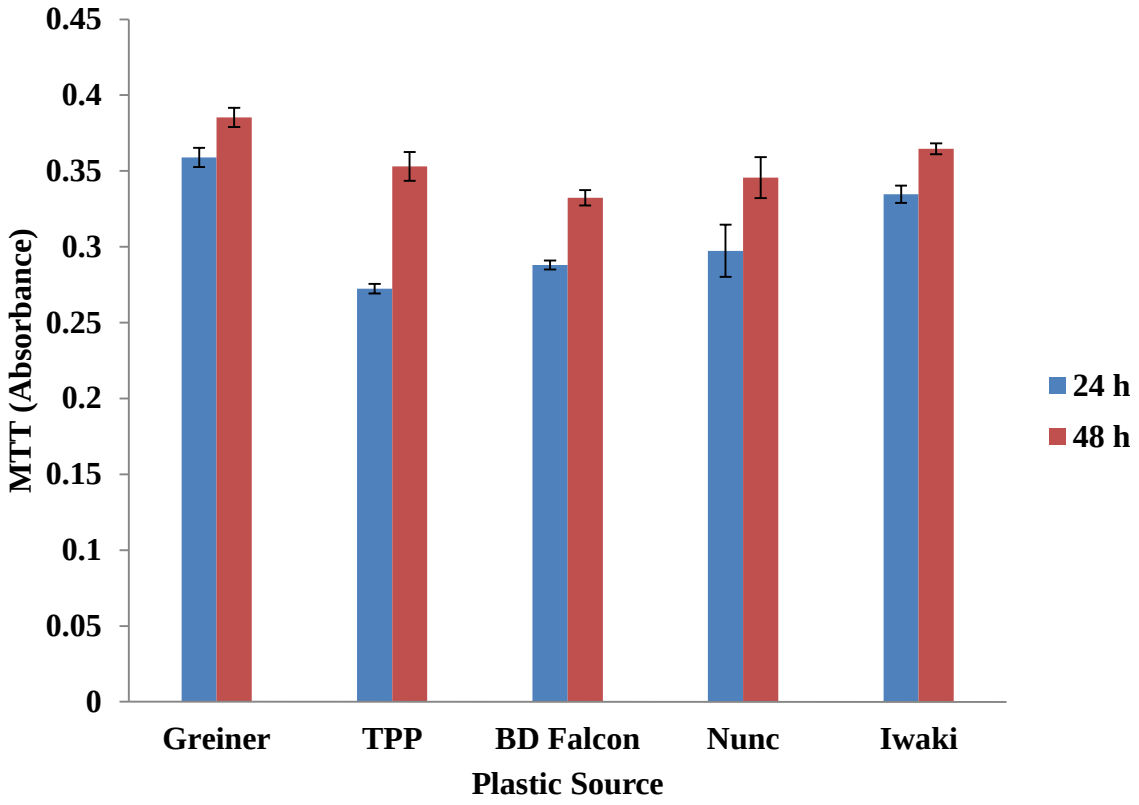

Figure 3-3 MTT assay results and different plastic sources.

Primary rat hepatocytes cultured on collagen coated 96 well plates after 24 and 48 h in culture. Results are Mean ± SEM, n = 3. No statistical difference was observed by ANOVA followed by Fischer's individual error rate

3.3.1.3 The effects of changing medium volume on culturing primary rat hepatocytes in vitro.

The effects of changing medium volume were investigated to determine an optimum depth in a 24-well plate. No statistical difference was observed with a NR assay (see Figure 3.5) when comparing medium depths within a time point (24 and 48 h). However, MTT assay resulted in a statistically ($p \leq 0.05$; significantly different ANOVA followed by Fischer's individual error rate) higher absorbance with a medium depth of 0.5 ml at 24 and 48 h (see Figure 3.4).

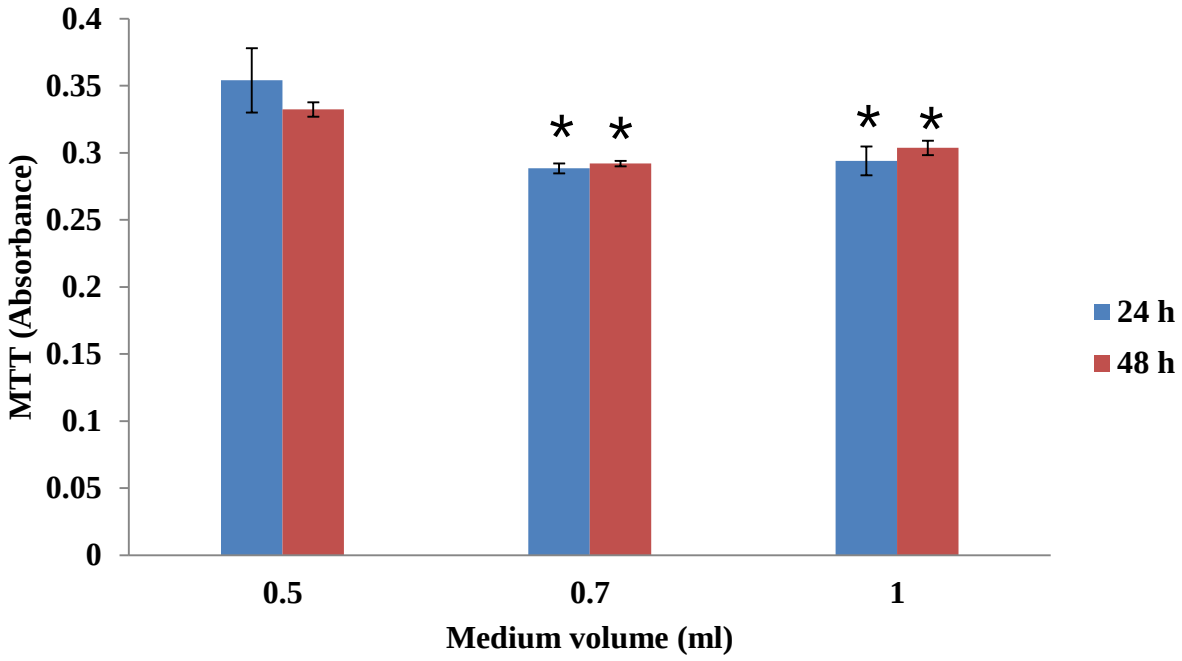

*Figure 3-4 MTT assay results with various medium volumes. Primary rat hepatocytes cultured on collagen (in-house prepared) coated 24 well plates with various volumes of medium after 24 and 48 h in culture. Results are Mean ± SEM, n = 3. * $p \leq 0.05$ significantly different (ANOVA followed by Fischer's individual error rate) in comparison to 0.5 ml medium.*

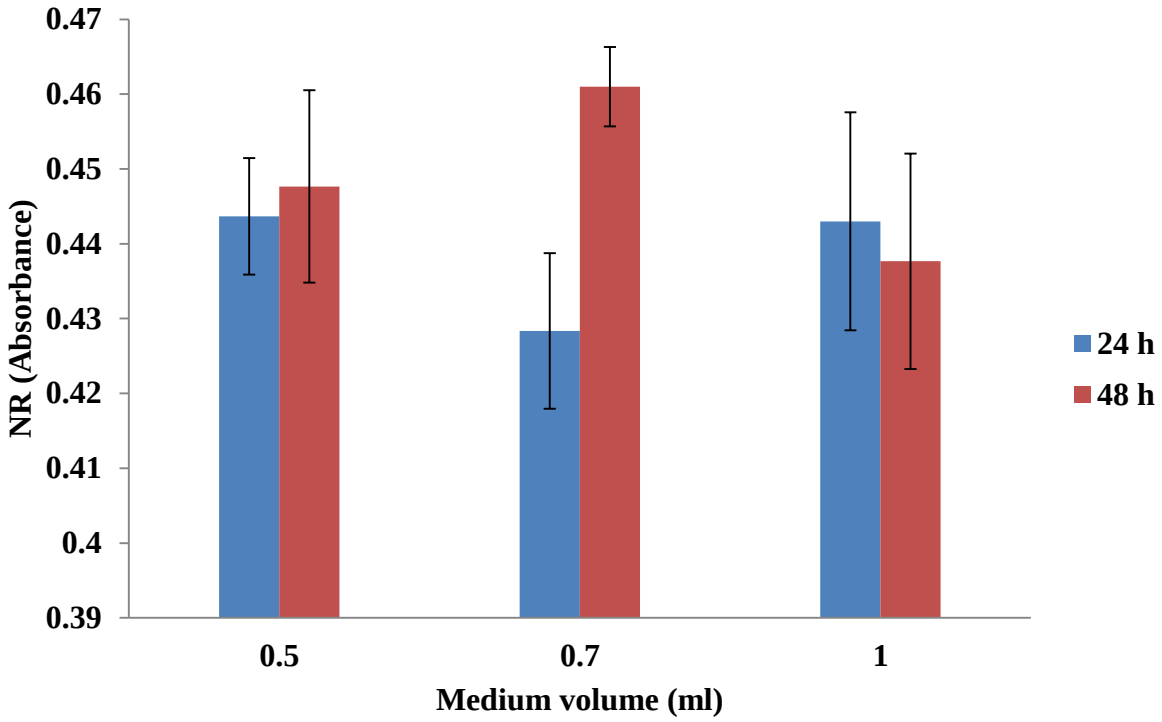

Figure 3-5 NR assay results and various medium volumes. Primary rat hepatocytes cultured on collagen (in-house prepared) coated 24 well plates with various depths of medium after 24 and 48 h in culture. Results are Mean ± SEM, n = 3. No statistical difference was observed by ANOVA followed by Fischer's individual error rate.

3.3.1.3 The effects of changing attachment time on culturing primary rat hepatocytes in vitro.

After freshly seeding plates with primary rat hepatocytes, cells are left for a period of time which is referred to here as attachment time. During this time the hepatocytes were left to adhere to the culture surface prior to the first medium change. Varying the attachment time on a 24 well plate demonstrated that a 24 h attachment time was not an optimum time for the cells, shown in Figure 3.6 with a significantly lower absorbance with MTT assay at both 24 and 48 h and with NR assay at 24 h (see Figure 3.7).

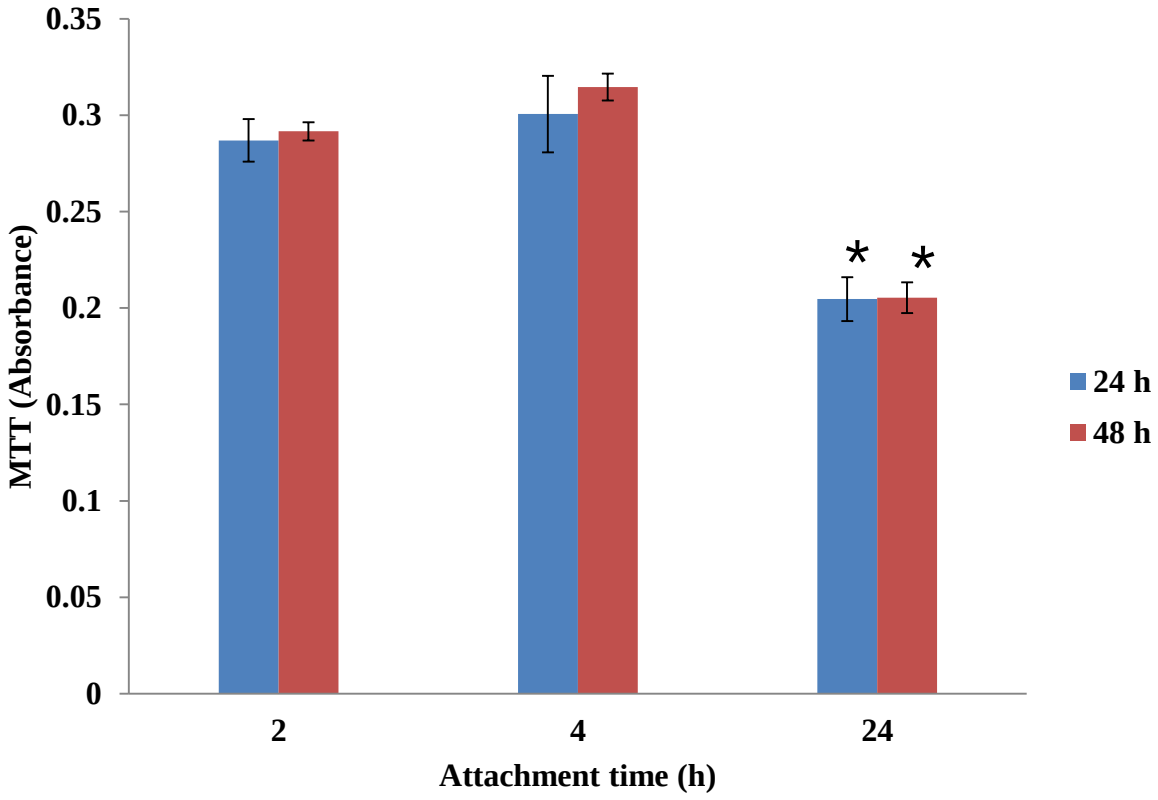

*Figure 3-6 MTT assay results and various attachment times. Primary rat hepatocytes cultured on collagen (in-house prepared) coated 24 well plates with various attachment times (h) after 24 and 48 h in culture. Results are Mean ± SEM, n = 3. * $p \leq 0.05$ significantly different (ANOVA followed by Fischer's individual error rate) in comparison with 4 h attachment time.*

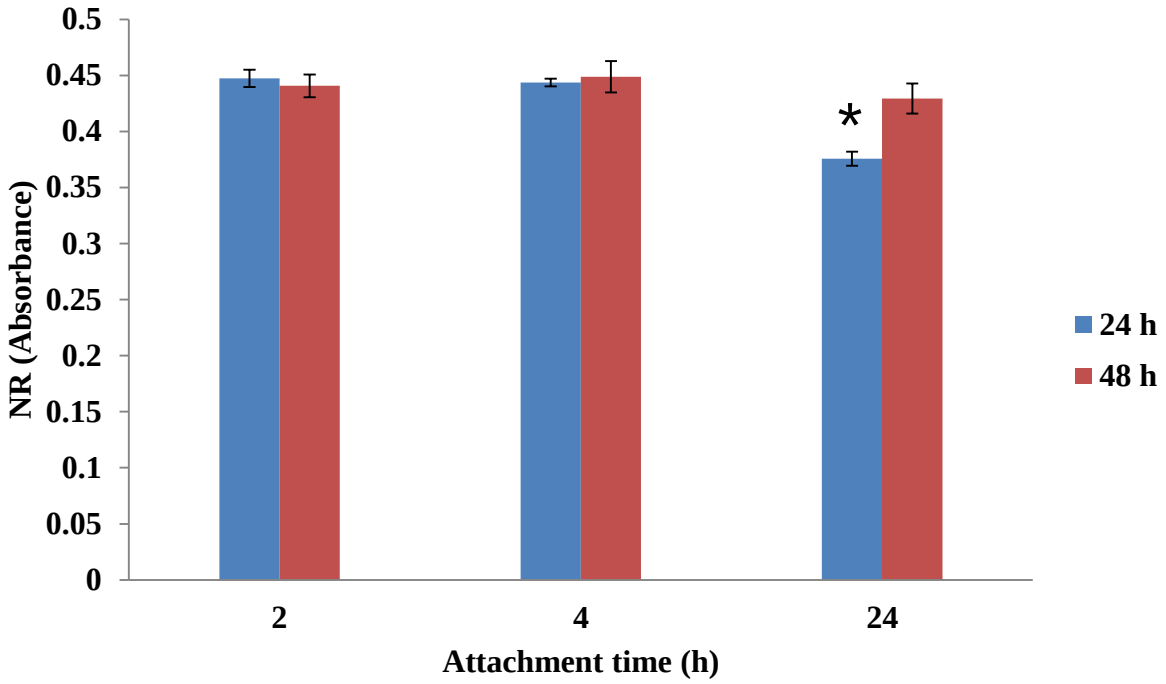

*Figure 3-7 NR assay results and various attachment times. Primary rat hepatocytes cultured on collagen (in-house prepared) coated 24 well plates with various attachment times (h) after 24 and 48 h in culture. Results are Mean ± SEM, n = 3. * $p \leq 0.05$ significantly different (ANOVA followed by Fischer's individual error rate) in comparison with 4 h attachment time.*

On 96 well plates, the effects of varying attachment times were not as obvious when compared with the results from medium depth. The results from an MTT assay demonstrated that the absorbance was significantly higher at 48 hr with 4 and 24 h attachment (see Figure 3.8). However, there was no significant difference when NR assay was carried out at 24 and 48 h (see Figure 3.9).

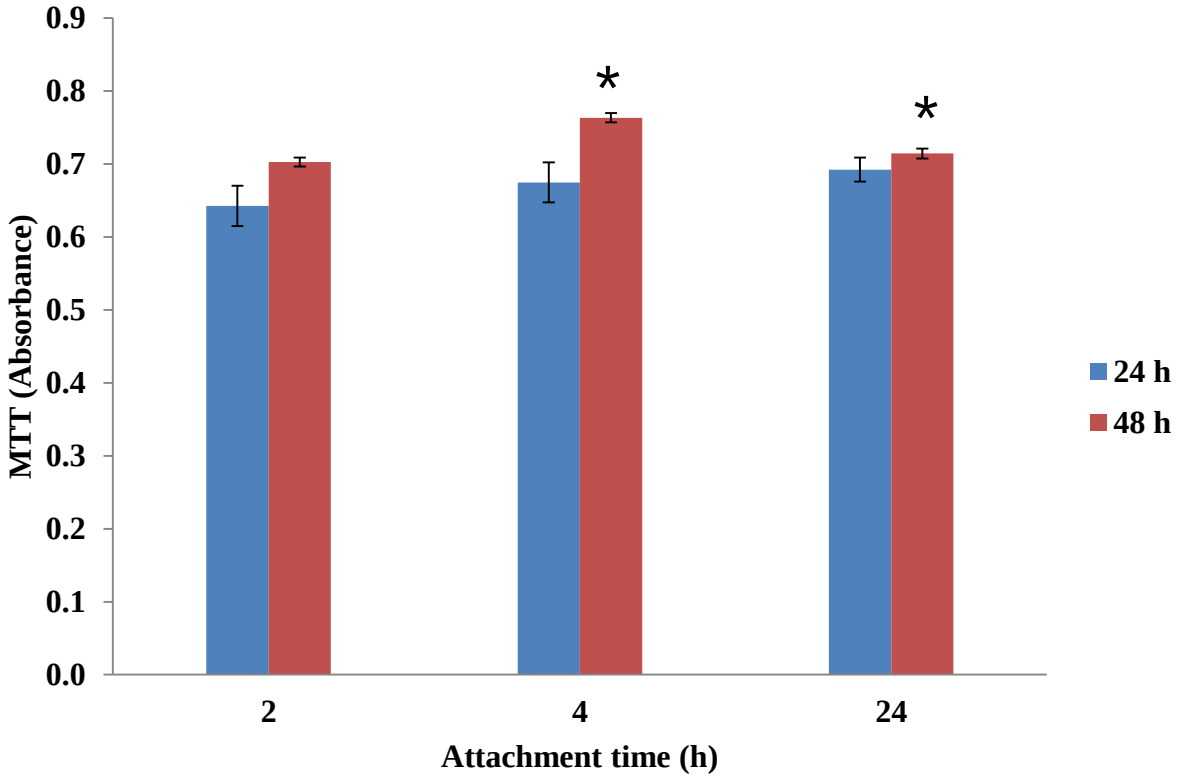

*Figure 3-8 MTT assay results and various attachment times. Primary rat hepatocytes cultured on collagen (in-house prepared) coated 96 well plates with various attachment times (h) after 24 and 48 h of total culture time. Results are Mean ± SEM, n = 3. * $p \leq 0.05$ significantly different from 2 h. (ANOVA followed by Fischer's individual error rate) in comparison with 4 h attachment time.*

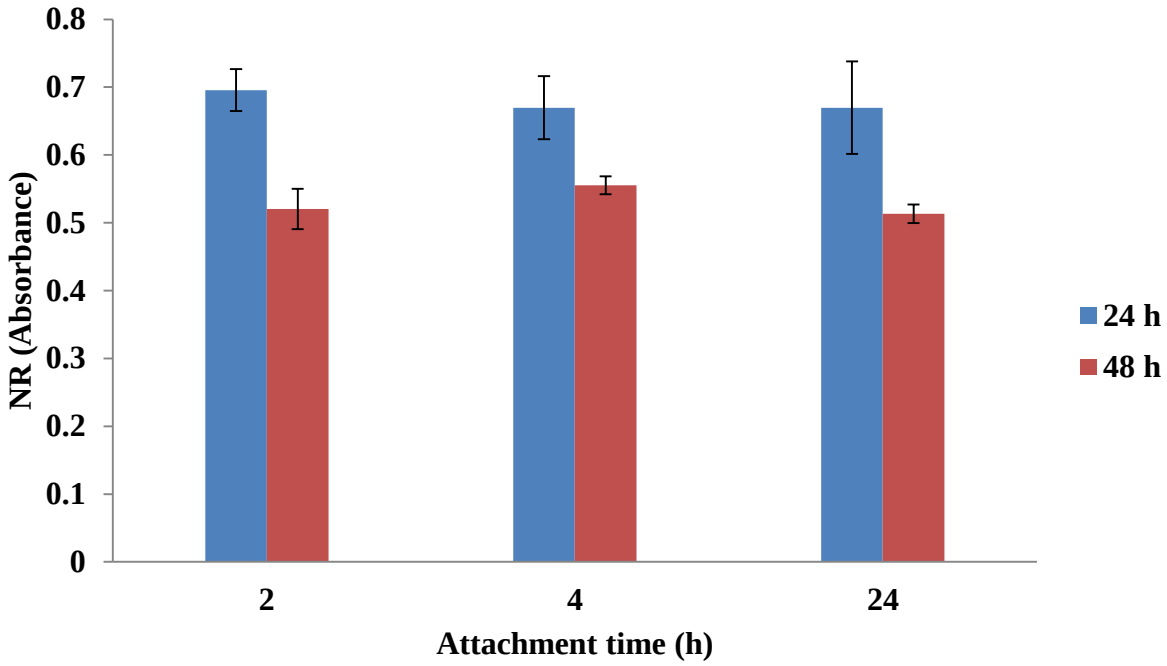

Figure 3-9 NR assay results and various attachment times. Primary rat hepatocytes cultured on collagen (in-house prepared) coated 96 well plates with various attachment times (h) after 24 and 48 h of total culture time. Results are Mean ± SEM, n = 3. No statistical difference was observed in comparison with 4 h attachment time.

3.3.2 GSTP1 expression

Figure 3.10 shows the GSTP1 expression by primary rat hepatocytes over 9 days in culture as measured by immunoblotting and subsequent densitometry. At 1 day the level of GSTP1 present is very low (53.37 ± 23.26). There is a significant increase in GSTP1 at day 2 and these day 2 levels increase also at day 3 and remain high at day 9 in comparison with day 1.

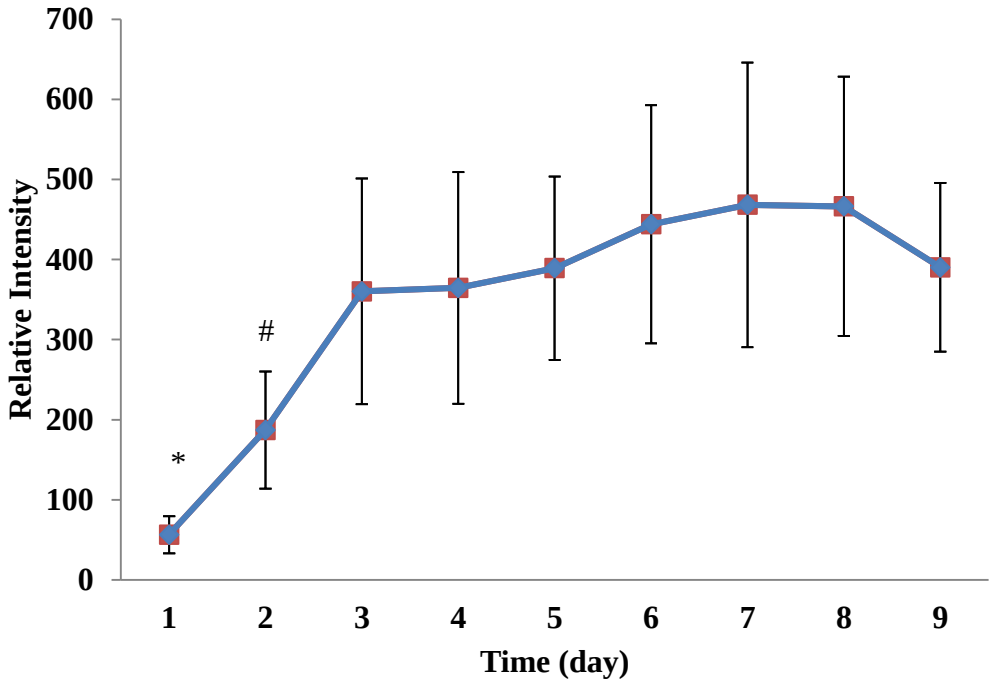

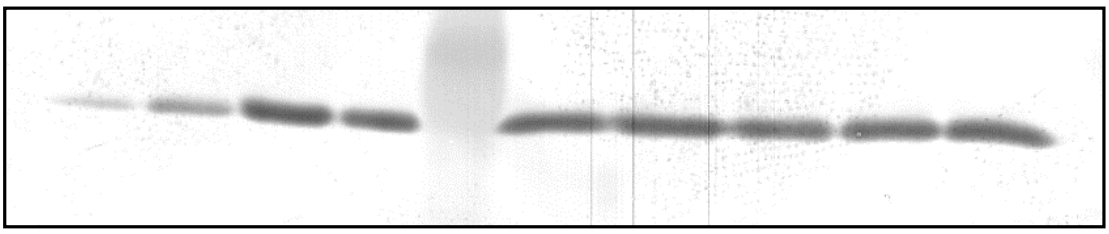

Day 1 Day 2 Day 3 Day 4 Marker Day 5 Day 6 Day 7 Day 8 Day 9

Figure 3-10 Typical immunoblot for GSTP1

*GSTP1 expression by immunoblotting of primary rat hepatocytes cultured on collagen (in-house prepared) films over 9 days. Cells were harvested, total protein content was measured and 10 µg protein was added to each lane. Results are Mean ± SEM, n = 3 separate experiments * $p \leq 0.05$ significantly different from day 2 to day 9, # $p \leq 0.05$ significantly different from day 6, 7 and 8 (ANOVA followed by Fischer's individual error rate)*

3.3.3 Testosterone hydroxylation in cultured primary rat hepatocytes

Testosterone in Hank II buffer was incubated with cultures of primary rat hepatocytes that had been in culture for up to 9 days. The testosterone was left on the samples for an hour after which time the testosterone and its metabolites were extracted in dichloromethane. Figure 3.11 shows the levels of testosterone metabolites formed by the cells from 1 to 9 day cultures. After 5 days in culture the levels of metabolites were below the limit of detection (LOD).

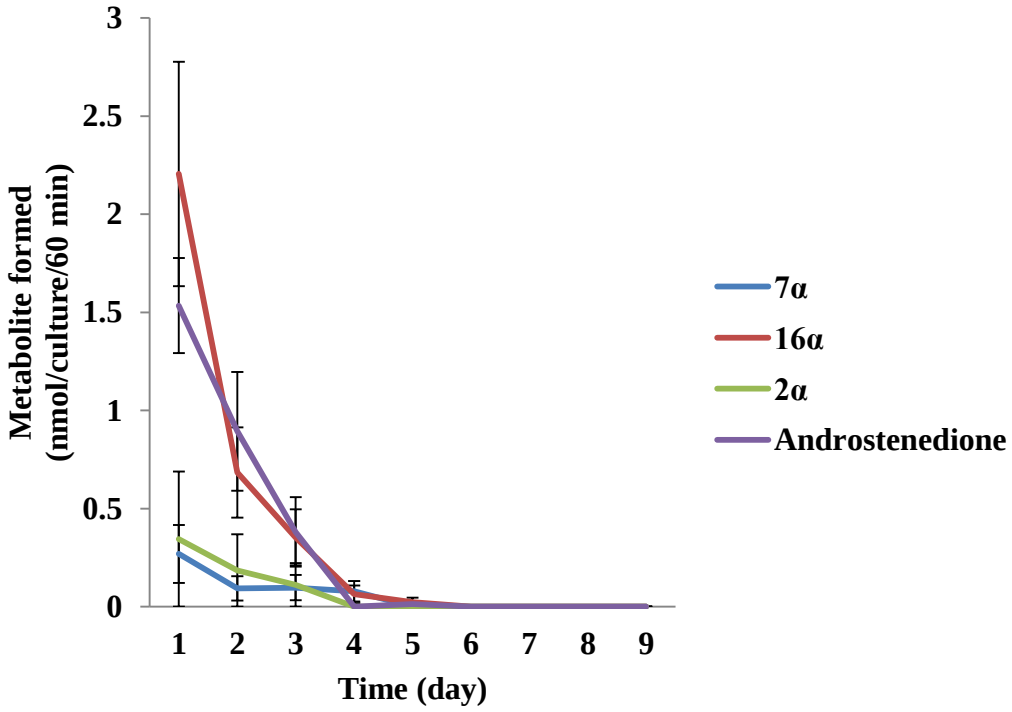

Figure 3-11 Formation of testosterone metabolites by primary rat hepatocytes.

Primary rat hepatocytes cultured on collagen (in-house prepared) films over a 9 day period. Formation of 7α, 16 α and 2 α hydroxytestosterone is indicative of CYP2A, CYP2C and CYP2C11 respectively. Results are mean ± SEM, n = 3 separate experiments

After extraction on dichloromethane the % recovery of testosterone was 75.65 ± 2.01 (mean ± SEM). Figure 3.12 shows the remaining testosterone after 60 min incubation with primary rat hepatocytes.

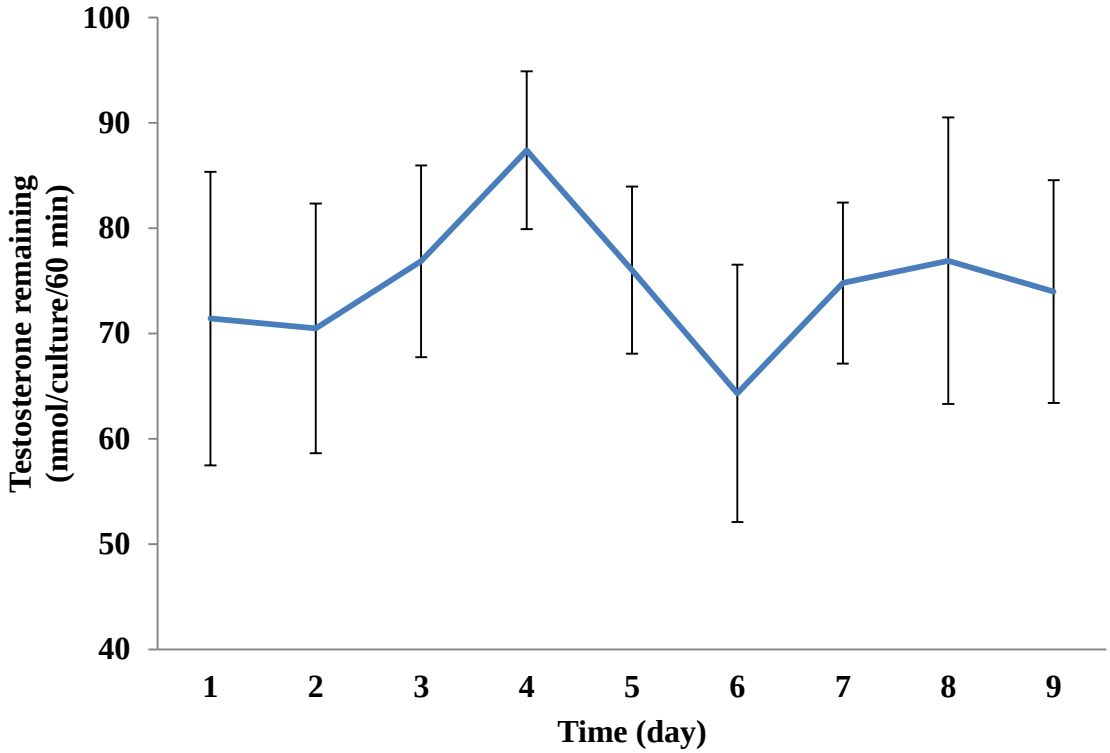

Figure 3-12 Testosterone remaining after 60 min incubation. Primary rat hepatocytes in culture on collagen films over a 9 day period. Results are mean ± SEM, n = 3 separate experiments

3.3.4 IGFBP-5 secretion in cultured primary rat hepatocytes

The IGFBP-5 release was measured from the conditioned medium taken from the cells over a 9 day period (see Figure 3.13). The levels of IGFBP-5 increased with time in culture. There was a medium change at 3 and 6 days, hence levels of IGFBP-5 are accumulating in the media for up to 3 days at a time. The levels of IGFBP-5 released are highest between 6 and 9 days in comparison with 0 and 3 days indicating that IGFBP-5 release increased as the cells aged in culture. Large error bars may be due to intra-culture variation in IGFBP-5 release. Hence, IGFBP-5 in culture medium at Day 6, 8 and 9 is only significantly higher than Day 1, despite the upward trend in IGFBP-5 release over time.

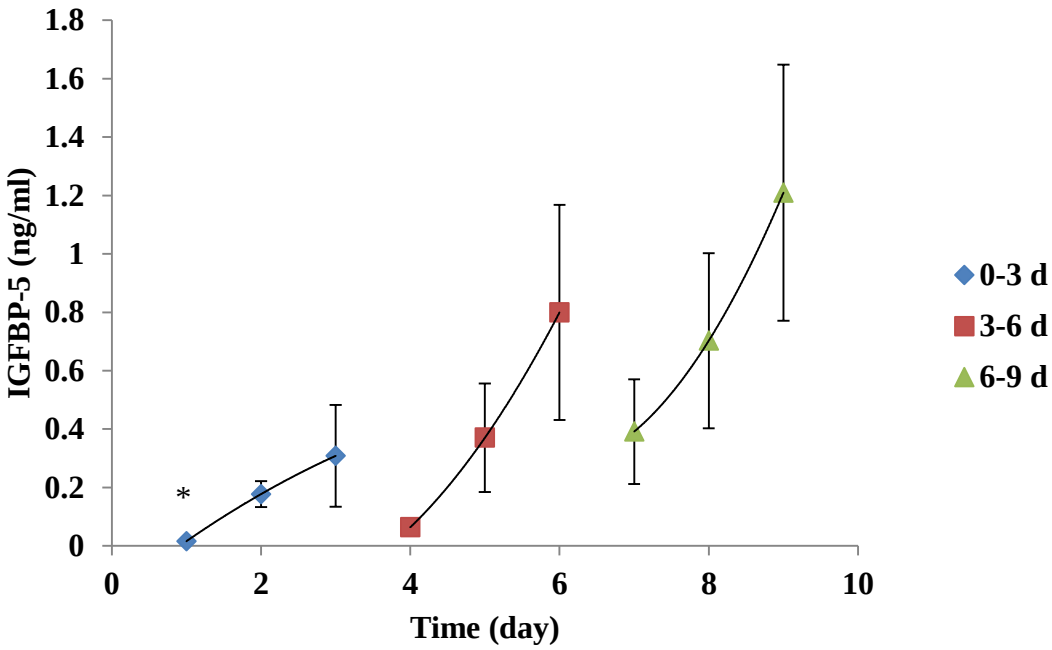

Figure 3-13 IGFBP-5 release over a 9 day culture.
*Primary rat hepatocytes on collagen (in-house prepared) films in culture over 9 days. Results are Mean ± SEM, n = 3 separate experiments * $p \leq 0.05$ significantly different from day 6, 8 and 9 (ANOVA followed by Fischer's individual error rate).*

3.4 Discussion

This chapter involved the optimisation of the in vitro model. Medium depth, cellular substratum and attachment times were all investigated. Several sources of collagen were used to determine any differences in the morphology of the cells cultured on them.

In this chapter, results on hydroxylation of testosterone and GSTP1 expression in primary rat hepatocytes in culture on collagen films over a period of 9 days demonstrated that the levels of GSTP1 expression significantly increased whereas the levels of testosterone metabolites formed significantly decreased. Along with this the levels of IGFBP-5 released into the medium during the 9 day period increased indicating that it could be a possible marker of dedifferentiation of primary rat hepatocytes.

Testosterone was used to monitor the levels of CYP isoenzymes present as the hepatocytes aged in culture. There are many reported metabolites of testosterone. Formation of 7α-, 6β-, 16α- and 2α- hydroxytestosterone is indicative of CYP2A, CYP3A4, CYP2C11 and CYP2C11 activity in the rat, respectively (Wortelboer et al., 1990). CYP2C11 is the major CYP isoenzyme in the male rat liver representing approximately 50 % of the total spectrally determined CYP. As discussed in 2.1.2 the expression of CYP2C11, a male specific ioenzyme is rapidly lost in culture. This is reflected in the decrease of 2α- and 16-α hydroxytestosterone observed in the present study. Androstenedione formation involves CYP2C11, CYP2B1, CYP2B2 and a cytosolic steroid dehydrogenase (Swales et al., 1996). In the experiments above, the hydroxylation of testosterone resulted in the detection of 2α-, 7α- and 16α-hydroxytestosterone and androstenedione. The formation of 6β- hydroxytestosterone was not detected in these experiments indicating the lack of CYP3A4 activity in non-induced primary rat hepatocytes cultured on collagen films. Levels of metabolites decreased as cells aged in culture. After 5 days in culture the levels of metabolites being formed were undetectable. It has been widely reported that the maintenance of differentiated status of hepatocytes in culture is dependent on a complex environment in which factors such as cell matrix and cell to cell interactions play a pivotal role. Some changes in the plating of the cells and the configuration can prevent this rapid

reduction in CYP activity. Sandwich cultures of primary rat hepatocytes have been reported to have relatively stable expression of CYP isoenzyme expression e.g. CYP1A1, CYP1A2 and CYP2B1 (Kern et al., 1997). Although sandwich cultures offer maintenance of CYP activity for longer in in vitro cultures of primary hepatocytes, they also present many issues. Matrigel derived from Engelbroth-Holm-Swarm mouse sarcoma rich in ECM protein is currently a widely used matrix used for sandwich cultures. Matrigel is an undefined matrix, with undisclosed components. The matrix not only contains structural proteins, but also growth factors and hormones. Diffusion of macromolecules may also be an issue, with medium components being excluded. Batch-to-batch variation should also be considered when designing and analysing experiments.

The results in section 3.3.2 showed that Phase II Glutathione S-transferase (GST) activity increased upon isolation and culture of primary rat hepatocytes in vitro. GSTA and GSTM are abundant in normal rat liver unlike GSTP1. The total GST activity after isolation has been shown to be reduced by 50% after 24 h in culture in comparison to levels in freshly isolated hepatocytes (Daniel, 1993). GSTP1 is not present in normal rat liver in vivo or in freshly isolated cells; however, expression is induced within 24 h in culture (Lockman et al., 2012). That was also shown to occur in the present experiments. GSTP1 expression was at 56.37 ± 23.26 OD just after 1 day in culture. The GSTP1 form has been shown to be most abundant in foetal liver but is almost absent postnatally (Tee et al., 1992). GSTP1 has been shown to have a specific developmental pattern in the foetal liver and is abundant in an 18 day old foetal liver. However, it has been shown that GSTP1 is only present in an adult liver during de-differentiation associated for example with hepatocarcinogenesis (Tee et al., 1992) . It has been suggested that GSTP1 expression in primary cultures could be attributed to hormones and growth factors present in the serum with which medium is often supplemented (Hatayama et al., 1991) . In the experiments carried out in this thesis the levels of GSTP1 detected were very low at 1 day which corresponds with previous published work (Lockman et al., 2012). An increase with time in culture was seen after 1 day in culture with a significant rise in GSTP1 expression to 187. 12 ± 73.09 OD at day 2 and 360.31 ± 140.82 OD at day 3 ($p \leq 0.05$).

An ELISA was carried out to correlate the IGFBP-5 release from cells into medium with the age of the primary rat hepatocytes in culture. The levels of IGFBP-5 secreted into media increased along with the reduction in testosterone metabolites formed and the increase in GSTP1 expression. The levels of IGFBP-5 secreted into the medium were low initially but increased as the hepatocytes aged in culture and lost function. The levels at day 1 were 0.01 ± 0.008 ng/ml and increased significantly to 1.2 ± 0.43 ng/ml. IGFBP-5 was not measured in the cells with time in culture. This would have highlighted if mRNA levels were changing within the cells resulting in the increase in release into the cell culture medium.

This would suggest that IGFBP-5 is a potential marker of de-differentiation. It has been suggested that the Insulin-like growth factor (IGF-1) axis is involved in aging. Longo and Firth (2003) have suggested some drug treatments for the treatment of some age related diseases and have targeted the IGF-axis and in particular the release of IGF-1 from the liver. IGFBP-5 has also been shown to be involved in cellular senescence. In this context Kim et al (2008) showed that in IGFBP-5 knockout human umbilical endothelial cells a reduction in some senescent phenotypes such as cell proliferation and β-galactosidase staining were observed

Chapter 4 In vitro 9 day chronic oxidative stress model

4.1 Introduction

Excessive oxidative stress can cause cell death via apoptosis and necrosis. There are many inducers of oxidative stress including reactive oxygen species (superoxide radical, hydroxyl radical and hydrogen peroxide), metals (iron, cadmium and mercuric chloride), pathological conditions (hyperglycaemia, Alzheimer's and Parkinson's disease) and drugs (cisplatin, taxol and antimycin D).

4.1.1 Menadione (2-methyl-1,4-napthoquinone) and Hydrogen Peroxide Toxicity

Menadione (vitamin K_3) is a synthetic analogue of vitamin K (for structure see figure 4.1). It is a member of a large group of quinone compounds found in the diet and occurring naturally in the environment. It can undergo either one electron reduction to a semiquinone radical or two electron reduction to a more stable hydroquinone (Thor et al., 1982). Most semiquinone radicals rapidly enter a redox cycle resulting in the formation of reactive oxygen species (ROS) such as superoxide anion, hydrogen peroxide and hydroxyl radical. Menadione has been widely used as a model of oxidative stress for several cell models. Badr et al. (1989) demonstrated that menadione causes zone specific hepatotoxicity. Perfusion of rat livers with high concentrations of menadione increased the oxygen tension exclusively in the periportal region of the liver indicating that redox cycling of menadione occurred in this region. Perfusions with high concentrations of menadione (1 mM) also led to time dependent LDH release and positive Trypan Blue staining in the periportal region (Badr et al., 1989), indicating a toxic response. In validating a newly formed immortalised cell line, Anderson et al (1996) studied a range of concentrations of menadione on numerous markers of hepatic cell health. Concentrations $\geq$ 25 µM caused significant LDH leakage and GSH depletion in primary rat hepatocytes after 2 h exposure. In contrast to this, in suspension cultures 50 – 100 µM menadione did not cause a decrease in cell viability (Trypan Blue exclusion) (Di Monte et al., 1984). Concentrations above 200 µM did cause cell death and depletion of protein sulfhydryl groups indicating that perturbation of protein thiol homeostasis may represent a crucial step in the toxicity of menadione. For this to occur, complete depletion of GSH must have occurred, as

oxidation of protein sulfhydryl groups only takes places without GSH present. The treatment of hepatocytes with diethylmaleate to remove GSH, results in greater reduction in protein sulfhydryl groups and subsequent cell death. Di Monte et al (1984) have also demonstrated that at 50 µM menadione decreases in GSH content are evident, irreversible and dose-dependent.

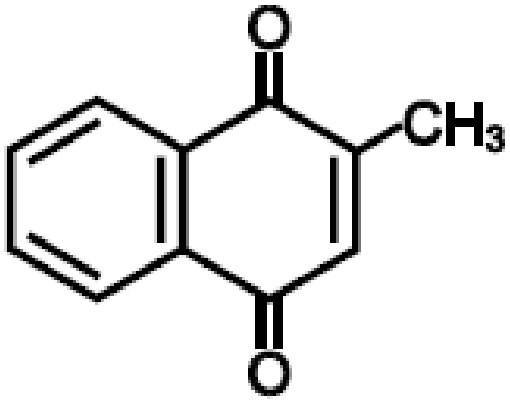

Figure 4-1 Chemical structure 2-methyl-1,4-naphthoquinone (Menadione).

Hydrogen peroxide (H_2O_2) is also a well-characterised toxin for the induction of oxidative stress in primary hepatocytes cultures. It is an endogenous ROS present at low levels in the mitochondria. H_2O_2 is present intracellularly at about 10 nM and in the liver it is generated at a rate of 50 nmol/min/gram of tissue equating to 2 % of total oxygen uptake at steady state (Sies, 2014). H_2O_2 is also formed as a result of metabolism, and can be implemented in redox signalling and oxidative stress when the balance of oxidants and antioxidants becomes imbalanced. Routine removal of ROS is carried out by antioxidant enzymes such as superoxide dismutase (SOD), catalase and glutathione peroxidase. SOD reduces superoxide radicals to H_2O_2 and glutathione peroxidase and catalase further reduce H_2O_2 to water. However, catalase is absent in

hepatocyte mitochondria. GSH also acts as an antioxidant defence towards H_2O_2, acting as a hydrogen donor to glutathione peroxidase in hepatocyte mitochondria, hence directly influencing its enzymatic function and antioxidant capacity (Wang et al., 2009, Kannan and Jain, 2000). Survival pathways, MAPK and NF-κB and activation of stress kinases e.g. c-Jun N-terminal kinases (JNK) (Iwakami et al., 2011) have also been described as having roles in attenuating oxidative stress (Conde de la Rosa et al., 2006). A study to compare the toxicities of menadione and H_2O_2, and their roles in progressing apoptosis or necrosis, also demonstrated the involvement of these cell survival pathways. Menadione, the superoxide anion donor caused increases in caspase-3 activity but H_2O_2 did not. In the same study, H_2O_2 concentrations of 2.5 mM and above caused necrotic cell death (increases in Sytox Green staining) (Conde de la Rosa et al., 2006). Menadione also caused a slight increase in necrotic cells death at 50 µM (Conde de la Rosa et al., 2006). In contradiction to this Han et al. (2006), demonstrated that concentrations as low as 100 µM H_2O_2 (generated through glucose oxidase dosing; 1 h exposure) caused necrosis in primary mouse hepatocyte cultures, and this was confirmed by bolus dosing of H_2O_2 at the same concentrations (5 min exposure).

Utilising the optimised model of primary rat hepatocyte culture that was developed in Chapter 3, a range of low concentrations of menadione (Vitamin K_3) and hydrogen peroxide, two classic oxidative toxins, were investigated to determine their effects on primary rat hepatocytes. Menadione (Morrison et al., 1984, Sun et al., 1990, Ip et al., 2002) and H_2O_2 (Starke and Farber, 1985) have been widely used in models of oxidative stress on hepatocytes. Hence there is a wide general understanding of both these molecules and their effects on hepatocytes. Low concentrations of these toxins were used to show chronic toxic insult on hepatocytes over a long period of time, to try to mimic a situation of chronic toxic insult on the liver, characteristic of that resulting in liver fibrosis and subsequently cirrhosis and liver failure. On consideration of the literature described above, concentrations below 10 µM and 0.5 mM for menadione and H_2O_2 respectively were selected.

Toxicity was characterised using WST-1 and Crystal Violet (CV) assays as well as determining intracellular reduced Glutathione (GSH) concentrations. Several parameters were used to assay cell health post chronic dosing with menadione and H_2O_2 (see Table 4.1). MTT and WST-1 were used to measure the metabolic activity of cells. NR and CV bind to cellular lysosomes and DNA respectively, indicating cell numbers present in cultures. The assays determine changes in cell viability or cell number. GSH will show any subtle changes occurring within the cells due to toxicity, as it plays an integral role in cellular protection against drug induced toxicity. Conde de la Rosa (2006) demonstrated the role of GSH in menadione induced apoptosis, by adding buthionine sulfoximine (BSO) to cultures of primary rat hepatocytes before and during menadione exposure. BSO inhibits γ-gluyamyl-cysteinyl-synthetase, a rate limiting step in the biosynthesis of GSH. This method reduced GSH levels by as much as 80 % and increased superoxide anion induced apoptosis in primary hepatocytes. In contrast, the addition of glutathione donor GSH-MEE, slightly decreased menadione induced apoptosis (Conde de la Rosa et al., 2006).

Methods	**Parameter measured**
Neutral Red Assay	Cell viability
MTT Assay	Metabolic Activity/Cell Viability
WST-1 Assay	Metabolic Activity/Cell Viability
CV Assay	Cell number
Intracellular GSH content	Oxidative stress/toxicity

Table 4-1 Methods used to determine toxicity, and the parameters they measure.

4.1.2 Ethanol and Acetaldehyde Toxicity

ROS plays a role in the pathogenesis of alcoholic liver disease (Boers et al., 2006). Alcohol misuse is one of the major causes of liver fibrosis worldwide. The UK and Scotland in particular have seen an increase over the last decade in the mortality rates of both men and women from cirrhosis related to alcohol, in contrast to a decrease in mortality from cirrhosis being witnessed elsewhere, in Southern Europe in particular (Bosetti et al., 2007).

Chronic toxic insult from alcohol to the liver results in a loss of functional tissue due to the accumulation of extracellular matrix proteins which distort the hepatic architecture by forming fibrous scar tissue and hence lead to the development of liver fibrosis. Progression in liver fibrosis then lead to the development of cirrhosis and liver failure (Friedman, 2003). The effects of alcohol have been shown to vary with dose, with some evidence suggesting that it may even have some beneficial cardiovascular effects at low consumption rates, particularly in the prevention of coronary heart disease (Renaud and de Lorgeril, 1992). However, alcohol is a known hepatotoxin and induces several types of liver disease including fibrosis ((Mello et al., 2008, Bataller and Brenner, 2005) and hepatocellular carcinoma (HCC) (Yang et al., 2005). About 90% of alcohol taken into the body is metabolised by the liver to acetaldehyde and acetic acid at a maximal rate of between 10-20 ml/h. Ethanol is metabolised in the body by alcohol dehydrogenase (ADH), CYP2E1 and catalase. Acetaldehyde is the predominant metabolite formed by the oxidation of ethanol by ADH. It is then oxidised to acetic acid by the enzyme acetylaldehyde dehydrogenase (ALDH) in the mitochondria (Figure 4.2). The major metabolite, acetaldehyde, plays the central role in the pathogenesis of liver fibrosis (Mello et al., 2008, Gutierrez-Ruiz et al., 2001). It has also been concluded that chronic alcohol ingestion inhibits ALDH production and hence results in an increase in tissue and plasma acetaldehyde levels (Lieber, 1997).

Acetaldehyde, the major metabolite produced by ADH induces the expression of the collagen I genes in hepatic stellate cells (HSC) at relevant concentrations measured in

hepatic venous blood during alcohol consumption (200 µM) (Svegliati-Baroni et al., 2001). The mechanisms underlying this are not well known, however, some work is being carried out in the field to elucidate the factors. Svegliati-Baroni et al. (2001) have also demonstrated that acetaldehyde induces α2(I) collagen and fibronectin gene expression at transcriptional levels, as early as 2 h after incubation with human HSC in vitro.

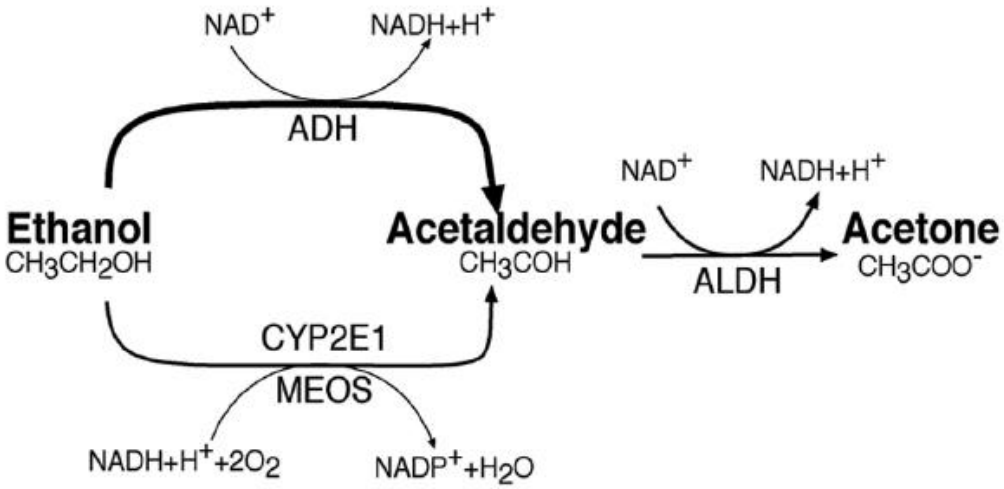

Figure 4-2 Metabolic pathways of ethanol involving alcohol dehydrogenase (ADH) and the microsomal ethanol oxidising system (MEOS).

Adapted from (Setshedi et al., 2010)

4.1.3 Primary rat hepatocytes and HepG2 cells

Much work has been carried out to elucidate the functional differences between both cellular models (Gerets et al., 2012, Xu et al., 2005, Guo et al., 2010). HepG2 cells are often perceived as an ideal alternative to primary hepatocytes due to their maintenance of a somewhat differentiated state, unlimited availability and ease of use. However, their main limitation is their low metabolic capacity. This would make HepG2 cells suitable for determining the toxicity of parent molecules but not necessarily for screening the turnover of a parent molecule to a toxic metabolite. Wilkening et al. (2003) demonstrated, at the mRNA level, the differences in expression of Phase I and Phase II enzymes between primary human hepatocytes and HepG2 cells, concluding

that primary human hepatocytes exhibited much higher levels of Phase I enzymes. In particular, they reported that CYP3A4, regarded as the most important drug metabolising enzyme in human liver, has undetectable at mRNA level in the HepG2 cells. This should be kept in mind when interpreting the differences in toxicity of ethanol in HepG2 versus primary rat hepatocytes.

The aim of this chapter was to determine if IGFBP-5 secretion was affected in the model of primary rat hepatocytes developed in Chapter 3 when the hepatocytes were under oxidative stress using two well characterised oxidative toxins, hydrogen peroxide and menadione as well as ethanol and its primary metabolite acetaldehyde.

4.2 Methods

4.2.1 Preparation and isolation of primary rat hepatocytes

Hepatocytes were isolated as previously described in Chapter 2 (see sections 2.2.1 – 2.2.3).

4.2.3 Hepatocyte cultures treated with menadione and hydrogen peroxide

Primary rat hepatocytes were cultured on collagen coated (30 µg/cm^2) 24- and 96- well plates and were seeded at a density of 1.5 x 10^5 cells/cm^2. Plates were incubated at 37 °C for 2 h after which time the medium (William's E containing 5 % v/v foetal calf serum (FCS), L-glutamine (2mM), penicillin G (50 units/ml), streptomycin sulphate (50 µg/ml) and fungizone (250 µg/ml)) was removed and replaced with Hydrogen peroxide (0.01 – 0.5 mM; in a total volume of 0.5 ml for 24 well plate and 0.2 ml for 96 well plate) or Menadione (0.1 – 10 µM; in a total volume of 0.5 ml for 24 well plate and 0.2 ml for 96 well plate) diluted in medium and incubated for 2, 3, 4, 6 and 9 d at 37 °C. Control wells had medium only added (0.5 ml for 24 well plate and 0.2 ml for 96 well plate). Wells allocated for 2, 3, 4 and 6 d had drug added every day but did not get a medium change, 9 d wells had a medium change at 3d and 6 d with fresh toxin added daily. Differences in medium change days was to allow IGFBP-5 accumulation in the medium to levels above the level of detection for the ELISA kits used in this study. Figure 3.13 demonstrated that at early timepoints in culture IGFBP-5 measured in cell culture medium was low. Allowing for the accumulation over longer periods of time would help in measuring the IGFBP-5. Supplementing drug into each well was carried out in a 5 µl volume on the days required, but ensuring that the dimethylsulfoxide (DMSO) concentration always remained lower than 0.1 % v/v.

At the end of the incubation with toxins, the medium was removed and stored at 4 °C overnight awaiting LDH activity analysis, and at -70 °C awaiting IGFBP-5 ELISA assays. Samples for GSH (Section 2.12) and total protein (Section 2.6) were prepared as stated elsewhere.

For WST-1, a 10 % dilution of WST-1 (50 µl) was added to each well of a 96 well plate containing cell and medium and incubated for 1 h at 37 °C in a humidified atmosphere of 5 % CO_2 in air. Plates were shaken thoroughly for 1 min prior to measuring the absorbance (450 nm) on a plate reader (see section 2.13). Wells were then washed with PBS and 100 µl 4 % paraformaldehyde (PFA) was added for 30 min to fix the cells. After 30 min, PFA was removed and wells were washed with 100 µl PBS (2x) before adding 100 µl CV for 20 min. After 20 min, CV was removed and wells were washed with 200 µl PBS (3x). The stain was then solubilised overnight with 0.1 % Triton X-100 in PBS. Plates were shaken thoroughly prior to measuring the absorbance (540 nm) on a plate reader (See section 2.14).

4.2.4 Hepatocyte cultures treated with Ethanol and Acetaldehyde

4.2.4.1 Seeding cells and sample preparation with Sodium Bicarbonate containing medium

For MTT and NR assay, 96 well plates were seeded with Hep G2 cells (200 µl) at a seeding density of 3.25 x 10^4 cells/cm^2. Plates were incubated at 37 °C for 24 h to allow cell attachment after which time medium (refer to section 2.10) was removed and replaced with medium (refer to section 2.10) containing ethanol (0.02 M to 1 M; in a total volume of 200 µl) and incubated for 24 h at 37 °C. Control wells had medium only added (200 µl).

For LDH activity, GSH determination and Lowry Assay with Hep G2 cells, 24 well plates were seeded at a density of 3.25 x 10^4 cells/cm^2. Plates were incubated at 37 °C for 24 h after which time medium was removed and replaced with medium containing ethanol (100 mM to 500 mM; in a total volume of 1 ml) and incubated for 24 h, 48 h and 72 h at 37 °C. Control wells had medium only added (1 ml). For plates being incubated for longer than 24 h, medium (refer to section 4.2.2) was changed every 24 h.

For LDH activity, GSH determination and Lowry Assay with rat hepatocytes, collagen coated (30 µg/cm^2) 24 well plates were seeded at a density of 1.5 x 10^5 cells/cm^2. Plates were incubated at 37 °C for 4 h after which time medium (Williams' E containing 5 % v/v foetal calf serum (FCS), penicillin G (50 units/ml), streptomycin sulphate (50 µg/ml) and fungizone (250 µg/ml)) was removed and replaced with ethanol diluted in medium (100 mM to 500 mM; in a total volume of 1 ml) and incubated for 24 h and 48 h at 37 °C. Control wells had medium only added (1 ml). For plates being incubated for longer than 24 h, medium was changed after 24 h.

At the end of the incubation with ethanol, the medium was removed and stored at 4 °C overnight awaiting LDH activity analysis. Wells were washed once with PBS, and then GSH was extracted by adding 200 µl of 10 % (v/v) TCA to each well. After 10 min the samples of TCA were frozen at -20 °C until analysis. Meanwhile the cells remaining on the surface of the wells were digested with 0.5 M NaOH for 18 h at 37 °C, and samples were stored at -20 °C in order to measure the protein content.

4.2.4.2 Seeding cells and sample preparation with HEPES containing medium

Problems arose with evaporation of ethanol from medium when culturing cells on multiwell plates, hence, a HEPES buffered medium was used to allow the culture of cells in sealed flasks. 25 cm^2 sealed culture flasks (BD Falcon™, BD Biosciences, UK) were collagen coated (30 µg/cm^2) and seeded with primary rat hepatocytes at a density of 1.5 x 10^5 cells/cm^2 in 10 ml of medium (Williams' E medium containing HEPES (25 mM) with 5 % v/v FCS, L-glutamine (2 mM), penicillin G (50 units/ml), streptomycin sulphate (50 µg/ml), fungizone (250 µg/ml) and non-essential amino acids (NEAA) (100 x; 5 ml)). Flasks were incubated at 37 °C for 2 h after which time medium was removed. All flasks were washed twice with Dulbecco's PBS (Lonza, Switzerland). Medium with 10 % FCS was replaced fresh medium (10 ml) containing ethanol (20, 50 and 80 mM) or acetaldehyde (125, 150 and 175 µM). Flasks were incubated for 3 days at 37 °C. Control flasks contained medium only. After 3 days in culture, medium was removed was stored in Eppendorf tubes, centrifuged at 1000 rpm and placed at -70 °C awaiting analysis for IGFBP-5 secretion. Another aliquot of medium was also removed and stored at 4 °C overnight awaiting LDH activity

analysis. The GSH was extracted by adding 200 µl of 10 % (v/v) TCA to the wells after the removal of medium. After 10 min incubation at room temperature, the samples of TCA were frozen at -20 °C until analysis. Meanwhile the cells remaining on the surface of the wells were digested with 0.5 M NaOH for overnight at 37 °C in order to solubilise the protein content.

4.2.5 MTT Microplate Assay

MTT was measured as previously described in Chapter 2 (see section 2.4).

4.2.6 Neutral Red (NR) Assay

NR was measured as previously described in Chapter 2 (see section 2.5).

4.2.7 Measurement of lactate dehydrogenase (LDH) activity

LDH was measured as previously described in Chapter 2 (see section 2.11)

4.2.8 Determination of reduced glutathione (GSH) by fluorimetry

GSH was measured as previously described in Chapter 2 (see section 2.12)

4.2.9 Determination of total protein

Total protein was measured as previously described in Chapter 2 (see section 2.6).

4.2.10 Measurement of IGFBP-5 by ELISA

Mouse IGFBP-5 was measured as previously described in Chapter 2 (see section 2.9).

Human IGFBP-5 was measured as previously described in Chapter 2 (see section 2.15).

4.3 Results

4.3.1 Chronic 9 day dosing of hydrogen peroxide on primary rat hepatocytes

GSH determination in the hepatocytes after dosing of hydrogen peroxide for 9 days demonstrated that the concentration chosen for this work did not affect the oxidative capacity of the cells in vitro until Day 9 and only at the highest concentration of 0.5 mM (see Figure 4.3). Despite the oxidative capacity being unaffected with the addition of H_2O_2, a drop in GSH from 4.79 ± 0.18 nmol/well to 1.35 ± 0.39 nmol/well between Day 3 and Day 9 controls respectively is evident.

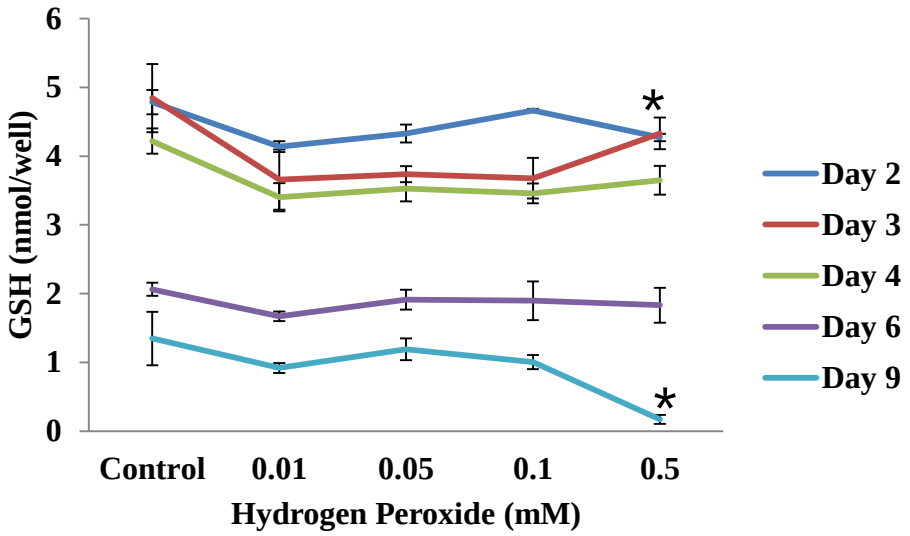

*Figure 4-3 GSH determination after H_2O_2 incubation. Primary rat hepatocytes on collagen (in-house prepared) coated 24-well plates with hydrogen peroxide (0.01 – 0.5 mM) in medium for 2, 3, 4, 6 and 9 d. Results are Mean ± SEM, n = 3; * p < 0.05 (ANOVA followed by Dunnett's multiple comparison test) in comparison with control cultures.*

The amount of formazan salt formed in the WST-1 assay is indicative of the number of metabolically active and viable cells and is dependent on the presence of NADPH. As shown in Figure 4.4, after dosing cells for 9 days a significant decrease in the formation of formazan salt was measured at Day 9 with concentrations of 0.05 – 0.5 mM H_2O_2. At Day 2, the formation of formazan salt is increased above the control at all concentrations of H_2O_2. Interestingly, an increase in formazan formation is seen over time in the controls (see Table 4.2).

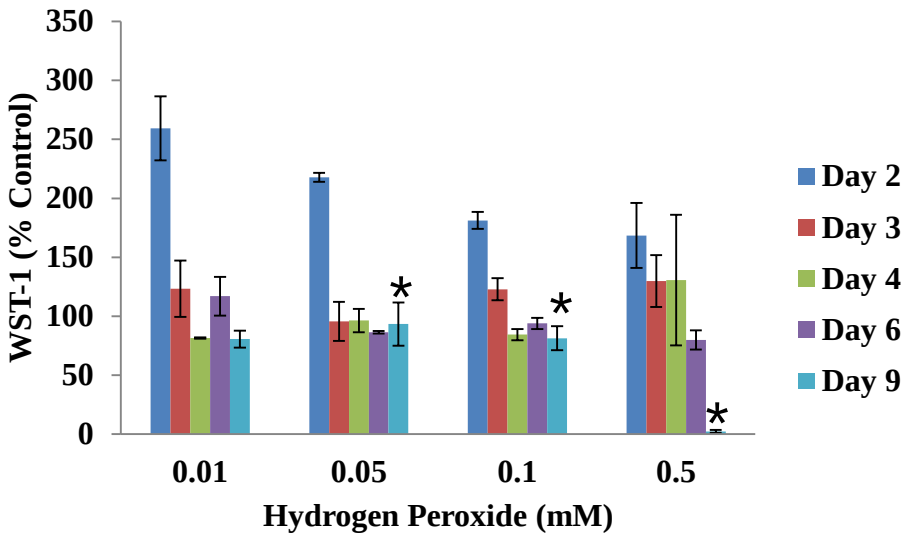

Figure 4-4 WST-1 determination after incubation with H_2O_2.

*Primary rat hepatocytes on collagen (in-house prepared) coated 24-well plates with hydrogen peroxide (0.01 – 0.5 mM) in medium for 2, 3, 4, 6 and 9 d. Results are Mean ± SEM, n = 3; * $p < 0.05$ (ANOVA followed by Dunnett's multiple comparison test) in comparison with control cultures.*

Day	Mean (OD at 450 nm)	SEM
2	0.19	0.01
3	0.21	0.02
4	0.28	0.09
6	0.30	0.01
9	0.47	0.02

Table 4-2 WST-1 determination of the control wells.

Primary rat hepatocytes over 9 days in culture. Results are Mean ± SEM, n = 3

CV staining after chronic dosing of H_2O_2 demonstrates a decrease in cell number at Day 9 at concentrations of 0.05 – 0.5 mM in comparison with controls (see Figure 4.5). Table 4.3 highlights the OD values for the control wells. The values indicate no major loss of hepatocyte number over the 9 days in culture.

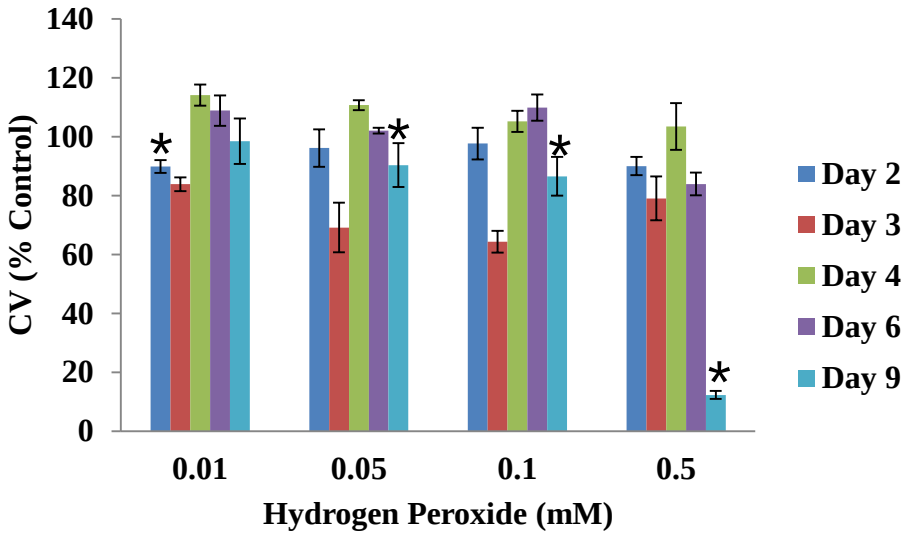

Figure 4-5 CV assay after incubation with H2O2.

*Primary rat hepatocytes on collagen (in-house prepared) coated 24-well plates with hydrogen peroxide (0.01 – 0.5 mM) in medium for 2, 3, 4, 6 and 9 d. Results are Mean ± SEM, n=3; * p < 0.05 (ANOVA followed by Dunnett's multiple comparison test) in comparison with control cultures.*

Day	Mean (OD at 450 nm)	SEM
2	1.67	0.14
3	1.35	0.03
4	1.35	0.10
6	1.17	0.02
9	1.57	0.08

Table 4-3 CV staining of the control wells.

Primary rat hepatocytes over 9 days in culture. Results are Mean ± SEM, n = 3

IGFBP-5 was measured in the supernatant from dosing of H_2O_2 on primary rat hepatocytes for 9 days. Significantly higher IGFBP-5 levels were measured in the medium from the control wells (3.32 ± 0.99 ng/ml accumulated between day 6 to day 9) in comparison with the medium from the H_2O_2 dosed wells (0.1 mM: 0.57 ± 0.20 ng/ml accumulated between day 6 to day 9). Similarly, the same trend was also demonstrated between days 3 and 6. These results are shown in Figure 4.6 and the effect was observed at both concentrations of H_2O_2.

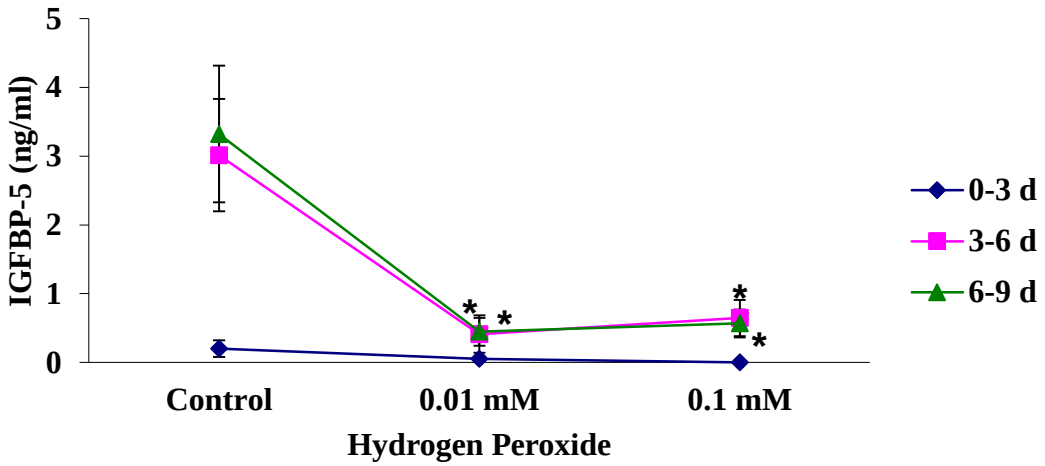

Figure 4-6 IGFBP-5 release after H2O2 exposure.

*Primary rat hepatocytes on collagen (in-house prepared) coated 24-well plates exposed to hydrogen peroxide. Results are Mean ± SEM, n = 3, * p < 0.05 (ANOVA followed by Dunnett's multiple comparison test) in comparison with control cultures.*

4.3.2 Menadione dosing on primary rat hepatocytes for 9 days

GSH levels were measured after 9 days of dosing of menadione on primary rat hepatocytes. No significant changes in GSH levels were demonstrated until Day 9 at the highest concentrations of 5 and 10 µM in comparison with the control as shown on Figure 4.7. However, the control levels of GSH were also decreasing with time, indicating the overall oxidative capacity was diminishing with time even without perturbation with menadione. GSH levels on Day 2 were 4.43 ± 0.22 nmol/well decreasing to 0.75 ± 0.05 nmol/well on day 9.

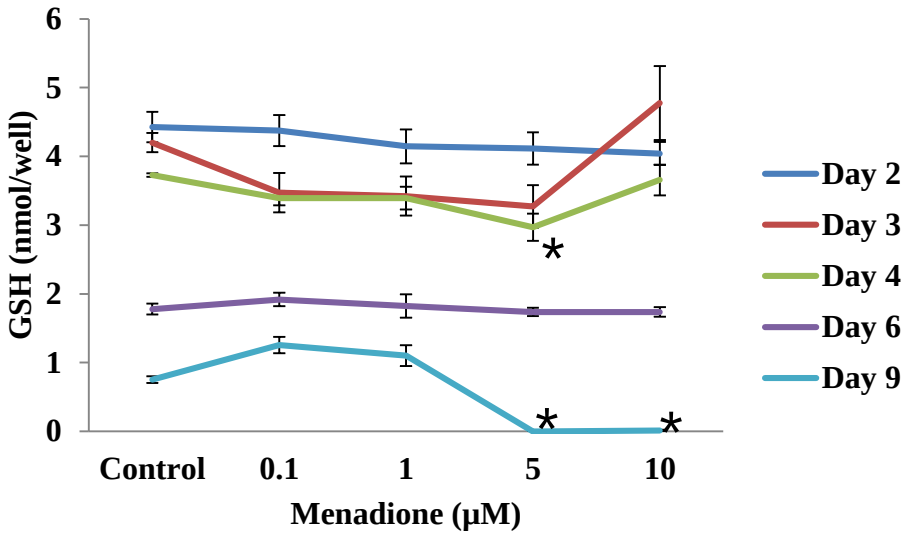

Figure 4-7 GSH determination after incubation with menadione.

*Primary rat hepatocytes on collagen (in-house prepared) coated 24-well plates with menadione (0.1 – 10 µM) in medium for 2, 3, 4, 6 and 9 d. Results are Mean ± SEM, n = 3; * p < 0.05 (ANOVA followed by Dunnett's multiple comparison test) in comparison with control cultures.*

WST-1 demonstrated a decrease in cell number at Day 9 also at the highest concentrations of 5 and 10 µM menadione dosing in comparison with the control value (See Figure 4.8). Table 4.4 illustrates the formazan salt formation in the control wells over the 9 day culture period. With the addition of 5 and 10 µM menadione between Day 2 and Day 4, an increase in formazan salt formation is observed. However, after Day 6 this phenomenon is no longer evident.

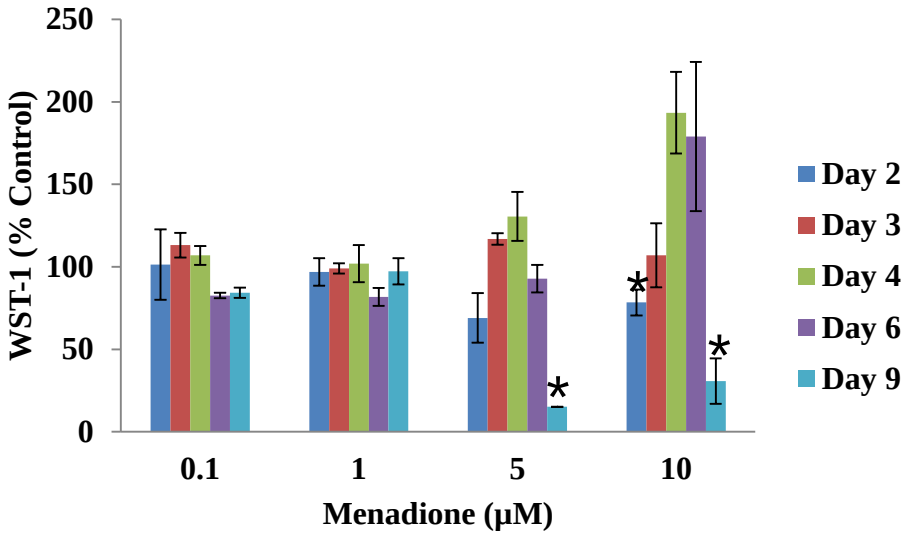

Figure 4-8 WST-1 determination after incubation with menadione.

*Primary rat hepatocytes on collagen (in-house prepared) coated 24-well plates with menadione (0.1 – 10 µM) in medium for 2, 3, 4, 6 and 9 d. Results are Mean ± SEM, n = 3; * p < 0.05 (ANOVA followed by Dunnett's multiple comparison test) in comparison with control cultures.*

Day	Mean (OD at 450 nm)	SEM
2	0.36	0.09
3	0.24	0.00
4	0.23	0.01
6	0.33	0.05
9	0.43	0.04

Table 4-4 WST-1 determination of the control wells.

Primary rat hepatocytes over 9 days in culture. Results are Mean ± SEM, n = 3

Using CV as a viability test, it demonstrated that no significant loss in attached cell numbers was demonstrated until Day 9 at the top concentrations used (5, 10 µM Menadione) as seen on Figure 4.9. CV staining in the control wells did not decrease with time (see Table 4.5), indicating that any reduction seen in menadione cultures was due to the addition of menadione and not the aging of the cultures.

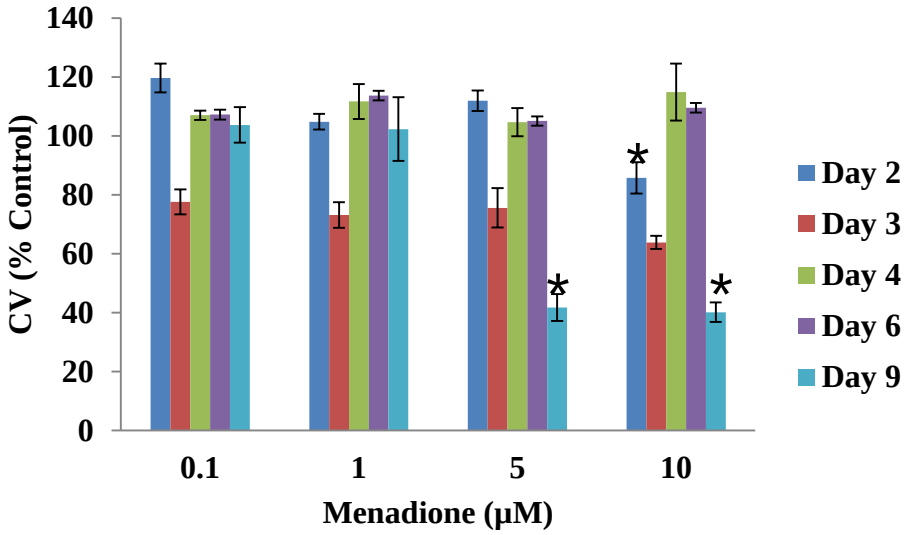

Figure 4-9 CV assay after incubation with menadione.

*Primary rat hepatocytes on collagen (in-house prepared) coated 24-well plates with menadione (0.1 – 10 µM) in medium for 2, 3, 4, 6 and 9 d. Results are Mean ± SEM, n=3; * p < 0.05 (ANOVA followed by Dunnett's multiple comparison test) in comparison with control cultures.*

Day	Mean (OD at 450 nm)	SEM
2	1.40	0.05
3	1.40	0.09
4	1.57	0.05
6	1.19	0.08
9	1.59	0.03

Table 4-5 CV staining of the control wells.

Primary rat hepatocytes over 9 days in culture. Results are Mean ± SEM, n = 3

Similar trends were seen with IGFBP-5 release into the medium with 9 days of dosing with menadione (see Figure 4.10). The highest concentrations were measured in the medium from the control cells (3.77 ± 1.02 ng/ml accumulated between day 6 to day 9), with the IGFBP-5 in the medium from treated cells being significantly lower (1 µM: 0.35 ± 0.20 ng/ml accumulated between day 6 to day 9), and similarly decreses were also seen between day 3 and day 6.

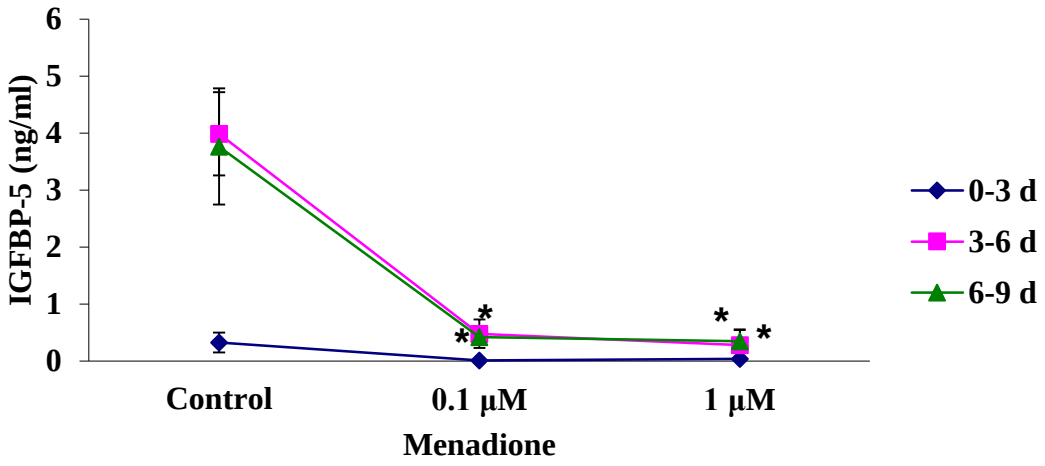

Figure 4-10 IGFBP-5 release after menadione exposure.

*Primary rat hepatocytes on collagen (in-house prepared) coated 24-well plates exposed to menadione. Results are Mean ± SEM, n = 3, * p < 0.05 (ANOVA followed by Dunnett's multiple comparison test) in comparison with control cultures*

4.3.3 Exposure of HepG2 cells to Ethanol assessed by MTT and NR

The MTT assay (see Figure 4.11) demonstrated a decrease in the number of viable cells with the addition of ethanol (0.02 M to 1 M). Concentrations used in these experiments are supra-physiological (1 M ethanol is up to 40 times higher than that seen in human blood).

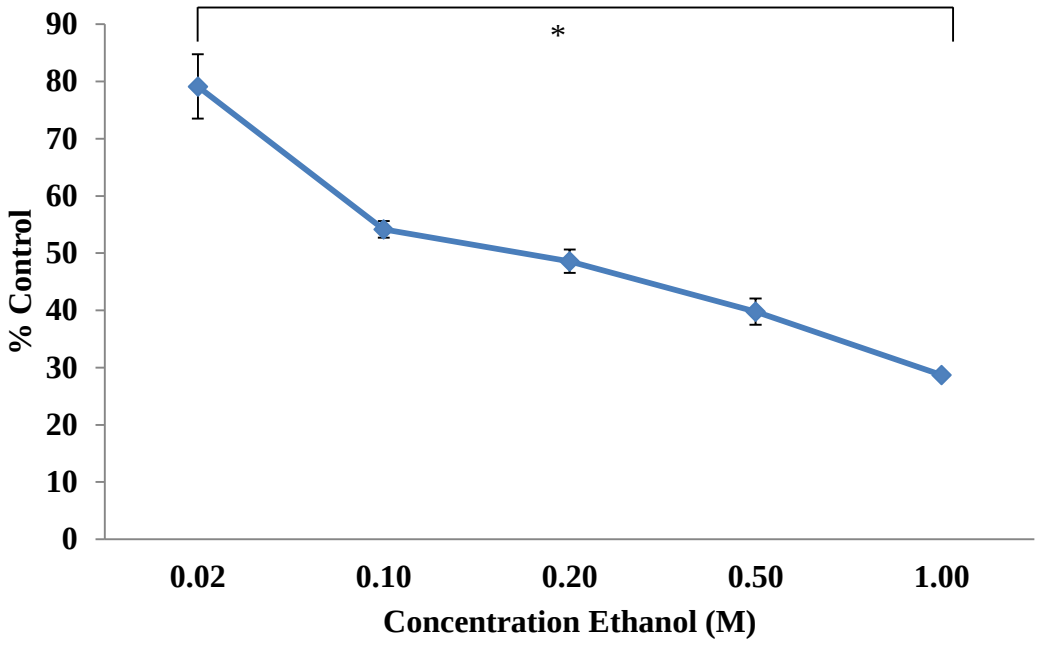

Figure 4-11 MTT assay after incubation of HepG2 cells with ethanol.

*HepG2 cells cultured in 24-well plates with varying concentrations of ethanol in medium for 24 h. Results are Mean ± SEM, n = 12. * $p \leq 0.05$ significantly different from control (ANOVA followed by Fischer's individual error rate). All values were significantly lower in comparison with control cultures.*

According to the NR assay, increasing ethanol concentration first resulted in increased cell numbers (see Figure 4.12), followed by a decrease with the addition of 0.5 M and 1 M ethanol after 24 h.

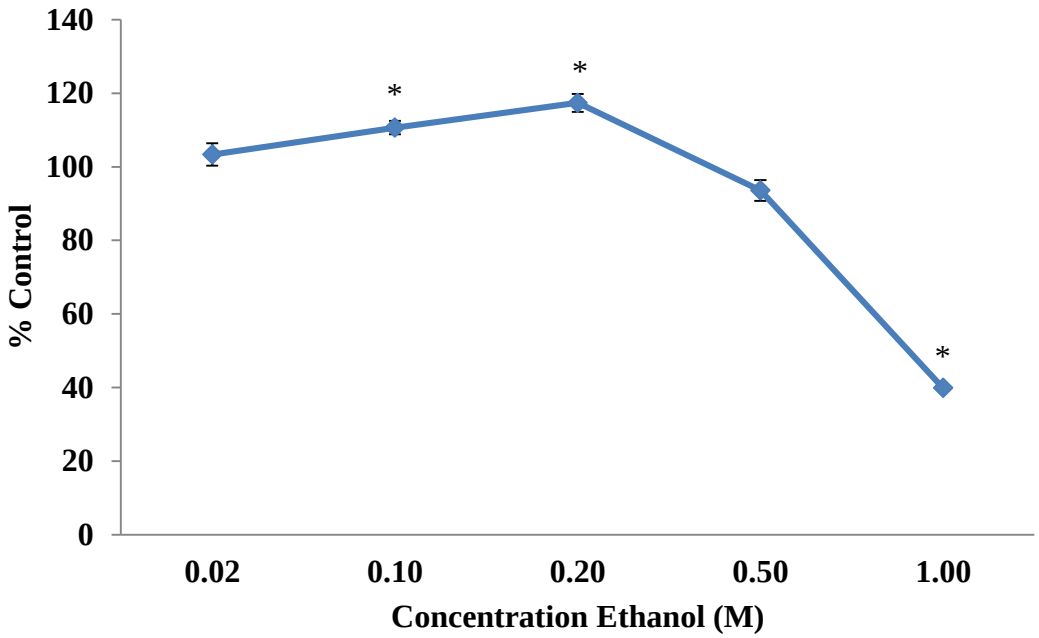

Figure 4-12 NR assay after incubation of HepG2 cells with ethanol

*HepG2 cells cultured in 24-well plates with varying concentrations of ethanol in medium for 24 h. Results are Mean ± SEM, n = 12. * $p \leq 0.05$ significantly different from control (ANOVA followed by Fischer's individual error rate)*

4.3.4 Exposure of HepG2 cells to ethanol assessed by GSH content: Evaluating the effect of Ethanol Evaporation on HepG2 cells in Neighbouring Wells on a 24 Well Plate in HepG2 culture

This work was carried out to determine if evaporation of ethanol was the cause of the toxicity in the control wells. Previous work indicated that ethanol in wells adjacent to the control wells were exhibiting toxic effects. GSH determination with Hep G2 cells showed a decrease in GSH content after the initial 24 h incubation with ethanol (See Fig. 4.13). An undetectable value for GSH was observed after 24 h with the addition of 250 mM and 500 mM ethanol in medium. An increase in GSH content was observed with the control wells at each time point (24 h, 48 h and 72 h). The control wells directly adjacent (Column 3) to ethanol containing wells showed a significant decrease in GSH at 48 h in comparison to the levels at the same point in the control wells (Column 1) furthest away from the ethanol containing wells. Control wells in Column 2 also showed a significant decrease in GSH in comparison with the control wells in Column 1 indicating that the the addition of ethanol at 100 nM in Column 4 and potentially the 250 and 500 nM ethanol in Column 5 and 6 respectively were affecting the control wells.

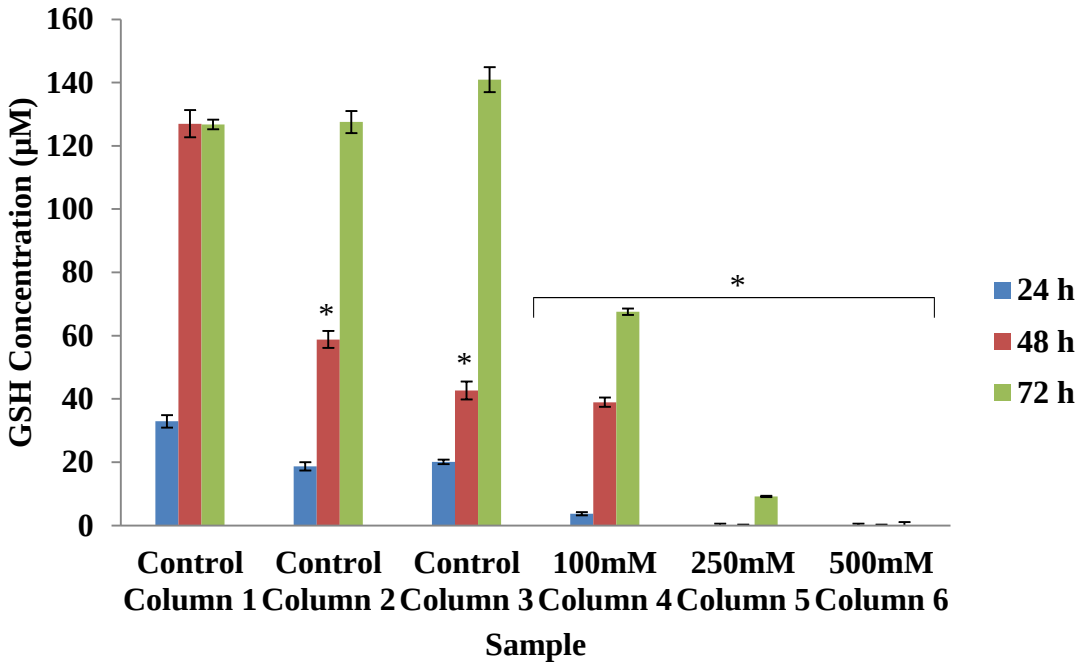

Figure 4-13 Intracellular GSH after incubation of HepG2 cells with ethanol.

*HepG2 cells cultured in 24-well plates with varying concentrations of ethanol in medium for 24 and 48 h. Results are Mean ± SEM, n = 4. Column numbers refer to the position of the sample on the 24 well plate. * $p \leq 0.05$ significantly different from column 1 (ANOVA followed by Fischer's individual error rate)*

LDH activity was similar for all samples, indicating that there was no detectable damage to the membranes of the cells by the insult of ethanol in medium at concentration between 100 mM and 500 mM after 24 h (see Figure 4.14). No significant difference was demonstrated between the control wells.

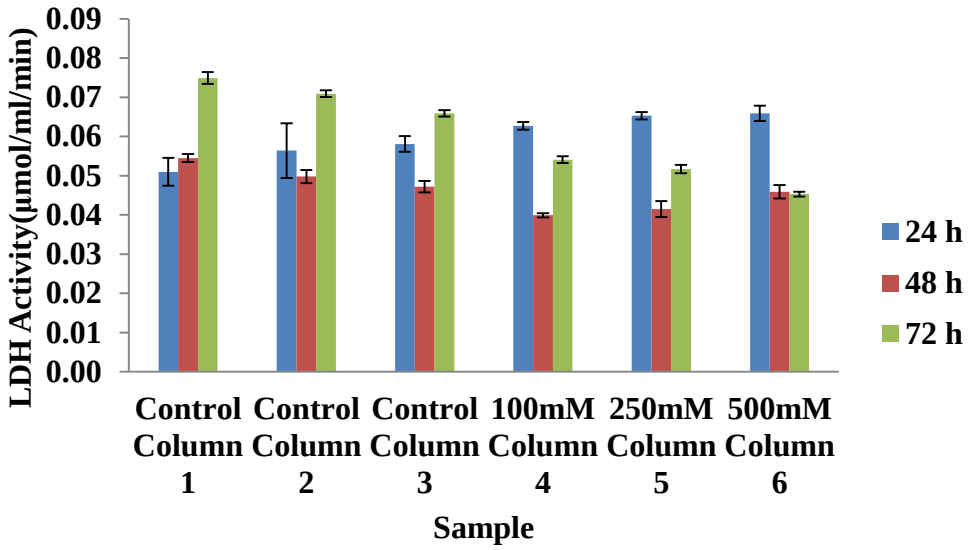

Figure 4-14 LDH activity after incubation of HepG2 cells with ethanol.

HepG2 cells cultured in 24-well plates with varying concentrations of ethanol in medium for 24 and 48 h. Results are Mean ± SEM, n = 4. Column numbers refer to the position of the sample on the 24 well. No statistical difference was observed in comparison with the controls.

The Lowry Assay provided data on the total amount of protein in each well after incubation of Hep G2 cells with ethanol (100 mM to 500 mM) in medium (see Figure 4.15). A decrease was noted after 24 h incubation with ethanol in medium in comparison with the controls, with a drop below the level of detection after 72 h incubation with 250 mM and 500 mM ethanol in medium, indicating that cell death had occurred and that cells were detached from the base of the wells and washed away. Column 3 control protein values at 24 h and 72 h are significantly decreased from the control protein values of Column 1 at the same time point.

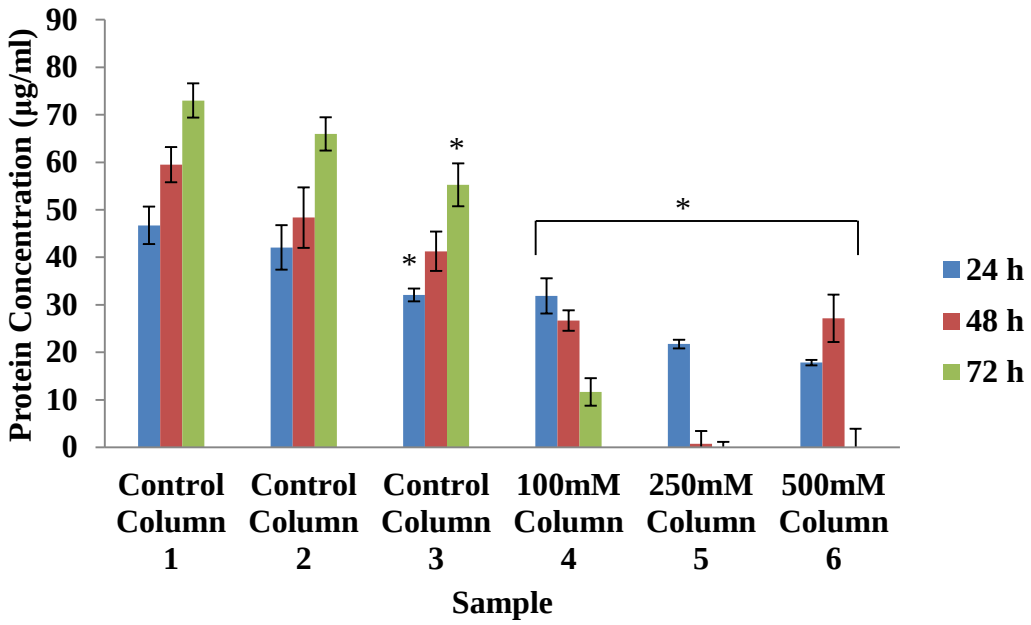

Figure 4-15 Protein content measured after ethanol exposure to HepG2 cells.

*Protein content measured using the Lowry assay after incubation of HepG2 cells cultured in 24-well plates with varying concentrations of ethanol in medium for 24 and 48 h. Results are Mean ± SEM, n = 4. Column numbers refer to the position of the sample on the 24 well plate. * $p \leq 0.05$ significantly different from column 1 (ANOVA followed by Fischer's individual error rate)*

4.3.5 Evaluating the effect of Ethanol Evaporation on Primary Rat Hepatocyte cultures in Neighbouring Wells on a 24 Well

GSH levels in rat hepatocytes, showed a decrease after 48 h incubation with ethanol in medium (see Figure 4.16). With the addition of ethanol (250 mM) in medium, a decrease in GSH was seen in cells between 24 h incubation to 48 h incubation from 45.82 ±1.35 µM to a value below the limit of detection. Similarly, with the addition of 500 mM ethanol in medium a decrease was seen in cells between 24 h incubation and 48 h incubation from 44.61 ± 1.18 µM to an undetectable level by the assay. Intracellular GSH concentration was significantly higher in cells at 24 and 48 h in Column 1 control in comparison with the other two control cell samples (Column 2 and 3) measured at the same time points.

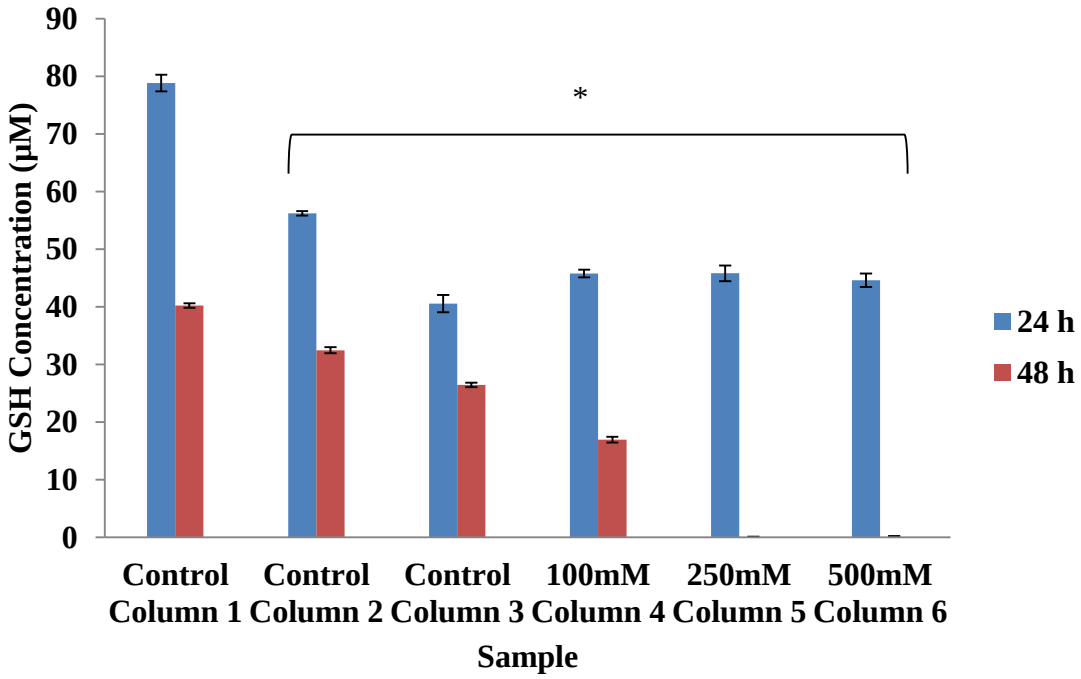

Figure 4-16 Intracellular GSH after exposure to ethanol.

*Primary rat hepatocytes on 24 well plates with varying concentrations of ethanol in medium for 24 and 48 h. Results are Mean ± SEM, n = 4. Column numbers refer to the position of the sample on the 24 well plate. * $p \leq 0.05$ significantly different from control column 1 (ANOVA followed by Fischer's individual error rate)*

After 24 h incubation of rat hepatocytes with ethanol in medium the LDH leakage ranged from between 0.61 ± 0.04 µmol/ml/min (Control Column 1) to 0.54 ± 0.03 µmol/ml/min (500 mM ethanol in medium) (see Figure 4.17). There were no significant differences.

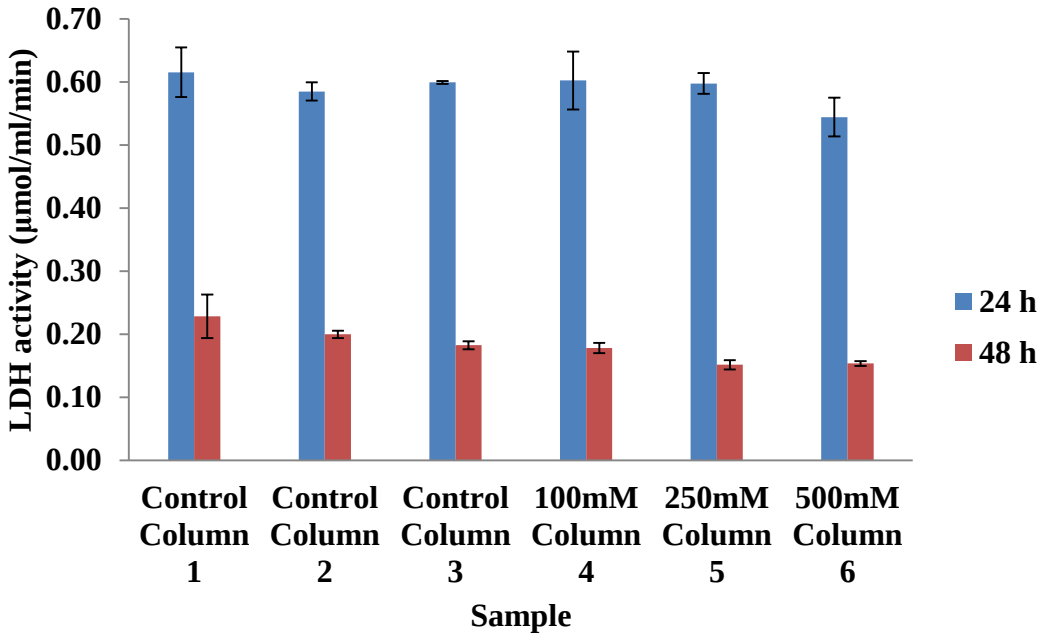

Figure 4-17 LDH activity after incubation ethanol.

Primary rat hepatocytes on collagen (in-house prepared) coated 24 well plates with varying concentrations of ethanol in medium for 24 and 48 h. Results are Mean ± SEM, n = 4. Column numbers refer to the position of the sample on the 24-well plate. No statistical difference was observed in comparison with the controls.

The Lowry Assay provided data on the total amount of protein in each well after incubation of rat hepatocytes with ethanol (100 mM to 500 mM) (see Figure 4.18). A slight decrease was noted after 48 h incubation with ethanol. However, this decrease was seen with the control samples also.

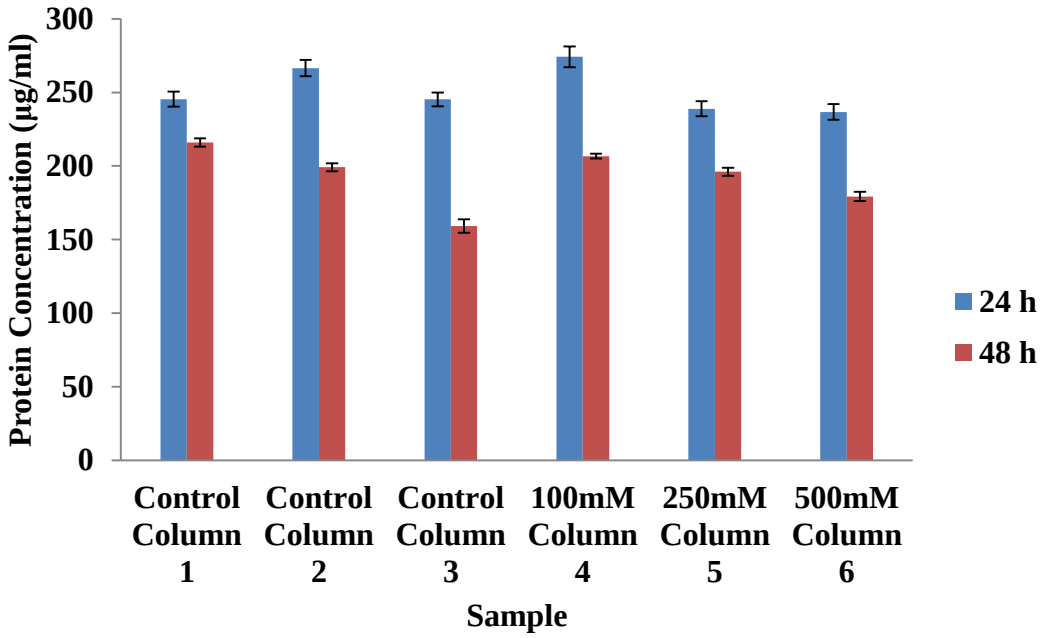

Figure 4-18 Protein content measured after exposure to ethanol.

Protein content measured using the Lowry assay after incubation of primary rat hepatocytes on collagen (in-house prepared) 24-well plates with varying concentrations of ethanol in medium for 24 and 48 h. Results are Mean ± SEM, n = 4. Column numbers refer to the position of the sample on the 24 well plate. No statistical difference was observed in comparison with the controls.

4.3.6 LDH activity in primary rat hepatocytes exposed to ethanol and acetaldehyde in sealed culture flasks

LDH activity in primary rat hepatocytes exposed to ethanol and acetaldehyde showed no significant decrease in comparison to controls. Figure 4.19 shows that the highest concentration of ethanol added (80 mM) did not increase the levels of LDH activity in the medium indicating that the membrane of the cells was not significantly compromised after 3 days exposure. LDH leakage for the control flasks which received no dose of ethanol was 4.26 ± 0.59 µmol/flask/min in comparison with 4.11 ± 0.46 µmol/flask/min from the flasks that received a dose of 80 mM ethanol.

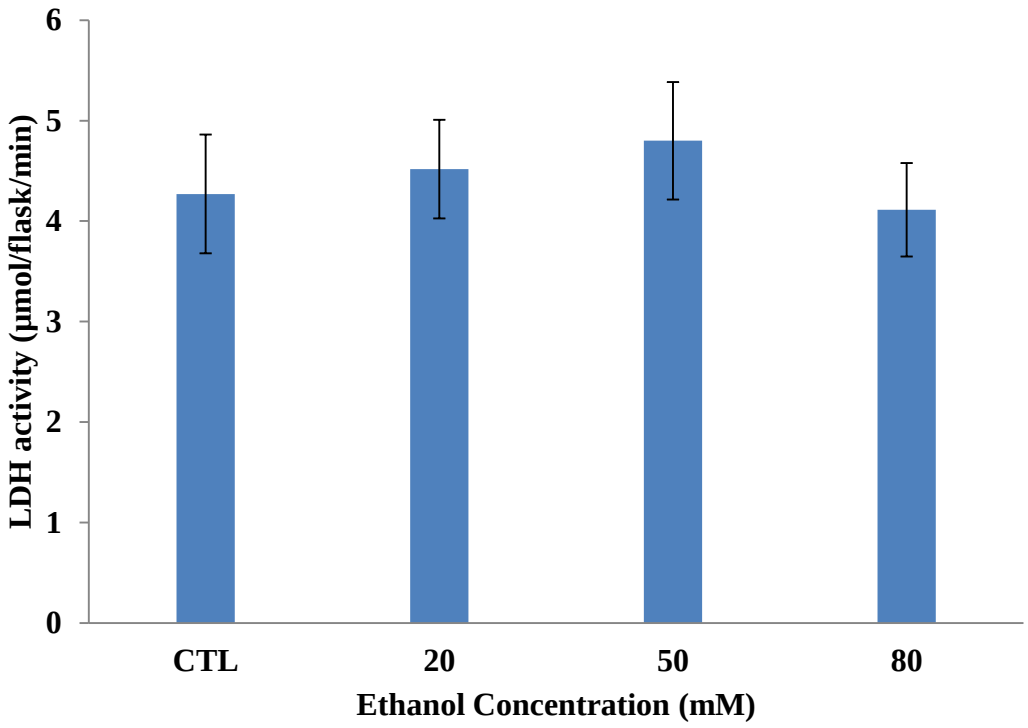

Figure 4-19 LDH activity after incubation with ethanol.

Primary rat hepatocytes with varying concentrations of ethanol in collagen (in-house prepared) coated sealed culture flasks for 3 days. Results are Mean ± SEM, n = 3 separate experiments. No statistical difference was observed in comparison with the control.

Similarly to the effect of ethanol on the primary rat hepatocytes, Figure 4.20 demonstrates that acetaldehyde at concentrations of 125 – 175 µM did not significantly increase LHD leakage. LDH leakage from control samples was 4.26 ± 0.59 µmol/flask/min in comparison with 2.91 ± 0.30 µmol/flask/min for the highest concentration of acetaldehyde added to samples.

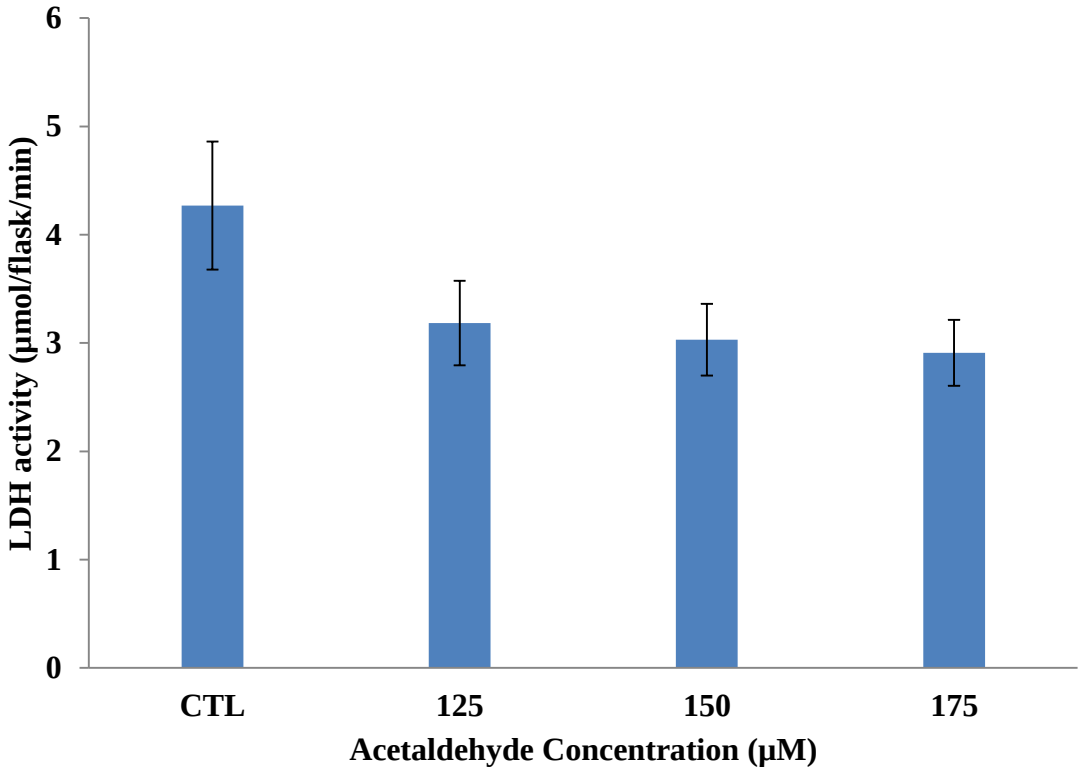

Figure 4-20 LDH activity after incubation with acetaldehyde.

Primary rat hepatocytes in collagen (in-house prepared) coated sealed flasks with varying concentrations of acetaldehyde for 3 days. Results are Mean ± SEM, n = 3 separate experiments. No statistical difference was observed in comparison with the control.

4.3.7 The effect of ethanol and acetaldehyde on GSH concentrations of primary rat hepatocytes in sealed culture flasks

Measurement of intracellular GSH was used as an indicator of oxidative stress to detect any subtle changes that ethanol and acetaldehyde caused. GSH content was also corrected for protein to eliminate changes in cell number as a possible cause of any changes in GSH levels. GSH concentrations per mg of protein decreased significantly ($p \leq 0.05$) in comparison with the control samples after 3 days in culture with the addition of 50 and 80 mM ethanol (Figure 4.21). After 3 days in culture GSH concentrations from control samples was 27.91 ±1.39 nmol/mg in comparison with 21.99 ±1.59 nmol/mg with the addition on 80 mM ethanol.

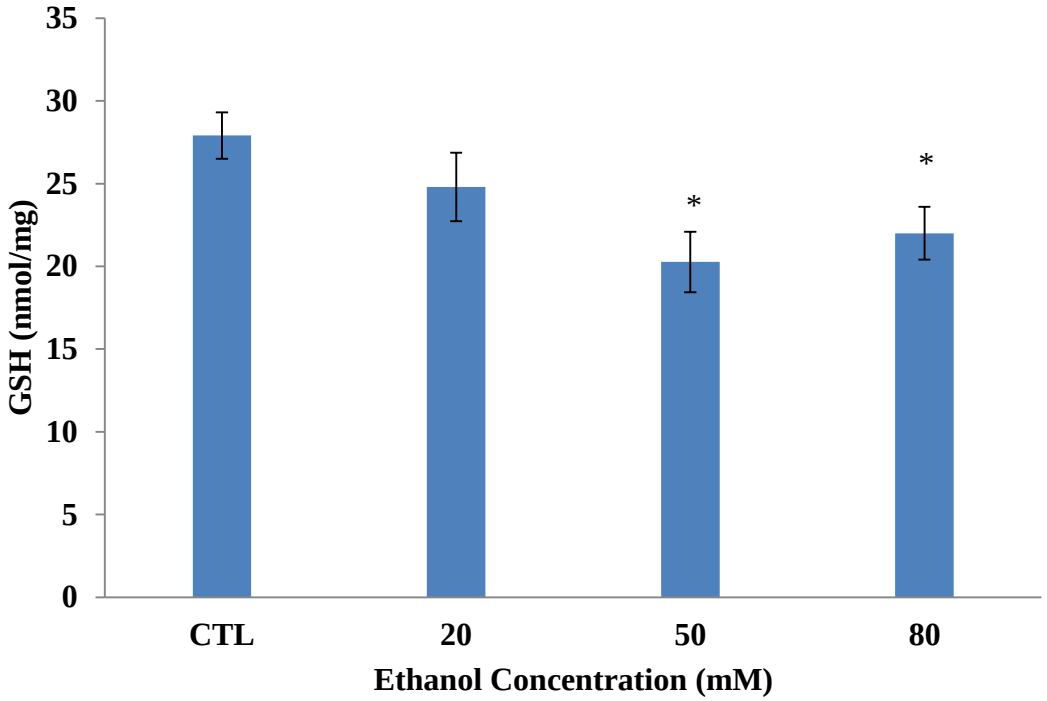

Figure 4-21 GSH concentrations corrected for protein (nmol/mg) after incubation with ethanol.

*Primary rat hepatocytes with varying concentrations of ethanol incubated in collagen (in-house prepared) coated sealed culture flasks for 3 days. Results are Mean ± SEM, n = 3 separate experiments. * $p \leq 0.05$ significantly different from control (ANOVA followed by Dunnet's multiple comparison test.)*

In contrast to the addition of ethanol to the sealed flasks of cultures of primary rat hepatocytes, the addition of acetaldehyde for 3 days did not cause a significant increase or decrease in GSH concentrations (Figure 4.22).

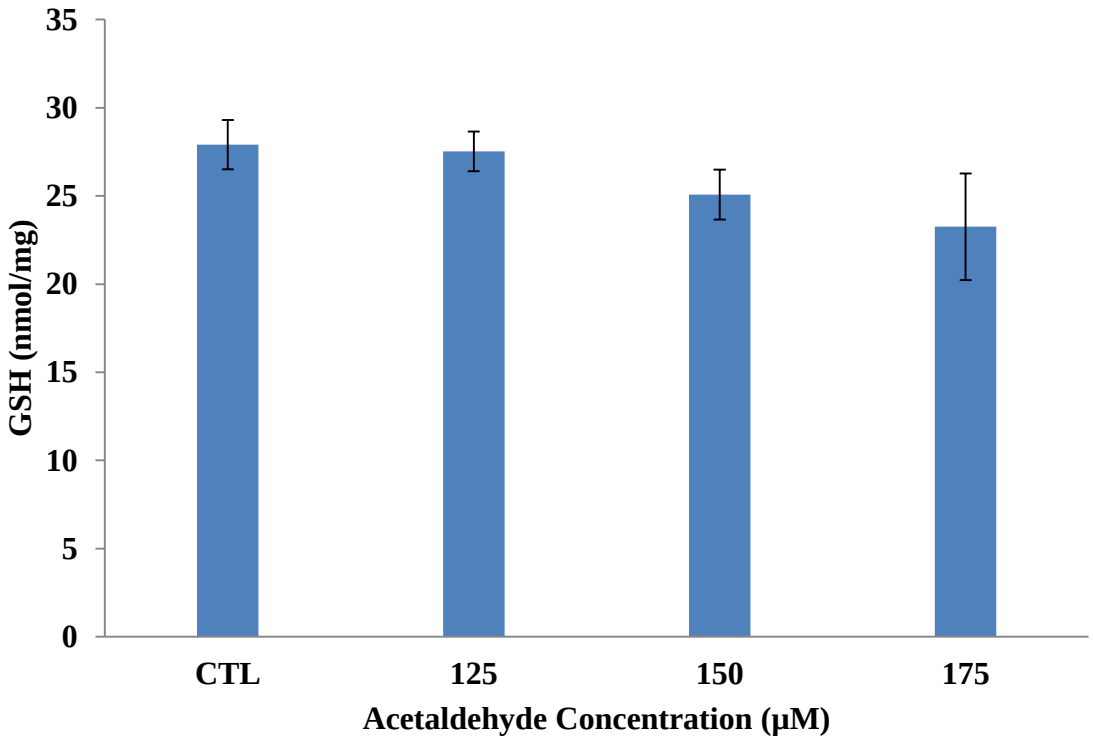

Figure 4-22 GSH concentrations corrected for protein (nmol/mg) after incubation with acetaldehyde.

Primary rat hepatocytes with varying concentrations of acetaldehyde for 3 days in collagen (in-house prepared) coated sealed culture flasks. Results are Mean ± SEM, n = 3 separate experiments. No statistical difference was observed in comparison with the control.

4.3.8 The effect of ethanol and acetaldehyde on total protein concentrations of primary rat hepatocytes in sealed culture flasks

Total protein concentration was measured to determine if the addition of ethanol or acetaldehyde affected the number of cells in the samples in sealed culture flasks. There was no statistical difference in the amount of protein in the control samples (Figure 4.23) and any of the samples treated with ethanol for 3 days. Protein concentration of 1.81 ± 0.09 mg/flask was measured for the control samples. The highest concentration of ethanol added to samples was 80 mM, the protein concentration calculated for these samples was 1.81 ± 0.11 mg/flask. Hence ethanol (20 – 80 mM) did not cause significant cell death at 3 days in culture.

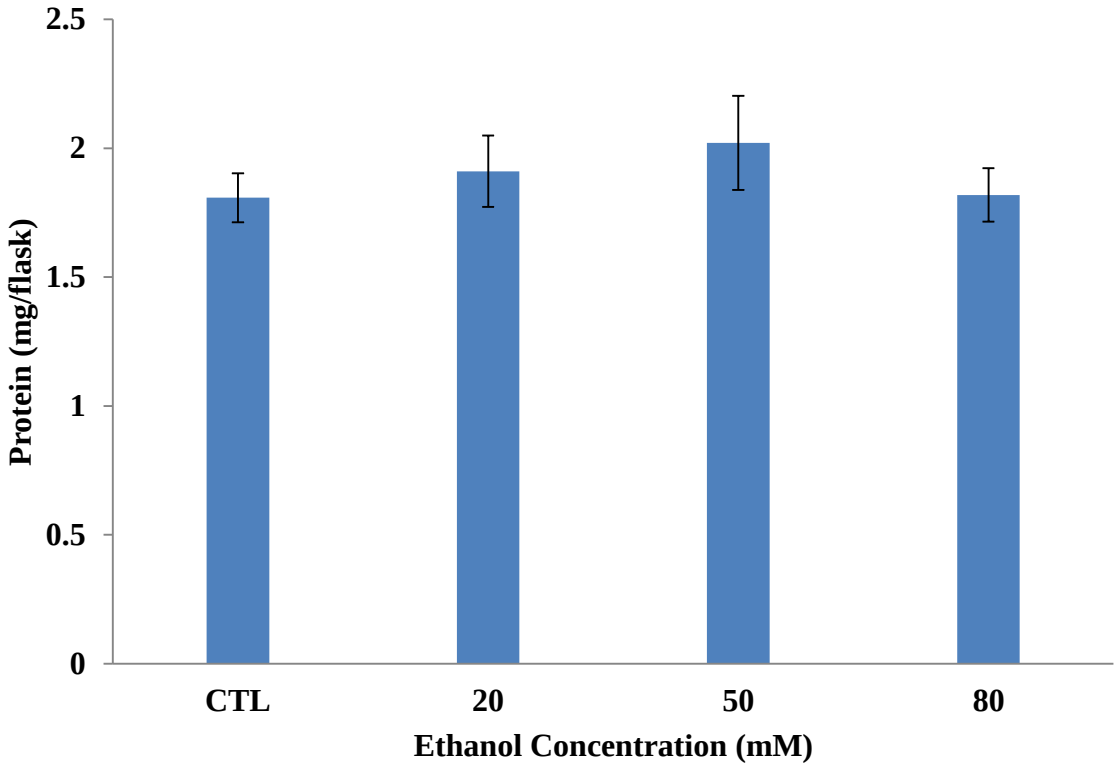

Figure 4-23 Total protein concentrations (mg/flask) after incubation with ethanol

Primary rat hepatocytes with varying concentrations of ethanol for 3 days in collagen (in-house prepared) coated sealed flasks. Results are Mean ± SEM, n = 3 separate experiments. No statistical difference was observed in comparison with the control.

Similarly with ethanol, acetaldehyde did not cause cell death at the concentrations added to the samples (125 – 175 µM). At these concentrations, Figure 4.24 shows that acetaldehyde did not cause a significant decrease in total protein concentration of cells exposed to the toxin for 3 days in sealed flasks.

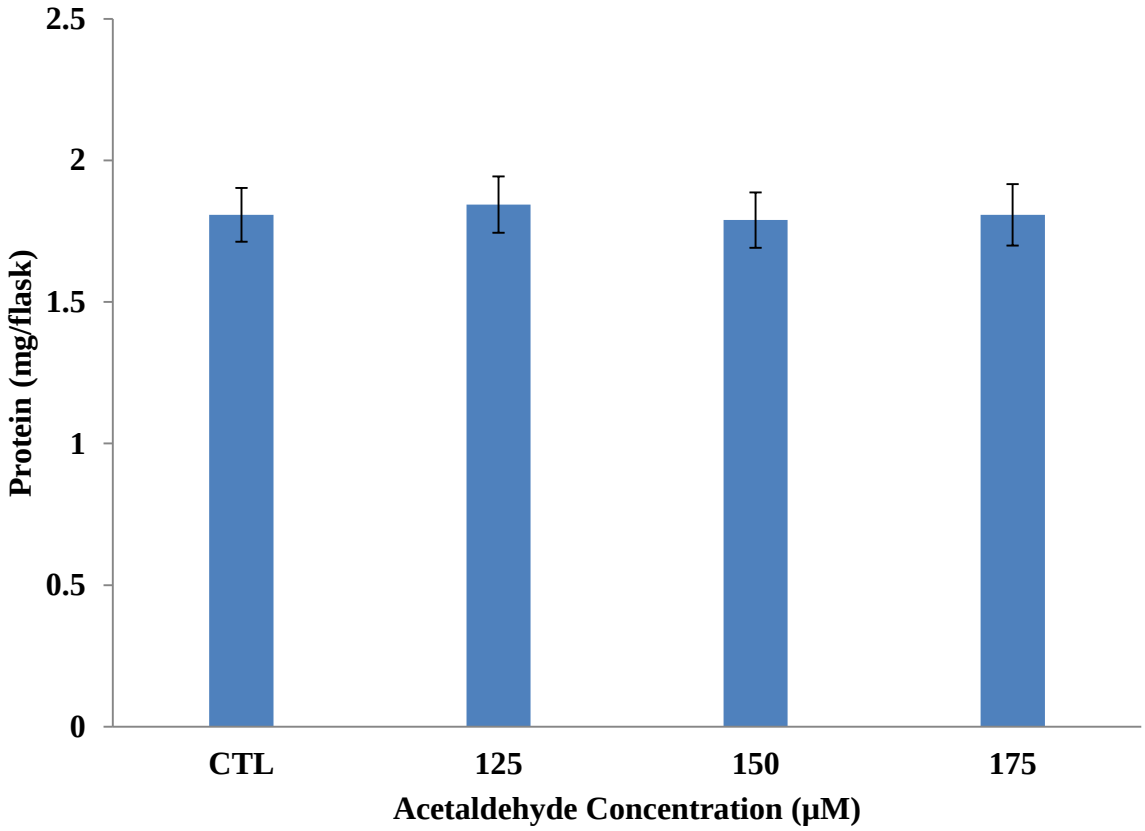

Figure 4-24 Total protein concentrations (mg/flask) after incubation with acetaldehyde.

Primary rat hepatocytes with varying concentrations of acetaldehyde for 3 days in collagen (in-house prepared) coated sealed flasks. Results are Mean ± SEM, n = 3 separate experiments. No statistical difference was observed in comparison with the control.

4.3.9 IGFBP-5 measured in conditioned medium

No IGFBP-5 was detected in the supernatant from the cultures insulted with ethanol or acetaldehyde. IGFBP-5 was also not detected in the culture medium from the control wells. Previously, IGFBP-5 secretion had peaked in cultures between Day 6 and 9 in culture (see Figure 2.13 and 4.7). In contrast, this culture was terminated at Day 3 in culture and was performed in sealed culture flasks in the presence of HEPES.

4.4 Discussion

With alcohol misuse and with alcohol related deaths on the rise in the UK and in Scotland in particular, a biomarker to detect early injury is necessary. In this chapter, an in vitro model of oxidative stress via menadione and hydrogen peroxide exposure as well as a model of ethanol toxicity was used.

Utilising the in vitro model developed in Chapter 3, chronic exposure of primary rat hepatocytes to menadione and hydrogen peroxide for 9 days was investigated to determine if IGFBP-5 was a suitable early marker of oxidative stress in vitro. In Chapter 3 it was demonstrated that IGFBP-5 was upregulated as the cells dedifferentiated in vitro. Chronic daily dosing for 9 days at sublethal concentrations of menadione (0.1 – 10 µM) and hydrogen peroxide (0.01 – 0.5 mM) was carried out and the cells were assessed for GSH content, WST-1 reduction, CV staining and IGFBP-5 secretion into the medium. For both menadione and hydrogen peroxide, no gross cell death was observed as assessed by CV staining as a marker of cell numbers until Day 9 in culture at the higher concentrations of both toxins. The oxidative capacity of the hepatocytes was monitored by measuring GSH in the cells. Similar to the results with CV, no significant decrease was observed in culture until Day 9 after dosing of both toxins at the highest concentrations. The metabolic capacity of the cells to carry out reduction reactions was monitored by WST-1, and again it was observed that the ability of the cells to reduce WST-1 was not significantly compromised until Day 9 in culture at the highest concentrations of both toxins. Both the decrease in cell number, in the ability to reduce WST-1 and in GSH levels of the cells could be attributed to the cells being highly dedifferentiated after 9 days in culture compounded by the continuous toxic insults from both menadione and hydrogen peroxide. The control wells from these experiments secreted increasing amounts of IGFBP-5 into the medium, as expected, further confirming the results demonstrated in Chapter 3. Interestingly, chronic dosing for 9 days with menadione and hydrogen peroxide suppressed the release of IGFBP-5 significantly between day 3 - 6 and day 7 - 9 into the medium, to levels just above that observed in control wells accumulating IGFBP-5 between days 1 – 3.

Ethanol and acetaldehyde toxicity is also well documented to involve oxidative stress. Initial work was carried out with HepG2 cells seeded on 24 well plates with varying concentrations of ethanol (0.02 – 1 M). It became evident that the absorbance values obtained for the control wells for the MTT and NR studies were lower than expected. This was attributed to the evaporation of ethanol from the medium in the wells adjacent to the control, and this resulted in contamination of control wells with ethanol. An experiment was designed to determine if this was the case. To determine if evaporation of ethanol from wells adjacent to the controls was causing the unexpectedly lower MTT and NR results, three columns of controls were placed in a 24 well plate, with the lowest ethanol concentration adjacent to one of the columns and the highest concentration furthest away. If ethanol was evaporating from the wells, some effects would be expected to be seen in some of the control wells closest to it. Figure 4.12 demonstrates that the intracellular GSH content was significantly higher in the control wells in Column 1 (furthest from the ethanol-containing wells) in comparison with Column 2 and 3 (closest to the ethanol-containing wells). This would suggest that the evaporation of ethanol from adjacent wells was affecting the biochemistry of the control wells.

A solution to this was to seal the flasks and use a HEPES buffer instead of sodium bicarbonate to buffer the pH in the medium. This kept all controls separate from the ethanol containing wells and avoided any cross contamination. In the initial experiments, concentrations of 20 – 80 mM ethanol and 125 – 175 µM acetaldehyde were used. It was critical to use concentrations that did not cause cell death, but caused subtle injury to the cells. LDH was used to monitor necrosis and intracellular GSH content was used to monitor redox injury caused to the cells.

Ethanol caused significant decreases in GSH content in primary rat hepatocytes when the cells were treated with 50 and 80 mM, however, this effect was not observed with any concentration of acetaldehyde used. Vina et al. (1980) demonstrated that ethanol and acetaldehyde decreased GSH content in primary rat hepatocytes with maximal

effects being observed with 20 mM ethanol after 60 min. Interestingly, higher concentrations of ethanol caused smaller decreases in GSH content. Acetaldehyde is a volatile liquid and has a boiling point of 20 °C. This makes it rather difficult to work with. It was kept on ice prior to adding it to medium on cells. The lack of an effect of acetaldehyde on the cells may be due to its volatility. Vina et al (1980) demonstrated that GSH decreased after 60 min with 0.1 mM acetaldehyde to 59 % of the control. They also demonstrated that this was dependent on the conversion of ethanol to acetaldehyde by ADH by using an inhibitor of ADH, Pyrazole. The addition of an inhibitor of ALDH, disulfiram, was shown to potentiate the effects of acetaldehyde on primary rat hepatocytes in suspension. In the present experiments, ethanol did not cause significant cell membrane damage, as no significant increase in LDH leakage was observed in comparison with the control at each timepoint. Decreases in GSH content associated with alcohol consumption has also been seen in vivo (Gao et al., 2012). Lack of differentiation of hepatocytes in this in vitro culture system may be the reason for the poorly observed toxicity with high concentrations of ethanol and acetaldehyde.

IGFBP-5 was the biomarker chosen for this study, as it had previously been implicated in the fibrosis of lung and skin and had been identified as a biomarker of ICC as previously discussed (Pilewski et al., 2005, Yasuoka et al., 2006a, Yasuoka et al., 2006b, Blechacz and Gores, 2008). IGFBP-5 secretion from the conditioned flasks containing primary rat hepatocytes 3 days post seeding was found to be below the level of detection for the ELISA used. The results from this in vitro model indicate that IGFBP-5 may not be a suitable biomarker for the detection of ALD, however, to determine this, extended cultured would have to be carried out.

As discussed in the introduction of this chapter, fibrosis plays a role in the pathogenesis of ALD. The activation of quiescent hepatic stellate cells to activated myofibroblasts is a major event leading to significant ECM formation in the liver. It has been previously described that ethanol and its major metabolite, acetaldehyde have the

ability to upregulate fibrogenic markers. Svegliati-Baroni et al. (2001) demonstrated that as early as 2 h post acetaldehyde administration to human stellate cells, collagen I and fibronectin gene expression are increased at transcription level. However, mild ALD is usually asymptomatic which would suggest that markers involving invasive liver biopsy to be carried out in order to assess ECM accumulation (Collagen I or fibronectin) would not be suitable. The diagnosis of mild ALD is determined by non-specific liver injury serum markers, including aminotransferases, in particular AST and gamma-glutamyl transpeptidase (GGT) (Bataller and Brenner, 2005, Gao et al., 2012). There is a potential to develop a co-culture model with primary rat hepatocytes and stellate cells to determine if that would be a more relevant model to determine if IGFBP-5 is a possible biomarker for ALD. Stellate cells are the major cell type involved in the pathogenesis of fibrosis, through their activation and ECM production after liver injury. Oxidative stress has been implicated in the activation of stellate cells (Hautekeete and Geerts, 1997). Evidence from clinical and experimental studies have implicated ROS in the pathogenesis of fibrosis. ROS has been demonstrated to increase stellate cell proliferation and invasion Galli et al. (2005).

The data collated in this chapter highlights the unsuitability of the monolayer culture of primary rat hepatocytes for chronic low toxicity studies, of both menadione and H_2O_2, and ethanol and its primary metabolite acetaldehyde. Rapid dedifferentiation of the hepatocytes in this in vitro culture could be attributed towards the poor predictivity of toxicity for the classic oxidative toxins and ethanol. As discussed above, other research groups have published data in contradiction to the results presented here. This could be attributed to the dedifferentiation of the hepatocytes. It is well understood that monolayer cultures of hepatocytes dedifferentiate in vitro rapidly. However, many advances are currently being made to maintain hepatic phenotype over time in culture (Elaut et al., 2006, Schug et al., 2008, Godoy et al., 2013, Soldatow et al., 2013, LeCluyse et al., 2012, Grant et al., 1985). Chapter 3 highlighted the rapid dedifferentiation of cells once plated after isolation. GSTP1 expression (Figure 3.10) after 1 day in culture was significantly lower than that observed thereafter up to 9 days in culture. Similarly, upon seeding, a loss in P450 activity was observed (Figure 3.11)

as monitored via testosterone metabolism. Schug et al. (2008) carried out a study comparing monolayer, Matrigel and sandwich cultures for the use in genotoxicity studies with particular interest in the following genes; Abat, Gsk3β, Myd116 and Sult1a1. Sandwich cultures of hepatocytes prepared by layering hepatocytes between two thin layers of collagen type 1 and Matrigel sandwich cultures prepared in the same way, outperformed the monolayer culture in maintenance of the genes of interest above (Schug et al., 2008). Layering hepatocytes between ECM maintains a more in vivo like structure of the hepatocyte and maintains polarity, in contrast to more fibroblastic like hepatocytes in monolayer culture, hence overcoming the rapid dedifferentiation. In comparison with the testosterone hydroxylation results shown in Chapter 3 with primary rat hepatocytes, studies have shown that collagen sandwich cultures can maintain testosterone hydroxylase activity for up to 6 days in culture and although the metabolic activity was decreasing, metabolites can be detected up to 14 days in culture (Kern et al., 1997). These authors also demonstrated the maintenance of Phase II activity for up to 14 days in culture. Matrigel is a protein mixture secreted by Engelbreth-Holm-Swarm (EHS) mouse sarcoma cells, and is commercially available through Corning Life Sciences. Although the exact contents of the mixture are unknown, it is well-known to contain levels of growth hormones including hepatocyte growth factor (HGF) and epithelial growth factor (EGF). It has also been suggested that co-culture of hepatocytes with non-parenchymal cells (stellate, sinusoidal endothelial or Kupffer cells) prolongs the life of hepatocytes in vitro. Bhatia et al (1999) demonstrated by micropatterning hepatocytes and murine 3T3 fibroblasts, hepatocyte phenotype was modulated. Collagen was micropatterned on tissue culture plastics where hepatocytes were seeded. Around these patterns of hepatocyte islands, murine 3T3 cells were seeded. Micropatterned co-cultures exhibited significantly higher liver-specific functions (albumin secretion) for up to 11 days in culture, in comparison with micropatterned mono-cultures. In conventional monolayer culture, Rogiers et al (1990) demonstrated that co-cultures of primary rat hepatocytes and rat liver epithelial cells outperformed monocultures of primary rat hepatocytes. Despite an initial decrease in P450 content, the level stabilised out to 14 days in culture in comparison with monocultures in which CYP content decreased as a function of time.

Likewise, P450 activity (ECOD activity) in co-cultures was also maintained to 14 days in culture outperforming the monocultures.

To conclude, a more sophisticated culture of hepatocytes, whether in mono or co-culture may be necessary to truly ascertain if IGFBP-5 is a suitable biomarker for chronic low toxicity in the liver as a more differentiated state of hepatocytes is required. However, monolayers of hepatocytes are cheap and readily available. The following chapter begins to determine if IGFBP-5 adenovirally transfected into the hepatocytes influences the toxic effects of menadione and H_2O_2. IGFBP-5 has already been shown to induce and exacerbate several fibrotic diseases, and both toxins contribute to an oxidative state in cells which chronically can lead to fibrosis in vivo.

Chapter 5 Transfection of Primary Rat Hepatocytes with WT-IGFBP-5 and toxicity with Menadione and Hydrogen Peroxide

5.1 Introduction

In Chapter 4, toxicity of menadione, H_2O_2, ethanol and its major toxic metabolite acetaldehyde was assessed to determine if chronic sub lethal dosing for 9 days would cause an increase in IGFBP-5 production from primary rat hepatocytes. In this chapter we aimed to determine if we could successfully transfect primary rat hepatocytes with adenoviral IGFBP-5 and subsequently determine if the presence of IGFBP-5 enhanced the toxic effects of both menadione and H_2O_2.

5.1.1 Liver Fibrosis

Liver fibrosis, the excessive accumulation of extracellular matrix proteins including collagen and fibronectin can be caused by persistent stress on the liver from many forms of toxins, including fat, xenobiotic drugs and alcohol (Bataller and Brenner, 2005f). Various types of autoimmune disease and hepatic infections are also common causes of fibrosis i.e. α_1-antitrypsin deficiency (de Serres and Blanco, 2014) and viral hepatitis (Su et al., 2014). After acute liver injury, parenchymal cells regenerate to replace apoptotic and/or necrotic hepatocytes. Limited deposition of ECM occurs with an associated inflammatory response. Occurring as an isolated case, this would not progress to fibrosis, however, if hepatic injury persists, eventually hepatic regeneration will cease and hepatocytes are substituted with ECM (Bataller and Brenner, 2005, Friedman, 2003).

It is well understood that hepatic stellate cells are the main source of extracellular matrix production. Hepatic stellate cells comprise of about 1.4 % of the total liver volume and are present in a 1:20 ratio with hepatocytes. They are typically located in the perisinusoidal Space of Disse and recess between endothelial cells and hepatocytes (Figure 1.1) (Moreira, 2007, Geerts, 2001, Martini et al., 2007). Stellate cells are the main storage site for vitamin A and are essential in the regulation of retinoic acid homeostasis. In a healthy liver, stellate cells are responsible for the maintenance of

levels of membrane matrix typically collagen types IV and VI in hepatic sinusoids. However, upon liver injury stellate cells become activated from a quiescent state to a myofibroblastic-like cell. Upon activation, stellate cells exhibit some phenotypic changes i.e. increased levels of α smooth muscle actin (αSMA), loss of retinoid storage capabilities and the acquisition of their fibrogenic potential. Activation leads to the deposition of ECM, including several types of collagen (e.g. I, V and VI), laminin, hyaluronan and proteoglycans. As well as producing several types of ECM, stellate cells and particularly activated stellate cells produce and secrete matrix metalloproteinases (MMPs) and their inhibitors (Geerts, 2001, Hautekeete and Geerts, 1997).

Oxidative stress plays a role in the progression of acute liver injury to fibrosis. This occurs when oxidative stress related molecules i.e. ROS are generated at a level that exceeds the intracellular antioxidant defences e.g. catalase, SODs, GSH and GSTs.

5.1.2 IGFBP-5 and its role in fibrosis

Given this body of evidence supporting a role for IGFBP-5 in fibrosis, in lung, skin and liver, we proposed to transfect primary rat hepatocytes with adenoviral IGFBP-5 and determine if this had any positive or negative effects on cell survival post-dosing with both of the commonly used oxidative toxins investigated in Chapter 4.

5.2 Methods

5.2.1 Preparation and Isolation of Primary Rat Hepatocytes

Primary rat hepatocytes were isolated as previously described in Chapter 2 (see section 2.2.1-2.2.3).

5.2.2 Transfection with wild-type (WT) IGFBP-5 and an Empty Vector

5.2.2.1 Production of recombinant wild type IGFBP-5 and IGFBP-5 adenovirus

Recombinant wild type IGFBP-5 was produced by the David J. Flint Laboratory at Strathclyde University (Allan et al., 2002) (see appendix i).

5.2.2.2 Adenoviral transfection with IGFBP-5 and a Null Vector

5.2.2.3 Assessment of viability and metabolic competence of primary rat hepatocytes in the presence of Ad IGFBP-5 or a Null vector.

24-well plates were prepared by coating with collagen at a concentration of 30 µg/cm^2 and subsequently seeded with primary rat hepatocytes at a density of 1.5 x 10^5 cells/cm^2 in serum containing complete medium (Williams' E containing 5 % v/v Foetal Calf Serum (FCS), L-glutamine (2 mM), penicillin G (50 units/ml), streptomycin sulphate (50 µg/ml) and fungizone (250 µg/ml)). Plates were incubated at 37 °C for 2 h after which time medium was removed and replaced with serum-free complete medium containing either Ad IGFBP-5 or null vector (NV) at known concentrations (See Table 4.1). After a further 2 h in culture, 5 % serum was supplemented into each well. 24 h after seeding, medium was removed from each well, cells were washed with dPBS x 2 and 500 µl of fresh complete medium was placed in each well. After 72 h in culture, a variety of assays were performed including WST-1, CV, and IGFBP-5 release into the cell culture medium to determine the effects of transfection of hepatocytes with Ad IGFBP-5 or a NV and to determine if the cells subsequently produced higher levels of de novo IGFBP-5.

MOI	Concentration of stock	µl of stock added
0 (control)	No addition	No addition
10	10^8 virus particles/ml	10
50	10^9 virus particles/ml	5
200	10^{10} virus particles/ml	2
1000	10^{10} virus particles/ml	10

Table 5-1 Multiplicity of infection (MOI) used for assessment of primary rat hepatocytes post infection with Ad IGFBP-5 and an NV.

5.2.2.2 Hydrogen peroxide and menadione dosing post infection with Ad IGFBP-5 and an NV.

Primary rat hepatocytes were cultured on collagen coated (30 µg/cm^2) 24- and 96- well plates were seeded at a density of 1.5 x 10^5 cells/cm^2. Cells were transfected as described in Section 5.2.2.1 at an MOI of 50. After transfection, medium was removed and replaced with medium containing hydrogen peroxide (0.5 mM) or menadione (10 µM) in a total volume of 0.5 ml. After 24 h exposure, hydrogen peroxide and menadione were spiked into cultures at 0.5 mM and 10 µM, respectively. Control wells had medium only added (0.5ml). After a further 24 h incubation, the medium was removed and stored at -70 °C awaiting analysis of IGFBP-5 release into the medium. Samples were also stored for GSH analysis, total protein measurement and CV staining.

5.2.3 WST-1 Assay

WST-1 was carried out as previously described in Chapter 2 (see section 2.13).

5.2.4 Crystal Violet (CV) assay

Crystal violet assay was performed as previously described in Chapter 2 (see section 2.14).

5.2.5 LDH

Lactate dehydrogenase release into the medium was assayed as previously described in Chapter 2 (see section 2.11).

5.2.5 Determination of reduced glutathione (GSH) by fluorimetry

GSH was measured as previously described in Chapter 2 (see section 2.12).

5.2.6 Measurement of IGFBP-5 by ELISA

Human IGFBP-5 was measured as previously described in Chapter 2 (see section 2.15) and mouse IGFBP-5 was measured as previously described in Chapter 2 (see section 2.9).

5.3 Results

5.3.1 Assessment of viability and metabolic competence of primary rat hepatocytes in the presence of WT IGFBP-5 and an EV.

After 48 h in culture post transfection with either Ad IGFBP-5 or NV, medium samples were analysed for the release of IGFBP-5. IGFBP-5 was released into the cell culture medium in a dose dependent manner in the presence of increasing concentrations of Ad IGFBP-5 (see Figure 5.1). WST-1 activity (Figure 5.2) demonstrated that the addition of an empty vector to hepatocytes in culture does not impact on the cells basic metabolic competence. There was however a drop in WST-1 activity seen at the highest MOI of IGFBP-5. Despite an impact on the cells ability to reduce WST-1, there is no impact on CV and total protein content (Figure 5.3 and 5.4) between each condition. Reduced intracellular glutathione (Figure 5.5) is also not affected in comparison with controls with the addition of either null or Ad IGFBP-5. Figure 5.6 demonstrates that the addition of either the empty vector or the Ad IGFBP-5 did not affect the cells morphology.

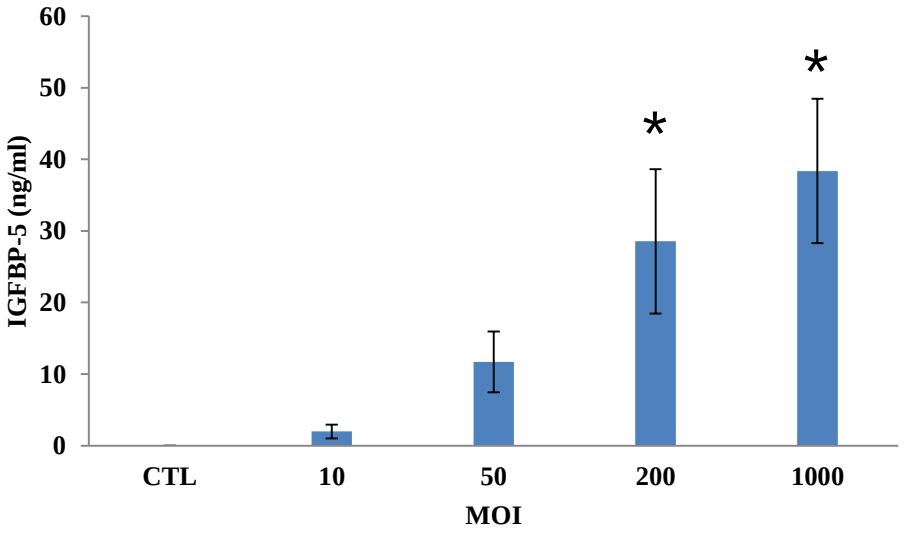

Figure 5-1 IGFBP-5 secreted after Ad IGFBP-5 infection.

*IGFBP-5 secreted into the medium from primary rat hepatocytes 48 h post infection with Ad IGFBP-5 in collagen (in-house prepared) coated 24-well plates. Results are Mean ± SEM, n = 3 separate experiments. * $p \leq 0.05$ significantly different from control (0 MOI) (ANOVA followed by Dunnett's individual error rate)*

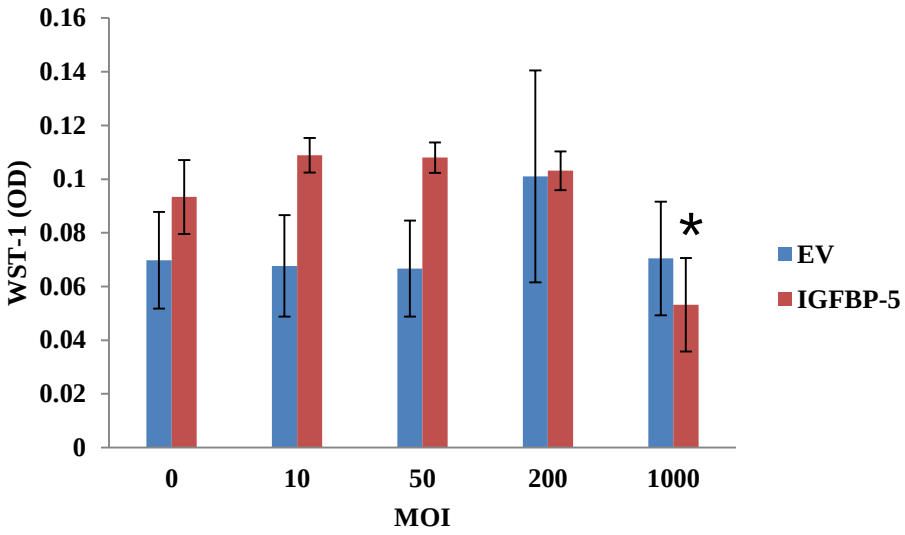

Figure 5-2 WST-1 activity after infection with EV or Ad IGFBP-5.

*Primary rat hepatocytes 48 h post infection with either Ad IGFBP-5 or an EV in collagen (in-house prepared) coated 96-well plates. Results are Mean ± SEM, n = 3 separate experiments. * $p \leq 0.05$ significantly different (ANOVA followed by Dunnett's individual error rate), compared with controls.*

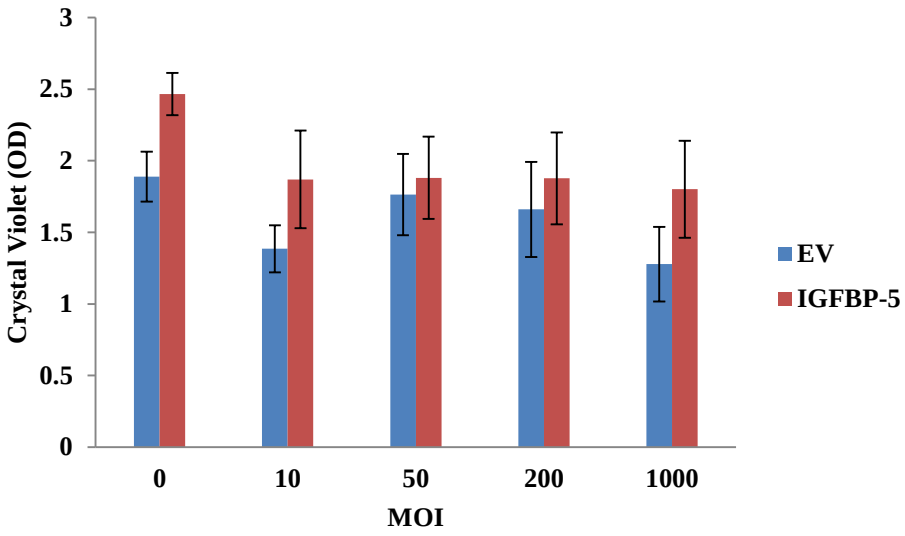

Figure 5-3 CV assays results afterinfection with EV or Ad IGFBP-5.

Primary rat hepatocytes 48 h post infection with either Ad IGFBP-5 or an EV in collagen (in-house prepared) coated 96-well plates. Results are Mean ± SEM, n = 3 separate experiments. No statistical difference was observed by ANOVA followed by Dunnett's individual error rate.

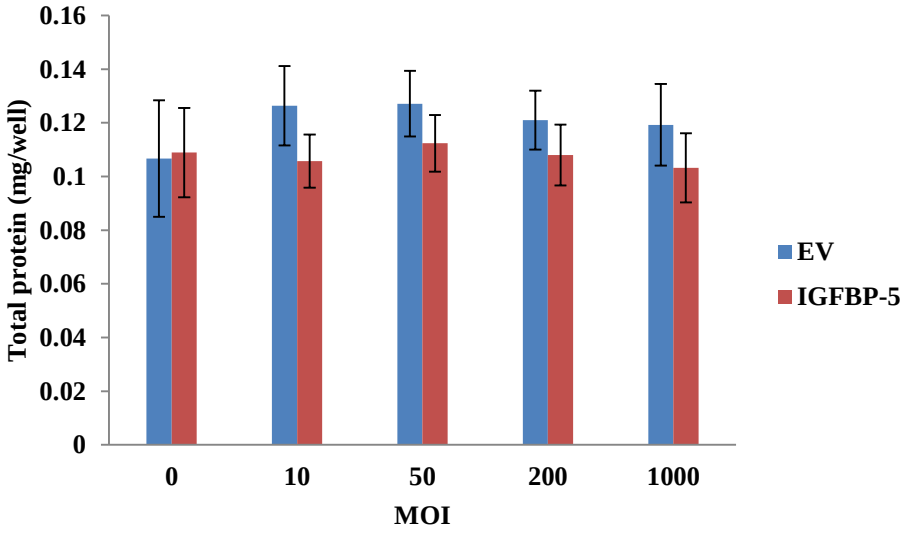

Figure 5-4 Total protein results after infection with EV or Ad IGFBP-5.

Primary rat hepatocytes 48 h post infection with either Ad IGFBP-5 or an EV in collagen (in-house prepared) coated 24-well plates. Results are Mean ± SEM, n = 3 separate experiments. No statistical difference was observed in comparison with control by ANOVA followed by Dunnett's individual error rate

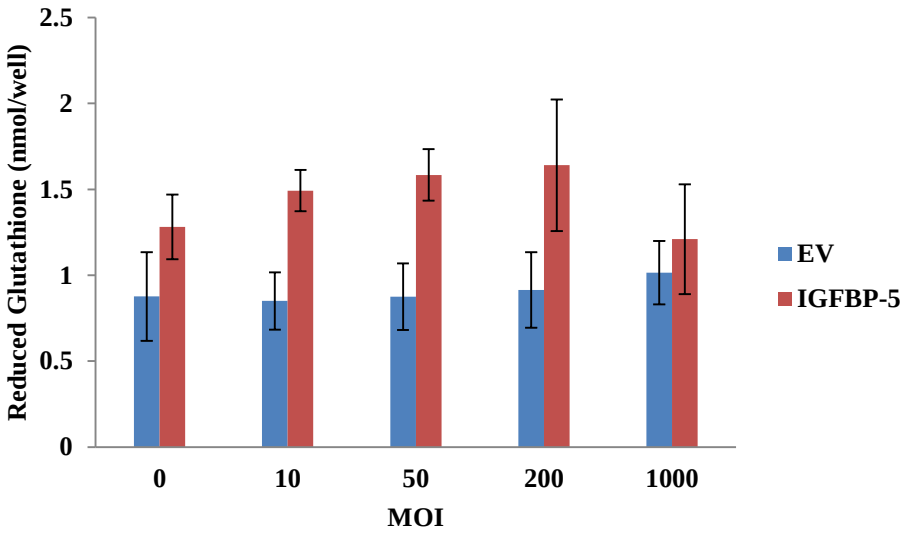

Figure 5-5 Reduced Glutathione results after infection with EV or Ad IGFBP-5.

Primary rat hepatocytes 48 h post infection with either Ad IGFBP-5 or an EV in collagen (in-house prepared) coated 24-well plates. Results are Mean ± SEM, n = 3 separate experiments. No statistical difference was observed in comparison with control by ANOVA followed by Dunnett's individual error rate

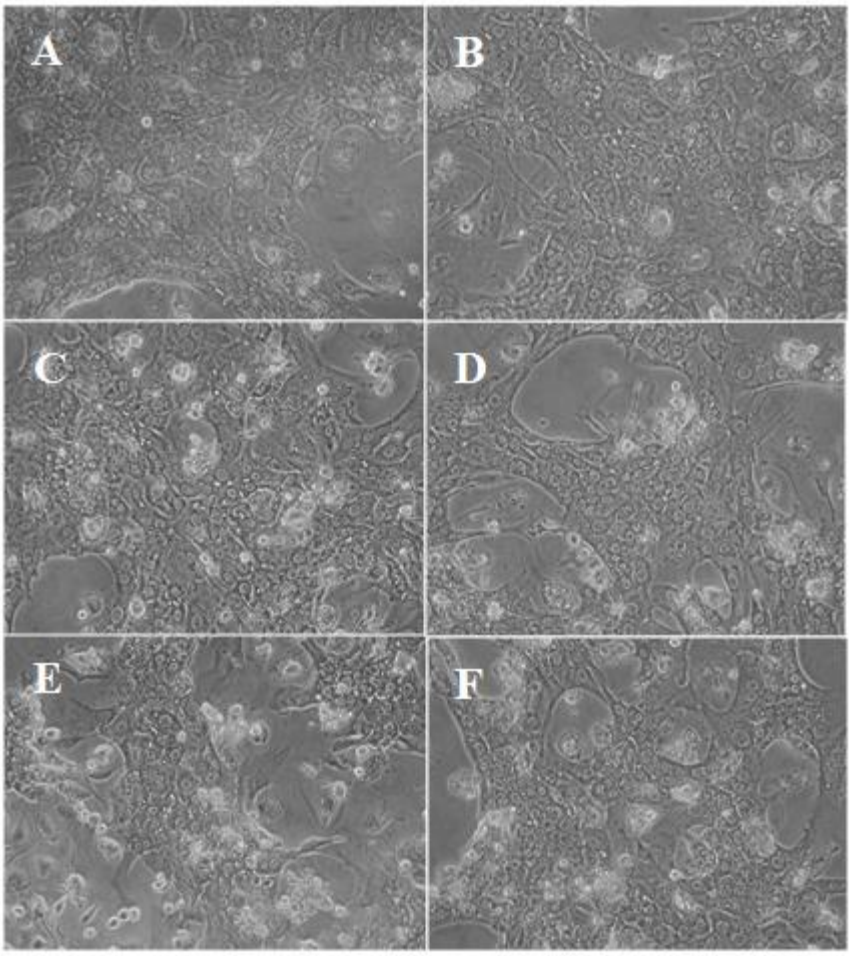

Figure 5-2 Images (of primary rat hepatocytes after infection with Ad IGFBP-5 or an EV.

Images (10x magnification) of primary rat hepatocytes on collagen coated 24-well plate after 48 h after infection with Ad IGFBP-5 or an EV. A, B Control wells; C 50 MOI of Ad IGFBP-5; D 50 MOI of EV; E 200 MOI of Ad IGFBP-5; F 200 MOI of EV.

5.3.2 Assessment of the effects of hydrogen peroxide and menadione dosing for 48 h post adenoviral infection with WT-IGFBP-5 and Null Vector.

Hydrogen peroxide was demonstrated to be non-toxic at concentrations between 0.01 and 0.5 mM in Chapter 4. Again, chronic dosing of 0.5 mM H_2O_2 48 h after hepatocytes transfection with Null vector or IGFBP-5 was not acutely toxic. CV staining showed no decrease with transfection of either a Null vector or IGFBP-5, or after 48 hr exposure to H_2O_2 (see Figure 5.7). After 24 h exposure to H_2O_2, no drop in

WST-1 (Figure 5.8) activity was measured, this was also the case after 48 h. An increase was seen, however, between the 24 and 48 h measurement for all conditions. Reduced glutathione (Figure 5.9) was also measured after 24 and 48 h exposure to the oxidative toxin. In the presence of 0.5 mM H_2O_2, a drop in GSH was observed, however, this was not compounded by the transfection of the hepatocytes with either a null vector or IGFBP-5. Total protein (Figure 5.10) confirmed that no gross cell death was observed over the duration of the culture (72 h).

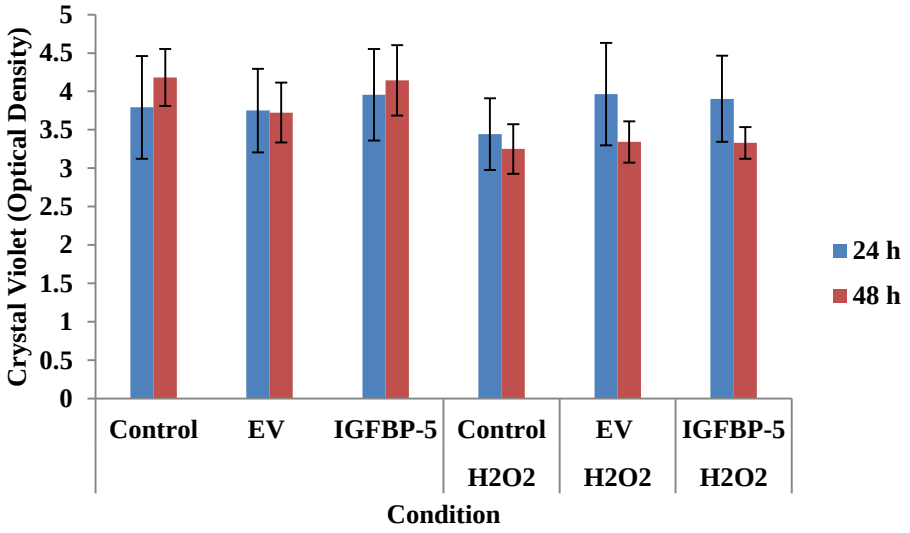

Figure 5-3 CV staining: infection with EV or Ad IGFBP-5 and H_2O_2 co-dosing.

Primary rat hepatocytes infected with either Ad IGFBP-5 (MOI 50) or an EV (MOI 50) 24 and 48 h post exposure with hydrogen peroxide (H2O2) in collagen (in-house prepared) coated 96-well plates. Results are Mean ± range, n = 2 separate experiments.

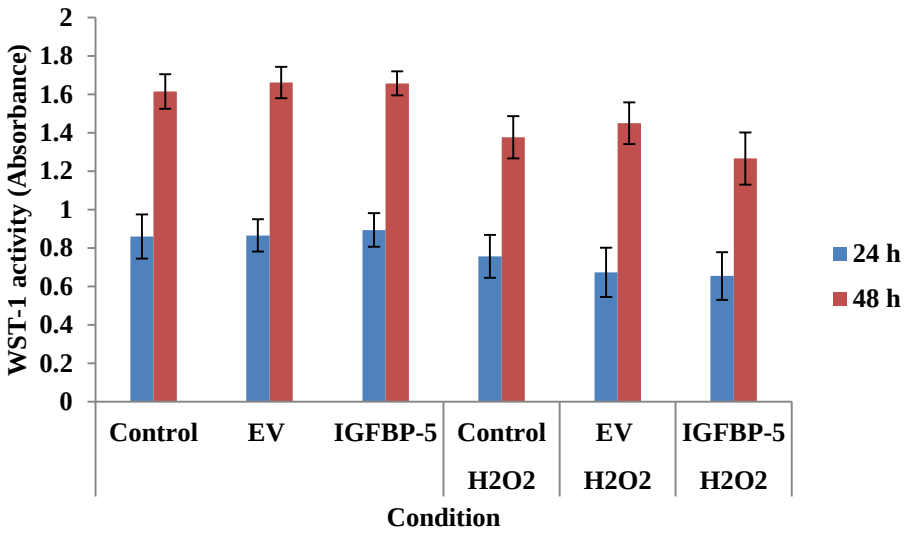

Figure 5-4 WST-1 activity: infection with EV or Ad IGFBP-5 and H_2O_2 co-dosing.

Primary rat hepatocytes infected with either Ad IGFBP-5 or an EV 24 and 48 h post exposure with hydrogen peroxide (H2O2) in collagen (in-house prepared) coated 24-well plates. Results are Mean ± range, n = 2 separate experiments.

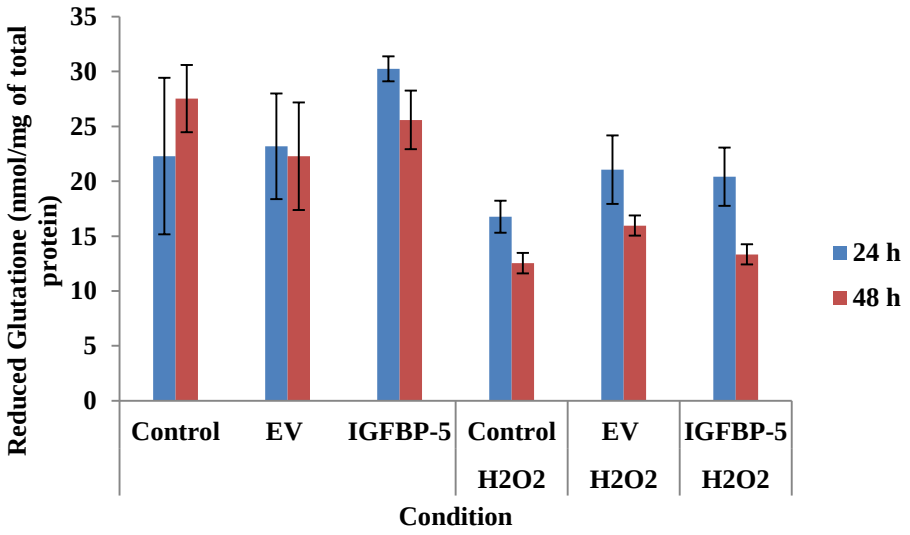

Figure 5-5 Intracellular GSH: infection with EV or Ad IGFBP-5 and co-dosing with H_2O_2.

Primary rat hepatocytes infected with either Ad IGFBP-5 or an EV 24 and 48 h post exposure with Hydrogen Peroxide (H2O2) in collagen (in-house prepared) coated 24-well plates. Results are Mean ± range, n = 2 separate experiments.

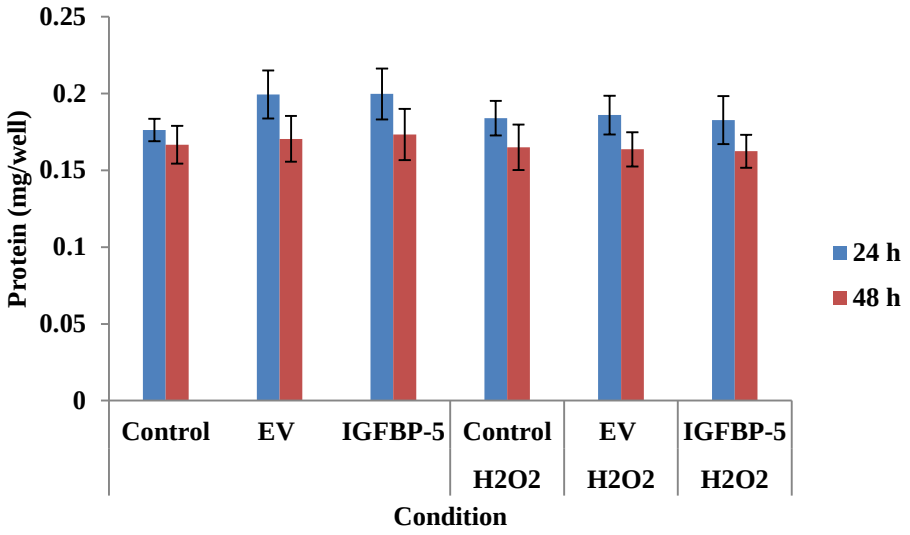

Figure 5-6 Total cellular protein: infection with EV or Ad IGFBP-5 and co-dosing with H_2O_2.

Primary rat hepatocytes infected with either Ad IGFBP-5 or an EV 24 and 48 h post exposure with Hydrogen Peroxide (H2O2) in collagen (in-house prepared) coated 24-well plates. Results are Mean ± range, n = 2 separate experiments.

A sub-toxic concentration of 10 µM was chosen to determine if the presence of IGFBP-5 in the cells had any effect on the toxicity. Crystal violet assay (Figure 5.11) demonstrated that no toxic effects were elicited post transfection and exposure to menadione for 24 and 48 h. Likewise, WST-1 assay demonstrated that no toxic effects were seen (Figure 5.12) after transfection and exposure to 10 µM menadione. Reduced glutathione was decreased from 33.38 nmol/mg to 28.50 nmol/mg of total protein in the presence of menadione for 24 h, and decreased again to 24.34 nmol/mg with both transfection with IGFBP-5 and menadione dosing for 24 h. This effect, however, was not seen after 48 h (Figure 5.13). Total protein (Figure 5.14) values from each well after both 24 and 48 h exposure to menadione in the presence and absence of transfected IGFBP-5 confirmed that no gross toxicity was observed.

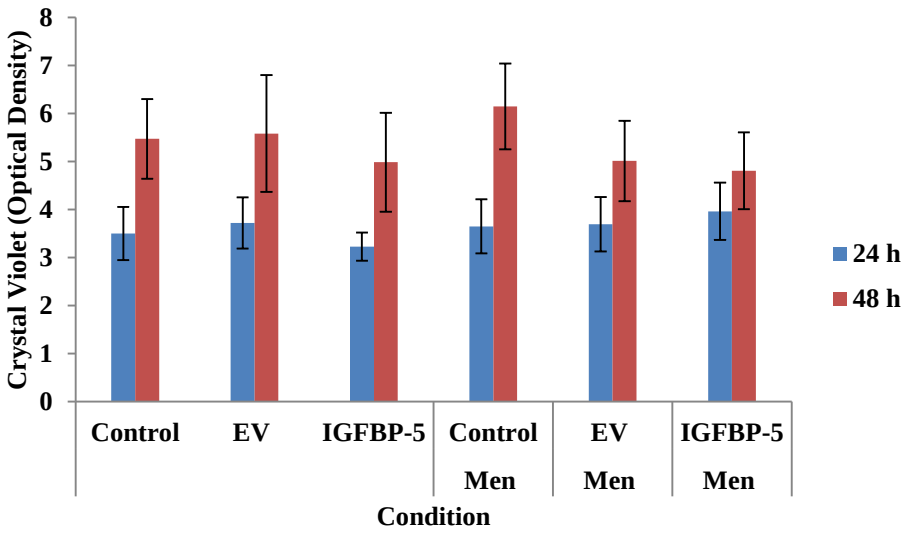

Figure 5-7 CV staining: infection with EV or Ad IGFBP-5 and co-dosing with menadione

Primary rat hepatocytes infected with either Ad IGFBP-5 or an EV 24 and 48 h post exposure with menadione (Men) in collagen (in-house prepared) coated 96-well plates. Results are Mean ± range, n = 2 separate experiments.

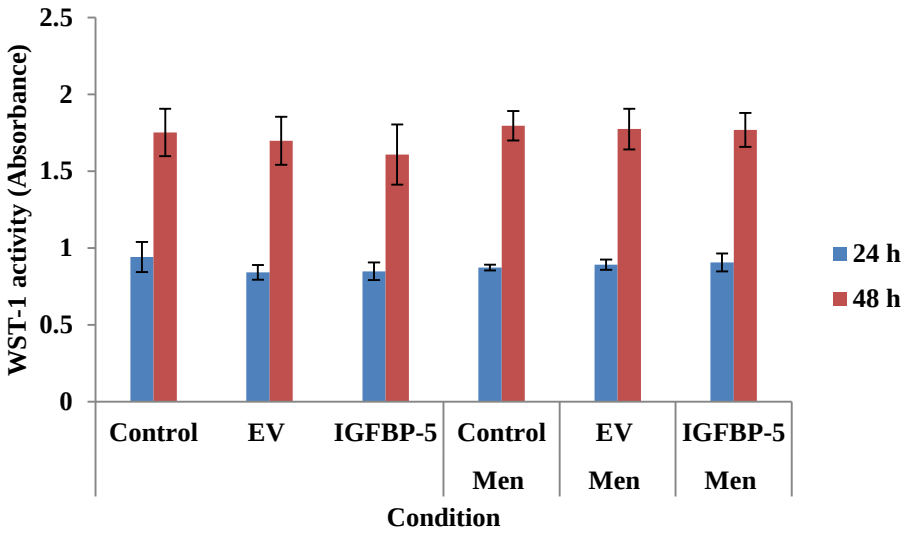

Figure 5-8 WST-1 activity: infection with EV or Ad IGFBP-5 and co-dosing with menadione.

Primary rat hepatocytes infected with either Ad IGFBP-5 or an EV 24 and 48 h post exposure with menadione (Men) in collagen (in-house prepared) coated 24-well plates. Results are Mean ± range, n = 2 separate experiments.

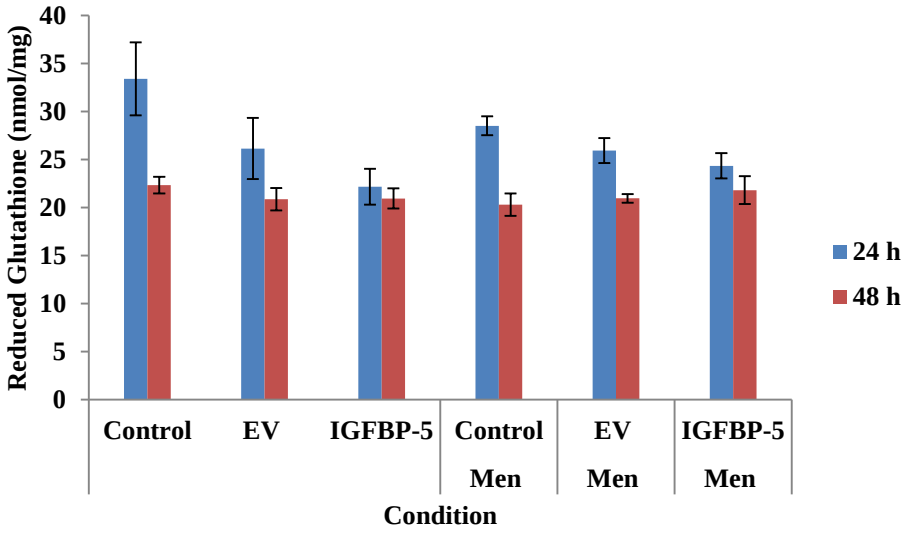

Figure 5-9 Intracellular GSH: infection with EV or Ad IGFBP-5 and co-dosing with menadione.

of primary rat hepatocytes infected with either Ad IGFBP-5 or an EV 24 and 48 h post exposure with menadione (Men) in collagen (in-house prepared) coated 24-well plates. Results are Mean ± range, n = 2 separate experiments.

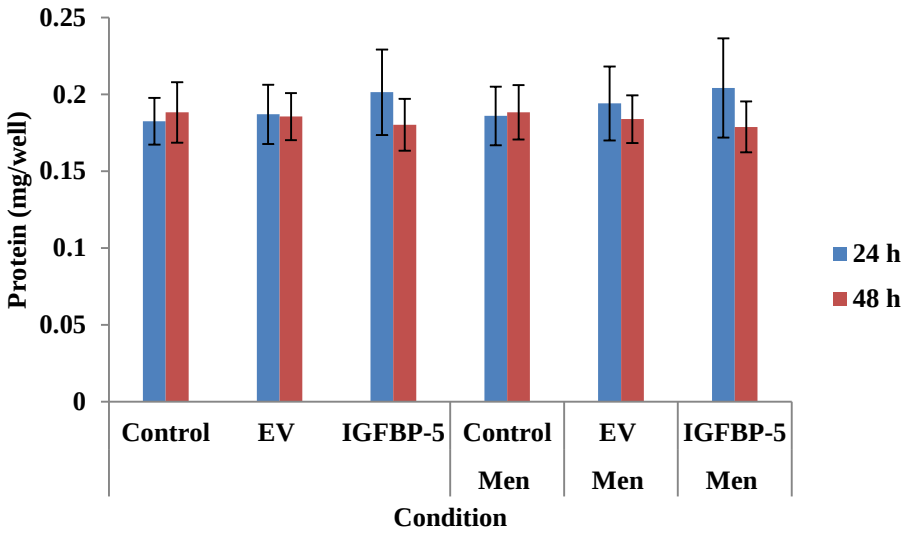

Figure 5-10 Total cellular protein: infection with EV or Ad IGFBP-5 and co-dosing with menadione.

Primary rat hepatocytes infected with either Ad IGFBP-5 or an EV 24 and 48 h post exposure with menadione (Men) in collagen (in-house prepared) coated 24-well plates. Results are Mean ± range, n = 2 separate experiments.

5.4 Discussion

The ability to infect primary rat hepatocytes with IGFBP-5 using adenovirus permitted the study of its effects on oxidative stress induced by the addition of H_2O_2 and menadione.

The first aim of this chapter was to determine if primary rat hepatocytes could be successfully infected with adenoviral IGFBP-5 without compromising the viability of the hepatocytes. Sokolovic et al (2012) successfully demonstrated in vivo transfection of IGFBP-5 in mouse liver. Modifications to the culture protocol designed in Chapter 2 were made to allow for the transfection of the hepatocytes in the absence of serum for 2 h in the early stages of attachment post seeding. A number of MOI were assessed for both the adenoviral IGFBP-5 and a null vector as a control. Several parameters were measured in assessing cell health 48 h post infection with both vectors. WST-1 demonstrating the reductive capacity of the cells showed no significant effects in comparison with the control except for the highest MOI of 1000 ($p \leq 0.05$) with adenoviral IGFBP-5 (0.09 ± 0.01 optical units to 0.05 ± 0.01 optical units respectively). Crystal violet staining, a marker of cell number per well, demonstrated no significant loss in cell number with either adenoviral IGFBP-5 or the null vector in comparison with control. This was also verified by the total protein values 48 h post infection with the IGFBP-5 adenovirus or the null vector. Despite the response seen with WST-1 at the highest MOI, no significant changes were seen in intracellular GSH levels post infection. As a result of this, we could conclude that all MOI except IGFBP-5 at 1000 would be acceptable for the infection of primary rat hepatocytes. Following this, IGFBP-5 secretion into the medium was assessed by ELISA. As expected, from results in Chapter 2 and 3, levels of IGFBP-5 are low (~0.2 ng/ml) or not measurable at early time points post seeding. In this work, medium was conditioned for 48 h post infection, when IGFBP-5 was measured. As expected, IGFBP-5 was not measurable in medium from the control well where no IGFBP-5 adenovirus was added. Converse to that, the addition of 10 MOI IGFBP-5 adenovirus resulted in a secretion of 1.98 ± 0.95 ng/ml IGFBP-5 (Figure 5.5). The secretion of IGFBP-5 was in a dose-dependent

manner, increasing with higher MOI. The increase was not linear however, as an MOI of 1000 elicited IGFBP-5 concentrations in the medium of 38.37 ± 10.09 ng/ml.

Transfection with IGFBP-5 has been successfully achieved in vivo, in skin (Yasuoka et al., 2006a), lung (Pilewski et al., 2005) and liver (Sokolovic et al., 2012) previously. No literature is available for the transfection of primary rat hepatocytes with IGFBP-5 in vitro, however. Transfection of primary rat hepatocytes in vitro is achievable, and has been demonstrated with many hepatic genes in the literature to study areas including cellular pathways and transcription factor activities (Ginot et al., 1989, Gardmo et al., 2005, Gao et al., 2012). It is widely accepted that primary rat hepatocytes are more difficult to infect with genes in comparison with cell lines such as Huh7.5.1, a human hepatoma cell line used to study Hepatitis C virus in vitro (Gao et al., 2012).

Upon the successful transfection of primary rat hepatocytes with IGFBP-5, a toxicity study was undertaken to determine if the presence of IGFBP-5 enhanced the toxicity on hepatocytes of either H_2O_2 or menadione, both well understood oxidative toxins. An MOI of 50 was chosen as the optimum for IGFBP-5 transfection prior to the addition of toxins, with high levels of IGFBP-5 secretion into the medium without any detrimental effects to the cells. This MOI gave IGFBP-5 concentrations of 11.71 ± 4.25 ng/ml secreted into the medium. Although not significant, this concentration was almost 10 times higher than that produced by normal primary rat hepatocytes in culture for over 9 days (Figure 3.13). Once again, no toxicity was observed with the addition of Null vector or adenoviral IGFBP-5. As demonstrated in Chapter 4, no toxicity was observed with the addition of 0.5 mM H_2O_2. Although, a significant ($p \leq 0.05$) decrease in GSH was observed for all H_2O_2 containing cultures in comparison with control, this was not compounded by the presence of either the null vector or adenoviral IGFBP-5.

Menadione at 50 µM depleted GSH in primary rat hepatocytes culture after 20 min exposure (Thor et al., 1982). Similarly, Starke and Farber (1985) demonstrate 40 % cell death after exposure to 175 µM menadione, by LDH leakage. The aim of this work was not to completely diminish the culture oxidative capacity and cause apoptosis and necrosis, but to impair the cells oxidative capacity chronically over a long period of culture. However, two doses of 10 µM menadione did not elicit any effect. This was also demonstrated by no significant decrease in CV and no impairment of the reductive capacity of the cells as monitored by WST-1. GSH depletion has been demonstrated as the main toxic pathway of menadione in vitro rat hepatocytes culture (Ip et al., 2002, Sun et al., 1990). The presence of IGFBP-5 in the transfected cells did not influence the toxicity of menadione under these conditions.

In this Chapter, it was demonstrated that monocultures of hepatocytes alone dosed with oxidative toxins and transfected with IGFBP-5 did not show any overt toxicity in comparison with results shown in Chapter 3 despite many papers describing the role of IGFBP-5 in fibrosis (Pilewski et al., 2005a, Sureshbabu et al., 2009, Yasuoka et al., 2006a, Yutaka et al., 2008), albeit not in in vitro cultures of primary rat hepatocytes. To fully understand the impact of IGFBP-5 on the progression of fibrosis in in vitro cultures of primary rat hepatocytes, the role of stellate cells could be explored.

Chapter 6 In vitro Model of Non Alcoholic Fatty Liver Disease (NAFLD)

6.1 Introduction

In this chapter, the University of Edinburgh in vitro model of NAFLD (Filippi et al., 2004) was used to determine if IGFBP-5 is a suitable marker for the detection of this form of liver disease. C3A cells (a clonal derivative of the hepatoblastoma-based HepG2 cell line) were treated with either lactate, pyruvate, octanoate (saturated fatty acid) and NH_4Cl (LPON) or with Oleate for a period of up to 7 days as a model of lipid accumulation in vitro to generate an in vitro model of NAFLD. The C3A cell line was derived by James H Kelly at Baylor College of Medicine, Texas in the early 90s for use in liver assist devices to replace the use of primary cells (Kelly, 1994). C3A cells exhibit an enhanced hepatic phenotype over HepG2 cells, namely albumin secretion but also alpha feto protein (AFP) production.

LX2 cells (human hepatic stellate cell line) were also studied in the presence of IGFBP-5 and conditioned medium from C3A cells (a clone of HepG2 cells) treated with fatty acids to simulate NAFLD to determine if cell activation could be observed. Many studies have demonstrated the need for hepatic stellate cells for the study of fibrosis (Moreira, 2007, Hautekeete and Geerts, 1997, Poli, 2000, Bataller and Brenner, 2005). An in vitro model of non-alcoholic fatty liver disease (NAFLD) was investigated to determine if IGFBP-5 could be a potential biomarker to detect the early stages of this disease. Data from a model utilising C3A cells and fatty acids developed in the University of Edinburgh are presented in Chapter 5 on the potential of IGFBP-5 as a biomarker for the detection of NAFLD (Lockman et al., 2012, Filippi et al., 2004). Conditioned medium from the NAFLD C3A model was also used to determine if it initiated the transdifferentiation of stellate cells to myofibroblastic cells. In addition, some data are presented from a clinical study to measure IGFBP-5 in the blood of patients with liver disease. The patient study was undertaken to complement the in vitro study of NAFLD. Serum from patients with different liver diseases e.g. steatosis and Type II diabetes, were assessed for IGFBP-5 levels in the serum, and to

determine the potential role of IGFBP-5 as a novel biomarker for the detection of liver disease.

6.1.1 Lactate, Pyruvate, Octanoate and Ammonia (LPON)

LPON was used as a steatoic model of liver disease with ROS. It has previously been shown to induce ROS formation. Lactate and pyruvate are employed as substrates for gluconeogenesis and lipogenesis to enhance ATP turnover and mitochondrial respiration which in turn promote significant intracellular lipid accumulation, due to ROS formation e.g. superoxide anion. Ammonia, metabolised in the urea cycle, also promotes NADH formation, further fuelling the respiratory chain (Lockman et al., 2012). Octanoate is a medium chain fatty acid and does not require transport into the mitochondria by mitochondrial enzymes such as carnitine palmitoyl transferase (CPT). ROS are one of the many factors suggested to have a possible role in insulin resistance (IR). Mitochondrial oxidative phosphorylation has been identified as an important source in palmitate (saturated fatty acid) induced ROS generation also (Nakamura et al., 2009).

6.1.2 Oleate

In contrast to LPON, oleate was used as a steatoic model of liver disease without increased ROS. Oleate is an unsaturated fatty acid and has been shown not to induce insulin resistance in H1IIEC3 hepatocytes (a rat hepatocyte cell line) in vitro. Previous studies have shown that CPT-1a (carnitine palmitoyltransferase-1a) is not induced in the presence of oleate. CPT-1a is rate limiting enzyme in mitochondrial fatty acid β-oxidation (Nakamura et al., 2009). It was also shown that oleate did not increase the expression of the CPT-1a gene (Nakamura et al., 2009). Transport into the mitochondria via CPT for oxidation can be attributed to the higher storage of oleate in comparison to octanoate which diffuses into the mitochondria (Guo et al., 2000). Nakamura et al (2009) demonstrated recently that hepatic insulin resistance could be attributed to induced CPT-1a expression by palmitate and not oleate resulting in accelerated fatty acid oxidation, excess electrons for mitochondrial oxidative phosphorylation, and generation of ROS which in turn impact on insulin signalling

pathways by activating JNK and impairing tyrosine phosphorylation of insulin receptor substrate-2 (IRS-2).

The aim of this chapter was to determine if either model of steatosis had any influence on the secretion of IGFBP-5.

6.1.3 IGFBP-5 in Human Serum

The prevalence of NAFLD in Europe and the Middle East is reported to be in the range of 20 – 30 % of the population (Loomba and Sanyal, 2013). One third of the US population is obese and with correlations between NAFLD and obesity, speculation can be made about the percentage of the population with NAFLD (Loomba and Sanyal, 2013). A patient study was also carried out in collaboration with the Royal Infirmary of Edinburgh, Edinburgh, UK. Serum samples from patients with various liver diseases were collected and stored at -80 °C for further analysis. Primarily, the aim was to determine if patients at different stages of the NAFLD spectrum had measureable serum levels of IGFBP-5. Evidence in the literature suggests many roles of IGFBP-5 in the progression of fibrosis (Pilewski et al., 2005, Yasuoka et al., 2006, Yasuoka et al., 2006b), and potentially it may also play a role in the pathogenesis of chronic liver disease. Of interest in the set of patient serum samples were Type II diabetes patients. NAFLD has a strong association with metabolic syndrome (MS) (Adams et al., 2009), with IR being of huge interest (Adams et al., 2005, Tarantino et al., 2010). Samples from these patients allowed us to target the early stages of chronic insult on the liver, and investigate the role and expression of IGFBP-5 over a wide variety of liver diseases. The aim of this study was to determine if IGFBP-5 could be measured easily from human serum and evaluate its potential as a biomarker of early stages of liver disease. Samples were obtained from patients with the following liver disease: Type II diabetes, Steatosis, NAFLD non cirrhotic, NAFLD cirrhosis and NASH non cirrhotic. NAFLD was confirmed by histological imaging of liver tissue containing fat accumulation in the form of triglycerides in > 5 % liver cells without inflammation. NASH patients, a subgroup of NAFLD, presented with fat accumulation accompanied by inflammation and liver cells injury (Krawczyk et al., 2010).

6.2 Methods

6.2.1 In vitro Model of NAFLD

6.2.1.1 10 x PBS

NaCl	40 g	1.37 M
KCl	1 g	26.8 mM
Na_2HPO_4	7.2 g	101.4 mM
KH_2PO_4	1.2 g	17.64 mM

All chemicals were dissolved in 400 ml of distilled H_2O. pH was adjusted to 7.4 with 1 M NaOH and the volume was made up to 500 ml with distilled H_2O.

6.2.1.2 Octanoate 0.1 M

865.2 mg of caprylic (octanoic) acid was weighed out and added to 40 ml distilled water; the acid is a liquid. Mixing for 2 – 3 h was required to break up the oily droplets. The volume was then made up in 60 ml distilled water. The pH of the solution was adjusted to 7.0 – 7.4 with 3 M NaOH. The octanoate solution was aliquoted into 5 ml aliquots and stored at -20 °C in glass bottles.

6.2.1.3 Oleate 18 mM/BSA 18 % w/v solution

20 ml BSA solution was made up by adding 4 g BSA to 20 ml distilled water. To the 18 % w/v BSA solution, 109.6 mg oleate was added. The solution was placed in a sonication bath surrounded by ice and water for at least 1 working day to dissolve. The final solution was aliquoted and then stored at -20 °C in glass bottles.

6.2.1.4 C3A cell culture

C3A cells (ATCC, USA) were cultured in T 25 flasks (2.5 x 10^5 cells/cm^2) in 3 ml minimum essential medium Eagle (MEME; Sigma, UK) with 10 % FCS, penicillin (100 IU/ml) and streptomycin (100 mg/ml) and incubated at 37 °C with 5 % CO_2 until

80 % confluent. Once confluent, cells were divided in to 3 groups, Control, LPON (10/1/2/2 mM) and Oleate 250 µM. MEME was removed and replaced with 3 ml of either group (Control/LPON/Oleate) (see Table 6.1) and cells were cultured for up to 7 days. Medium was changed at 3 and 5 days.

LPON (10 ml)	0.1 M Octanoate	200 µl
	NH_4Cl	40 µl
	L/P	100 µl
	MEME + 10% FCS	9.66 ml
Oleate (10 ml)	18 mM Oleate	139 µl
	MEME + 10 % FCS	9.86 ml

Table 6-1 Formulations for LPON and Oleate for addition to C3A cells for preconditioning prepared on the day of culture.

6.2.1.5 Oil Red O

A stock solution was prepared by dissolving 0.5 g Oil Red O in 60 % alcohol by warming at between 56 and 60 °C for approximately 1 h. A working solution was prepared by dissolving 6 parts stock solution in 4 parts water. It was allowed to stand for 10 minutes, and then filtered for immediate use.

6.2.1.6 Haematoxylin/Oil Red O staining of intracellular lipids

C3A cells were cultured on chamber slides (Nunc, Lab-Tek Chamber Slide System) seeded at 2.5 x 10^5 cells/cm^2 under the same conditions as stated in Section 6.2.4. After 7 days in culture with LPON, oleate or control medium, cells were fixed with 10 % neutral buffered formalin. 60 % ethanol was then used to wash the cells on the slides. The cells were then stained for 15 min in Oil Red O. The cells were then differentiated (removal of excess stain) in 60 % ethanol, followed by washing in distilled water and counterstained with HARRIS Haematoxylin (Sigma Aldrich, Dorset UK), and washed in 1 % acid alcohol (1 ml HCl in 100 ml 70 % ethanol) followed by Scott's tap water

substitute (Sigma Aldrich, Dorset UK). The slides were then washed in water and examined microscopically. This resulted in unsaturated and hydrophobic acid and mineral oils staining red. This staining was kindly carried out by Anne Pryde at The Royal Infirmary, Edinburgh.

6.2.1.8 Measurement of IGFBP-5 by human ELISA (R&D Systems, UK)

IGFBP-5 secreted into the supernatant from day 3, 5 and 7 culture was measured by an ELISA using antibodies raised to human IGFBP-5.

The human IGFBP-5 ELISA (R&D Systems, UK) was carried out as previously described in Chapter 2 (see section 2.15).

6.2.1.9 Measurement of IGFBP-5 by human ELISA (Abcam, UK)

The human IGFBP-5 ELISA (Abcam Plc, UK) was carried out as per the manufacturer's instructions. This ELISA kit is specifically designed for use with human serum and plasma and urine.

Wash buffer

Prepare a 1 x working solution from the 20 x wash buffer concentrate

Assay diluent

Prepare a 1 x working solution with distilled water from 5 x concentrated buffer for standard and samples diluent

Standard Preparation

A vial of standard was spun down briefly in a centrifuge and 500 µl of 1 x Assay diluent was added to prepare an 800 ng/ml stock solution. 1 x assay diluent was used as a zero (0 ng/ml) on the standard curve. Serial 3-fold dilutions were used to create the standard curve.

Detection Antibody Preparation

A vial of detection antibody was spun down briefly in a centrifuge and 100 µl of 1 x Assay diluent was added to prepare the detection antibody concentrate. The detection antibody was diluted 80-fold in 1 x assay diluent for use in the assay.

HRP-Streptavadin concentrate

A 1 x solution was prepared from the 700 x concentrated stock in 1 x assay diluent

Stop solution

0.2 M H_2SO_4

All reagents and samples were brought to room temperature. 100 µl of samples and standards were added to the plate, covered and incubated at room temperature for 2.5 h with gentle shaking. After 2.5 h the solution was discarded and wells were washed 4 times with 1 x wash buffer. After the final wash, the plate was inverted and blotted on a paper towel to insure complete removal of wash buffer. 100 µl of 1 x biotinylated detection antibody was added to each well, covered and incubated at room temperature for 1 h with gentle shaking. The wash step was repeated. 100 µl of HRP-streptavadin was added to each well, covered and incubated for 45 min at room temperature with gentle shaking. The wash step was repeated. 100 µ TMB One-step Substrate solution was added to each well, covered and incubated at room temperature for 30 min with gentle shaking. After 30 min, 50 µl stop solution was added to each well and the plate was read at 450 nm immediately on a plate reader.

6.2.3 Induction of fibrosis after exposure to IGFBP-5

C3A cells were cultured as described in Section 6.2.1.4 for 7 days in the presence of LPON, oleate or control medium without any fatty acids added. LX2 cells, gifted from Professor John Plevris, University of Edinburgh, were seeded in T25 flasks at a density of 1 x 10^4 cells /cm^2 in DMEM with 10 % FBS. The LX2 cells were cultured for 3 days to coincide with day 7 culture of the C3A cells. Medium from the C3A cells was collected for immediate use with the LX2 cells. Several medium (DMEM, Life Technologies, UK) compositions were prepared and added to LX2 cells, see Table 5.2.

Wild type IGFBP-5 was produced in-house as previously described (Allan et al., 2002, Shand et al., 2003). LX2 cells were cultured in these compositions for 24 h, when medium was removed and cells were washed 3 x with PBS. Cells were scraped into RIPA buffer (See appendix ii for recipe) (0.5 ml) and homogenised with 7 strokes of a motor driven pestle in a Teflon glass homogeniser. Samples were frozen at -70 °C awaiting analysis for Collagen 1, fibronectin and α-SMA.

Addition	**Concentration**
Control	-
TGF-β (Lonza, Wokingham)	5 ng/ml
IGFBP-5	1 µg/ml
Preconditioned control	1 : 1 ratio with fresh medium
Preconditioned LPON	1 : 1 ratio with fresh medium
Preconditioned Oleate	1 : 1 ratio with fresh medium

Table 6-2 Medium compositions added to LX2 cells after 3 days in culture

6.2.4 Sodium dodecyl sulfate polyacrylamide gel electrophoresis (SDS-PAGE)

See Section 2.2.9

6.2.5 Immunoblotting for Collagen 1, Fibronectin and αSMA

Primary Antibody	**Dilution**	**MW (kDa)**	**Source**
Rabbit polyclonal to Collagen 1	1:5000	42.2	Abcam (ab292)
Rabbit polyclonal to Fibronectin	1:2000	220	Sigma Aldrich (F3648)
Rabbit polyclonal to α-SMA	1:400	400	Abcam (ab5694)

Table 6-3 Primary antibodies used for immunoblotting and dilutions.

5.2.1.7 Human serum samples

Archived patient serum samples were collected from the University of Edinburgh Hepatology Biobank. Patients with NAFLD cirrhosis confirmed by biopsy (n = 3), NASH non cirrhotic, insulin resistant (n = 4), NAFLD non cirrhotic insulin resistant (n = 6), Type II diabetes (n = 6), steatosis (n = 6) and negative controls (n = 6) had serum samples collected and IGFBP-5 was measured from these using commercially available ELISA kits from Abcam and R&D Systems, UK.

6.2.2 Development of assay for the detection of IGFBP-5 in human serum

6.2.2.1 Spiking serum samples with a known standard

Using both commercially available kits, serum samples were spiked with a known concentration of standard (R&D Systems: 10 ng/ml and Abcam: 20 ng/ml) to determine if the serum was having a quenching effect on the ELISA. Varying volumes of serum, between 2 and 50 µl, were used to establish this.

6.2.2.2 Addition of Calf or Chicken serum

Using R&D Systems ELISA kits, standards curves were spiked with 10 µl of chicken serum (Sigma, UK) to determine if it had any interference on the results from the assay. Following this, various volumes (0 – 50 µl) of chicken serum was added to the human serum. The total volume in each well was 100 µl. The addition of chicken serum was carried out to determine if it could prevent the antibodies in the human serum samples interfering from with the antibodies in the assay.

6.3 Results

6.3.1 Oil Red O staining

The images in Figure 6.2 show clearly that the presence of LPON or oleate in the medium increased the amount of lipids in the C3A cells in culture over time. The levels of lipids present in the controls at 3, 5, and 7 days remain similar, however with the addition of LPON or oleate the levels of lipids rise with time.

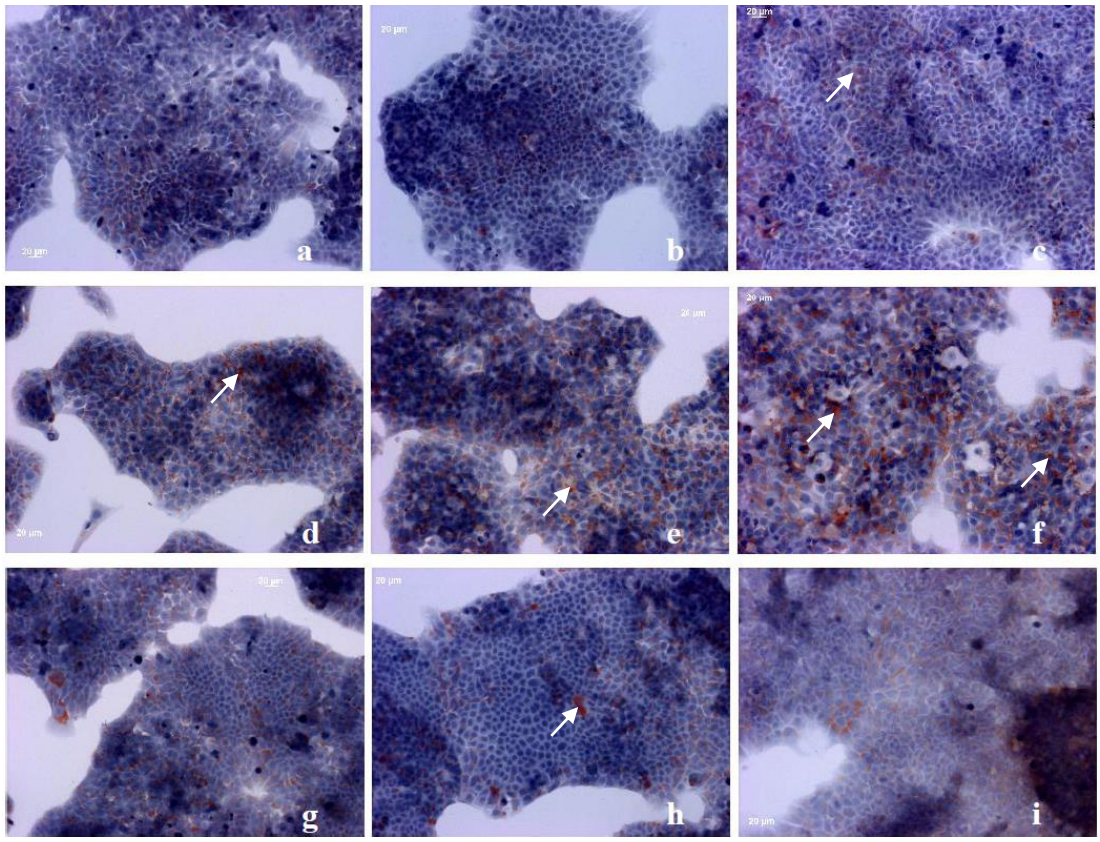

Figure 6-1 Microscopy images of C3A cells incubated with LPON and oleate.

C3A cells in culture for up to 7 days in the presence of LPON or oleate or MEME with FCS a, b and c are C3A cells in MEME with 10% FCS (control) at 3, 5 and 7 days respectively. d, e and f are C3A cells in LPON at 3, 5 and 7 days respectively. g, h and i are C3A cells in oleate for 3, 5 and 7 days respectively. Arrows indicate intracellular lipids stained with Haematoxylin/Oil Red O (10 x magnification). Intracellular lipids appear red.

6.3.2 IGFBP-5 secretion from C3A cells preconditioned with LPON or Oleate

IGFBP-5 release from C3A cells in the presence of LPON or oleate was measured (see Figure 6.3). IGFBP-5 release increased with time in culture with LPON to 0.3 ng/ml. Levels of IGFBP-5 released from cells in the presence of oleate were undetectable at 3 days and at approx. 0.1 ng/ml at 5 and 7 days. IGFBP-5 release from the controls wells were below the limit of detection (not shown on graph).

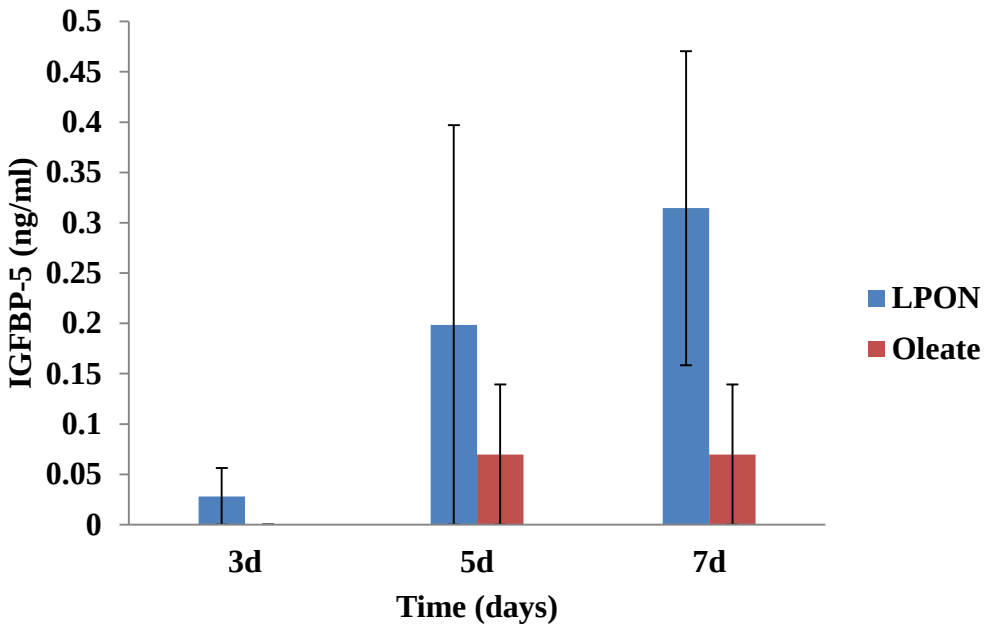

Figure 6-2 IGFBP-5 release from C3A cells in LPON or oleate

IGFBP-5 release into medium from C3A cells in the presence of LPON or Oleate for 3, 5, and 7 days. Cultures were naïve of adenovirus and in monoculture. Results are mean ± SEM, n = 3 No statistical difference was observed

6.3.3 IGFBP-5 measured in Human Serum with varying Liver Diseases

Initial ELISAs were carried out using the R&D systems ELISA kit, however, no IGFBP-5 was measured in the human serum. On consultation with literature, IGFBP-5 should be present in circulating serum at a concentration between 60 – 400 ng/ml. This led to the purchase of a commercially available kit that was specifically developed for measuring IGFBP-5 in human serum samples. Initially, this kit failed to measure any IGFBP-5 in the samples either. Both kits produced satisfactory standard curves, so this led to the thought that it was potentially the serum that was having a quenching effect on the kit.

6.3.4 Human serum samples spiked with a known standard

Using the R&D systems ELISA kit, varying concentrations of the same human serum sample were added to the assay and spiked with 10 ng/ml standard. It is clearly demonstrated that the wells containing more human serum have a greater quenching effect on the standard spiked into the sample. A sample with 50 µl human serum added gave an end result of 1.68 ng/ml IGFBP-5, compared with a sample that had 2 µl serum added which resulted in 8.63 ng/ml IGFBP-5 (Table 6.4).

µl serum sample added to well	Absorbance	IGFBP-5 (ng/ml)
50	0.487	1.68
50	0.481	1.61
20	0.653	3.50
20	0.647	3.44
10	0.806	5.19
10	0.696	3.98
5	0.966	6.95
5	0.927	6.52
2	1.139	8.85
2	1.119	8.63

Table 6-4 IGFBP-5 measured from the same human serum sample with varying dilutions.

Samples were spiked with 10 ng/ml standard. Total volume in each well is 100 µl (Mean, n = 2).

10 ng/ml on the standard curve (Figure 6.4) gave an absorbance reading of 1.474. This is still higher than that read from the wells with the lowest human serum added spiked with 10 ng/ml IGFBP-5 (which was 1.119 as shown on Table 6.4).

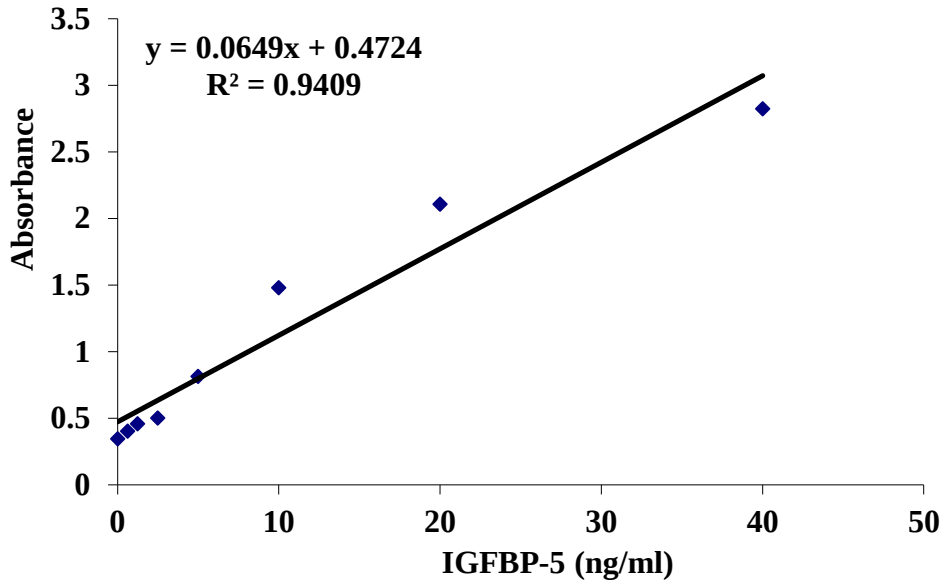

Figure 6-3 Standard curve using the R&D Systems human ELISA kit (Mean, n = 2)

Similarly, varying concentrations of the same human serum sample was added to the assay and spiked with 20 ng/ml standard. It is clearly demonstrated that the wells containing more human serum have a greater quenching effect on the standard spiked into the sample. A sample with 100 µl human serum added gave an end result of 3.98 ng/ml IGFBP-5, compared with a human sample that had 2 µl serum added which resulted in 7.54 ng/ml IGFBP-5 (Table 6.5).

µl serum sample added to well	Spiked 20 ng/ml standard	Absorbance	IGFBP-5 (ng/ml)
100	N	0.082	0
50	N	0.086	0
20	N	0.09	0
2	N	0.142	0
100	Y	0.239	3.98
50	Y	0.277	6.27
20	Y	0.243	4.22
2	Y	0.298	7.54

6-5 IGFBP-5 measured with the Abcam ELISA kit

The same human serum sample with varying dilutions was spiked with 10 ng/ml standard. Total volume in each well is 100 µl (Y = 20 ng/ml IGFBP-5 added, N = no standard added). (Mean, n = 1).

The standard 20 ng/ml on the standard curve gave an absorbance value of approximately 0.5 (Figure 6.5) and this value is again not achieved when the sample was spiked with even only 2 µl of human serum (Table 6.5).

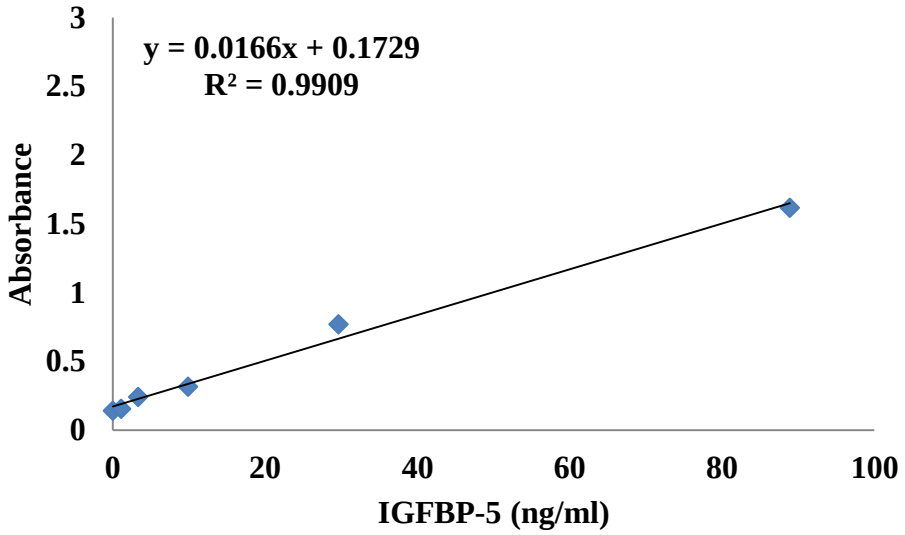

Figure 6-4 Standard curve using the Abcam human ELISA kit (Mean, n = 1)

6.3.5 Human serum samples spiked with a known volume of chicken serum

The addition of chicken serum (See Figure 6.6) gave similar results when added to the standard curve. This then led to chicken serum being added to the human serum sample to determine if it would decrease the quenching effect that had been demonstrated with human serum in the assay.

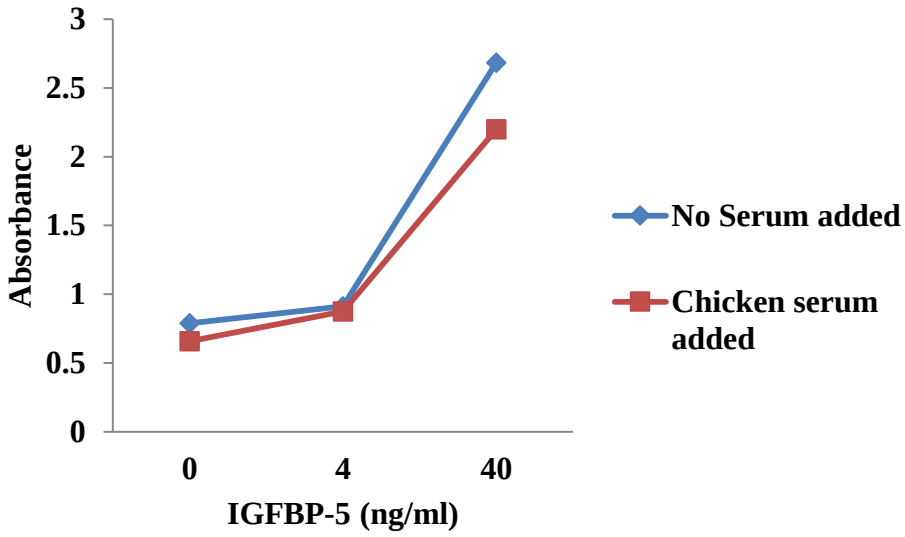

Figure 6-5 Standard curve from R&D Systems human ELISA kit with and without chicken serum (10 µl)

(Mean, n = 2)

Human serum containing no chicken serum had significantly higher levels of IGFBP-5 detected in comparison with the samples containing even 2 µl of chicken serum (see Figure 6.7). However, based on the data in Figure 6.6, the decrease is due to the presence of human serum.

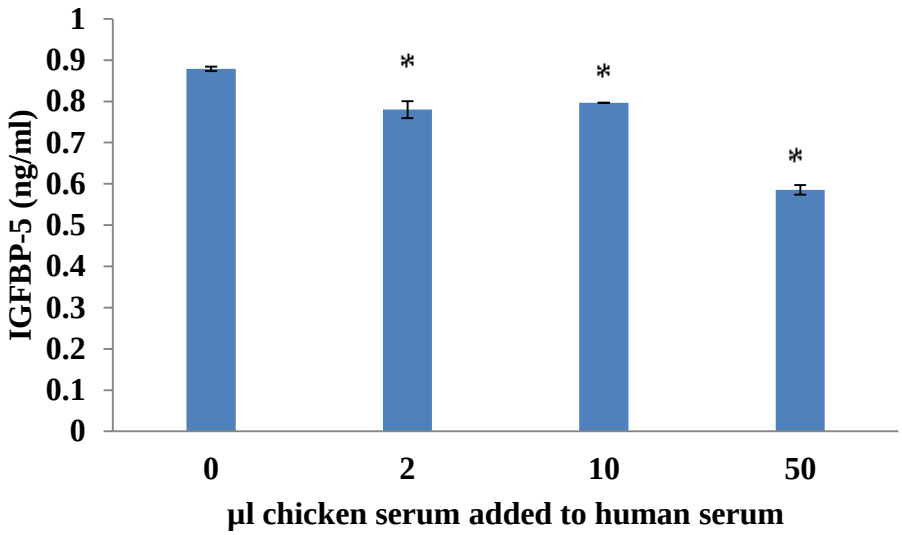

Figure 6-6 IGFBP-5 measured in a human serum sample with chicken serum.

*IGFBP-5 measured in a human serum sample with the addition of varying volumes of chicken serum (0 – 50 µl). (Mean ± SEM, n = 2). * $p \leq 0.05$ significantly different control (0 µl added) ANOVA followed by Dunnett's multiple comparison test)*

6.3.6 Expression of pro-fibrotic markers in LX2 cell cultures

LX2 cells were cultured with preconditioned medium from NAFLD C3A cell cultures. The conditioned medium used had previously been shown to contain increased amounts of IGFBP-5 which had been secreted from the cells. Fibronectin, αSMA and collagen 1 were measured by immunoblotting in the LX2 cells after 24 h exposure to the conditioned medium. Levels of collagen 1 were undetectable. Fibronectin was measurable in all cases (see Figure 6.8). A slight rise in fibronection expression occurred with the addition of IGFBP-5 to the medium, although this was not significant. Addition of TGF-β and IGFBP-5 to the medium both caused an increase in expression of αSMA (not significant) above control (see Figure 6.9). Decreases in αSMA expression were observed with exposure of the cells to all the preconditioned media types. Notably, both fibronectin and αSMA were measured in the controls with and without conditioning. An example immunoblot is shown in Figure 6.9.

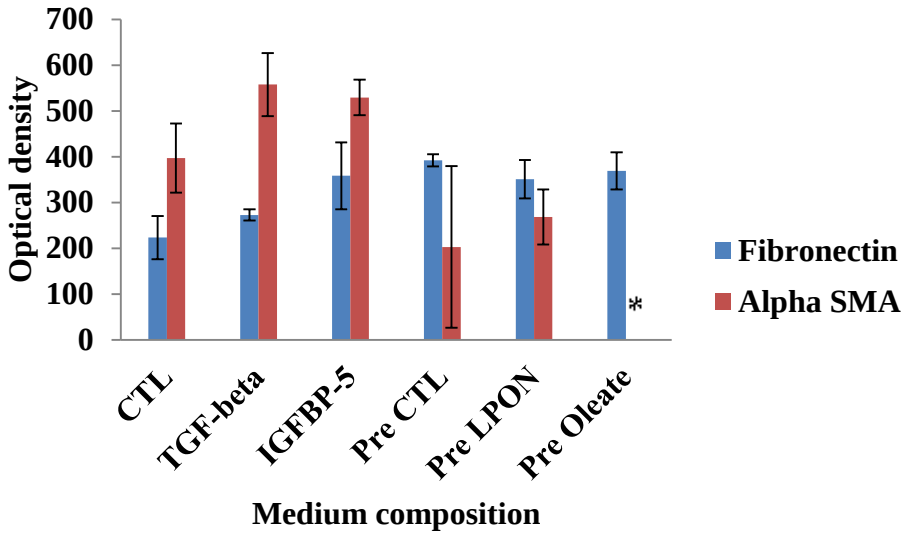

Figure 6-7 Fibronectin and αSMA expression in LX2 cells

*Cells were cultured in medium with no addition (CTL), TGF-beta (5 ng/ml), IGFBP-5 (1 µg/ml), preconditioned medium (Pre CTL), precondition LPON medium (Pre LPON) and preconditioned oleate (Pre Oleate) for 24 h. (Results are mean ± SEM, n = 3). * $p \leq 0.05$ significantly different from controls (ANOVA followed by Dunnett's multiple comparison test).*

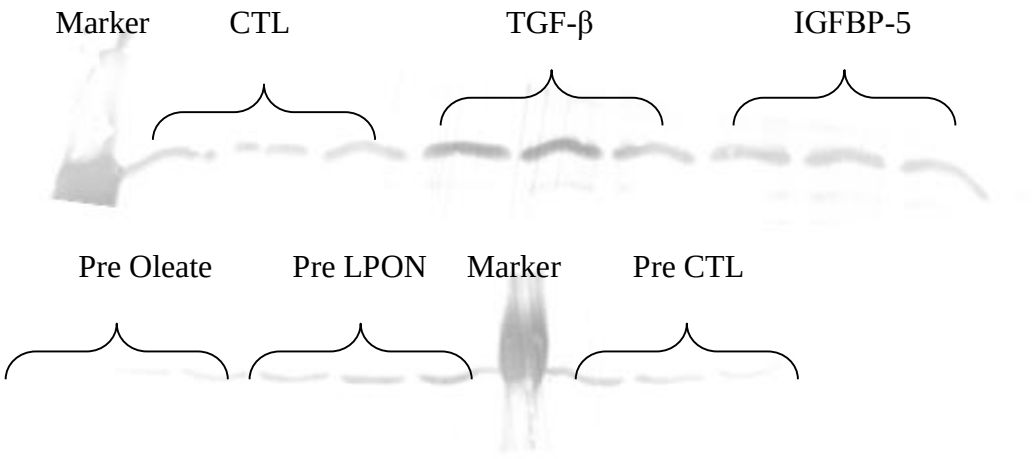

Figure 6-8 Typical immunoblot for αSMA obtained with 10 µg protein/lane.

Cells were cultured in medium with no addition (CTL), TGF-beta (5 ng/ml), IGFBP-5 (1 µg/ml), preconditioned medium (Pre CTL), precondition LPON medium (Pre LPON) and preconditioned oleate (Pre Oleate) for 24 h.Bands on the immunoblot correspond to the molecular weight of αSMA (400 kDa).

6.4 Discussion

With the prevalence of NAFLD on the increase in the developed world, mirroring the global epidemic of Type II diabetes and obesity, the need for a diagnostic marker for the detection of its early onset is necessary. As IGFBP-5 has already been implicated as playing roles in various fibrotic diseases including Idiopathic pulmonary fibrosis (Pilewski et al., 2005a) and skin fibrosis in a mouse model (Yasuoka et al., 2006d), it was chosen as a candidate biomarker for the detection on early liver disease.

An in vitro model of NAFLD with and without the presence of ROS has previously been developed at the Hepatology Department, University of Edinburgh (Filippi et al., 2004, Lockman et al., 2012). This model was utilised to determine if IGFBP-5 had potential as a biomarker for the early detection of this liver disease. The images in Fig 6.1 show clearly that the presence of LPON or oleate in the medium increased the amount of lipids in culture over time. The levels of lipids present in the controls at 3, 5, and 7 days remained similar. However, with the addition of LPON or oleate the levels of lipids rose with time as demonstrated by microscopy imaging of Oil Red O stained lipids.

IGFBP-5 release from C3A cells in the presence of LPON or oleate was measured (see Fig 6.3). IGFBP-5 release increased with time in culture with LPON to 0.3 ng/ml. Levels of IGFBP-5 released from cells in the presence of oleate were undetectable at 3 days and at approx. 0.1 ng/ml at 5 and 7 days. IGFBP-5 release from the controls was below the limit of detection (not shown on graph). Although the increase in levels was not significant, this indicates that IGFBP-5 could be utilised as a marker of NAFLD. IGFBP-5 secretion increased to a greater extent after preconditioning the C3A cells with LPON in comparison with oleate. The generation of ROS and subsequent oxidative stress with the LPON model may be a contributing factor to the increased secretion observed. Lockman et al (2012) demonstrated that LPON enhanced superoxide formation, to levels similar to the positive control oligomycin,

an ATP synthase inhibitor which increases the mitochondrial membrane potential. Dietary induced NAFLD is involved in the increase in energy substrates being made available to hepatocytes, hence within the mitochondria increasing the production of electron donors, i.e. NADH, fuelling the respiratory chain. This can lead to an increase in mitochondrial respiration and subsequent ROS formation. Increases in ROS formation have been established as playing a role in the advancement of IR (Pessayre and Fromenty, 2005, Newsholme et al., 2007). Excessive ROS will deplete intracellular stores of GSH, removing the cells ability to cope with dietary induced ROS leading to apoptosis, necrosis and scar tissue forming.

Following these findings, a clinical study was designed to determine if IGFBP-5 was also increased in patients with a spectrum of liver diseases. Using commercially available sandwich ELISA kits, the levels of IGFBP-5 in any patient samples were below the level of detection. IGFBP-5 has previously been measured in human serum using a specific radioimmunoassay (RIA) (Ehrnborg et al., 2007), but unfortunately in the laboratory where this current experimentation took place there was no resource for this type of assay. After a personal communication with Professor Jeff Holly, University of Bristol, chicken serum was added to the samples to determine if this could overcome the effects of human serum on the commercially available kit. Professor Holly is a renowned expert in the area of IGFs and their measurement, having published over 250 papers and book chapters on IGFs. IGFBP-5 is mostly bound to IGF in the circulation and this binding could be a possible cause of the interference in the ELISA. IGFBPs bind IGF with a high affinity (Hwa et al., 1999, Firth and Baxter, 2002), with over 95 % of circulating IGFs bound to IGFBP-3 (Colakoglu et al., 2007). The addition of a commercially available peptide NBI31773 (Merck, USA) could be used to displace IGF from IGFBP-5 (Perks et al., 2007, Liu et al., 2001). However, in March 2013, a research group in Turkey published data demonstrating how they used an ELISA to measure serum concentrations of human IGFBP-5 in patients with NAFLD (Colak et al., 2012). The study has yet to be repeated by another group. This study demonstrated that IGFBP-5 could be a useful marker to differentiate patients with advanced fibrosis from patients with early stages of fibrosis

and also patients with definite NASH and simple steatosis. IGFBP-5 levels were significantly higher in patients with moderate to high fibrosis in comparison to patients with mild to no fibrosis. There is no insight in the paper as to why an ELISA kit worked in this instance. The study consisted of 92 biopsy confirmed NAFLD patients and 51 healthy controls. The patient cohort consisted of patients from the wide spectrum of NAFLD, namely NASH (borderline and definite). Interestingly, 64 % of the patients tested had metabolic syndrome with NAFLD. Serum IGFBP-5 levels were measured using an enzyme-linked immunosorbent assay kit, commercially available from RayBiotech, USA, and was carried out per the manufacturers' instructions. The minimum detectable level of the kit was 2 µg/l. As this is a commercial kit, very few details are available about what antibodies are used in the kit (Colak et al., 2012) IGFBP-5 in healthy controls were between 200 and 690 µg/l and NAFLD patients were between 242 and 2683 µg/l. IGF1 levels were also measured, and no statistical difference was seen between controls and NAFLD patients, indicating that the commercially available kit was not measuring IGF1 bound to IGFBP-5. However, the IGF1/IGFBP-5 ratio was also not statistically significant. Despite this, IGFBP-5 and the IGF1/IGFBP-1 ratios differentiated patients with early fibrosis from those with advanced fibrosis as well as differentiating patients with definite NASH from patients with simple steatosis and borderline NASH. The IGFBP-5 measurements were not carried out using the same kit as was used in Colak et al., 2012.

Healthy patient IGFBP-5 in the Colak (2012) study correlates with other literature values of IGFBP-5 in human serum (Ehrnborg et al., 2007, Ulinski et al., 2000, Jehle et al., 2003, Jehle et al., 1998). However, a further 2013 paper from the same group in Turkey investigating IGFBP-5 in patients with Crohns Disease report much lower levels of IGFBP-5 in healthy controls at between 8 and 44.6 ng/ml (Adali et al., 2013) using the same kit as the NAFLD paper (Colak et al., 2012). Concentrations from control patients' serum in several studies are presented in Table 6.6.

IGFBP-5 Concentration	Reference	Assay
477 ± 8 ng/ml	(Jehle et al., 1998)	RIA
523 ± 225.5 µg/l	(Ehrnborg et al., 2007)	RIA
200 – 690 µg/l	(Colak et al., 2012)	ELISA
8 – 44.6 ng/ml	(Adali et al., 2013)	ELISA

Table 6-6 Human serum concentrations from literature measured by both ELISA and RIA.

In conclusion, in vitro studies indicated that IGFBP-5 could be a potential marker of NAFLD, however, the clinical study carried out proved unsuccessful in measuring IGFBP-5 in human serum using a commercially available ELISA kit. Yet, published data from Colak et al (2012) illustrated IGFBP-5 as a marker to differentiate severity of fibrosis and NASH using a commercial ELISA assay kit.

Further to this, an investigation was undertaken to determine if IGFBP-5 secreted from the C3Aa cells in the NAFLD model would initiate transdifferentiation of stellate cells (LX2) in vitro. TGF-β, a well-known inducer of α1a1 collagen was used as a positive control (Sysa et al., 2009, Leask and Abraham, 2004, Hellerbrand et al., 1999). A slight increase in fibronectin (not significant) was observed with the addition of 5 ng/ml TGF-β to LX2 cells. IGFBP-5 (1 µg/ml) also caused a slight increase, but not significant in fibronectin and αSMA expression. The preconditioned medium from the C3A NAFLD model had much lower levels (> 1000-fold) of IGFBP-5 in the medium. Interestingly, IGFBP-5 secreted into the medium from the oleate cultures was much lower, and no αSMA was detected via immunoblotting in comparison with LPON and the control wells. Reports in the literature have suggested that LX2 cells are already partially/fully activated cells once in culture in vitro (Xu et al., 2005). This could be one explanation as to why no significant increases in ECM protein production were observed. LX2 cells express glial fibrillary acidic protein (GFAP), which is more common in cells in a state of chronic liver disease. Also, they express receptors βPDGF-R, DDR2 and OB-R_L, phenotypic of activated stellate cells and not present in quiescent cells (Xu et al., 2005). IGFBP-5 expression has been shown to increase in in vitro culture of stellate cells by 200-fold (Boers et al., 2006). Sokolovic et al (2010a)

also describe LX2 cells as activated. In their study, they demonstrate that LX2 cells express 30 % more IGFBP-5 in comparison with stellate cells in a resting state.

Xu et al (2005) exposed LX2 cells to TGF-β (2.5 ng/ml for 20 h) which lead to 3-4 fold increases in α1a1 collagen mRNA. However, in this study, protein expression via immunoblot was used to assess increases in collagen and was unable to detect any protein expression. 24 h exposure to IGFBP-5 and TGF-β and the preconditioned medium may not have been sufficient time to observe changes at the protein level.

To conclude, the aim of the chapter was to determine if IGFBP-5 was a suitable marker for NAFLD. Firstly, an in vitro model developed by the University of Edinburgh was used. IGFBP-5 was successfully measured from this model, yielding higher secreted levels from the C3A cells after LPON addition than after oleate addition, indicating its potential role in the pathogenesis of the disease and its potential as a biomarker. Further to this, preconditioned medium from these cultures were used to determine if the secreted IGFBP-5 stimulated transdifferentiation of stellate cells to more fibroblastic like cells. No significant increases in markers of transdifferentiated stellate cells were observed, potentially due to the short exposure time, or perhaps to the activated state of the LX2 cells already in vitro. To conclude, a study of serum from patients with several types of liver disease was carried out to determine if IGFBP-5 was upregulated in any of the conditions, and indeed if there was any difference in serum levels between the different conditions. A component of human serum causing an inhibitory effect in the assay kits used in this study contributing to the failure to measure IGFBP-5 from human serum.

Chapter 7 Final Conclusions and Future Work

7.1 Final conclusions

The aim of this work was to elucidate if IGFBP-5 was a suitable biomarker of early liver disease. Several in vitro models of hepatocytes were utilised including long term culture of primary rat hepatocytes, and models of oxidative stress and NAFLD. IGFBP-5 had previously been described as playing roles in progression of fibrosis in several models (Feghali-Bostwick, 2005, Sureshbabu et al., 2009, Yasuoka et al., 2006a, Yasuoka et al., 2006b).

Firstly, Chapter 1 assessed modifications to the in vitro culture system with an aim to find the most suitable culture conditions. Collagen source, medium depth, plastic source for culture dishes and attachment times were all assessed. The optimal conditions (2 h attachment, BD Falcon plates, 0.5 ml medium and in-house prepared rat tail tendon collagen-1) were highlighted by NR staining and MTT assay and used in all future work throughout the project. Following this, an extended culture of primary rat hepatocytes was undertaken and differentiation status was assessed over 9 days in culture. GSTP1, testosterone hydroxylation and IGFBP-5 secretion into the medium were monitored. Rapid dedifferentiation was apparent from day 1 in culture, with GSTP1 protein expression increasing and testosterone metabolism decreasing. This result was not surprising as there is a large volume of published literature on loss of phenotype in hepatocytes during in vitro culture (Elaut et al., 2006, Paine et al., 1982, Rogiers et al., 1990, Stefan G. Hübscher, 2005). Despite the rapid decline in function of the hepatocytes, IGFBP-5 increased in cultures with time, reaching the highest concentration at day 9 in culture. The IGF signalling pathways play critical roles in cell growth, differentiation and aging, and literature suggests that IGFBP-5 plays a role in senescence (Kim and Younossi, 2008) . The correlation of loss of phenotype and upregulation of IGFBP-5 secretion could point to IGFBP-5's involvement in cellular injury and loss of function.

Following the characterisation of the in vitro model and understanding the patterns in IGFBP-5 secretion, the model was subjected to chronic oxidative stress via exposure to menadione and H_2O_2. Oxidative stress also plays a role in ethanol hepatotoxicity (Cahill et al., 2002, Kannan and Jain, 2000, Nanji et al., 2004, Wang et al., 2009), hence ethanol and acetaldehyde toxicity was also assessed to determine if IGFBP-5 played a role in their toxicity. No toxicity was observed using the selected markers (GSH, total protein, CV staining and WST-1 activity) with exposure to ethanol and acetaldehyde. However, despite this, IGFBP-5 was suppressed in the cultures that received menadione and H_2O_2. Contrary to the role of IGFBP-5 in cellular senescence (Kim et al., 2007), it has also been demonstrated to enhance the survival of LX2 stellate cells (Sokolovic et al., 2010). In order to determine if IGFBP-5 was progressing the cells into a state of stress, leading to a fibrotic state IGFBP-5 was adenovirally transfected into the rat hepatocytes, which were subsequently stressed with menadione and H_2O_2. No enhancement of the toxicity of either menadione or hydrogen peroxide was observed with the presence of adenoviral IGFBP-5. In contradiction to much of the published literature on IGFBP-5's role in the progression of fibrosis, Sokolovic and colleagues (2012) demonstrated that IGFBP-5 reduced liver fibrosis in mice with chronic cholangiopathy. IGFBP-5 could thus be playing a protective role within the hepatocytes.

NAFLD is a worldwide epidemic, mirroring Type II diabetes and obesity. Definite confirmation of a steatotic liver is via biopsy (Adams et al., 2005). Hence, there is a real need for a non-invasive biomarker for its detection. Using the University of Edinburgh NALFD model, IGFBP-5 release was upregulated with time in C3A cell cultures treated with LPON or oleate to simulate NAFLD with and without involvement of ROS. After the upregulation of IGFBP-5 production had been demonstrated in the in vitro NAFLD model, a patient serum study was undertaken to find out if its production was also upregulated in vivo in liver disease resulting in increased circulating serum concentrations. Unfortunately, both commercially available ELISA kits purchased for the detection of IGFBP-5 in the human serum did not detect any IGFBP-5. On further investigation, the addition of serum to a known

concentration of IGFBP-5 inhibited the ability of the assay to detect that quantity. The higher the concentration of human serum present, the more interference was observed. Most literature papers on IGFBP-5 in human serum use RIA for its detection (Ehrnborg et al., 2007, Jehle et al., 2003). However, this facility was not available in our laboratory at the University of Strathclyde. In 2013, a laboratory in Turkey published a paper describing the detection of IGFBP-5 in patient serum using a commercially available ELISA (Colak et al., 2012) to evaluate its potential as a biomarker for liver fibrosis. In this study, Colak et al. (2012) successfully measured IGFBP-5 from human patient serum and demonstrated that IGFBP-5 could be a useful marker to differentiate patients with advanced fibrosis from patients with early stages of fibrosis and also patients with definite NASH and simple steatosis. IGFBP-5 levels were significantly higher in patients with moderate to high fibrosis in comparison to patients with mild to no fibrosis. Stellate cells are well known to play a pivotal role in the progression of fibrosis. To confirm if IGFBP-5 had an effect on stellate cells, preconditioned medium from both LPON and oleate C3A cell NAFLD models, and IGFBP-5 itself, were cultured with LX2 cells. TGFβ was used as positive control. Neither preconditioned medium nor IGFBP-5 protein caused significant increases in markers of stellate cell activation. Similarly, TGFβ did not cause increases in αSMA or fibronectin. This could be due to two issues, either the stellate cells were already in an activated form (Sokolovic et al., 2010) or the time between exposure to all three conditions and harvest of samples was not long enough. Previously, increases in gene expression had been seen after 24 h, but the exposure time in the current experiments may not have been long enough to see upregulation in protein expression (Xu et al., 2005).

This work highlights some cases where IGFBP-5 could play a crucial role, namely in the aging of hepatocyte cultures and in the NALFD model, where an increase in secretion is demonstrated. Interestingly, the exposure to H_2O_2 and menadione suppressed its secretion into the medium. This was also the case with ethanol and acetaldehyde. More recent publications on IGFBP-5 have suggested its cytoprotective role, with both stellate cells (Sokolovic et al., 2010) and hepatocytes in vivo (Sokolovic

et al., 2012). Potentially, IGFBP-5 is involved in the aging process of the hepatocytes, but plays a different role in the presence of toxins and the progression of acute and chronic drug toxicity.

The secretion of IGFBP-5 may be a response to injury or insult in an attempt to maintain epithelial integrity. Sureshababu et al (2012) demonstrated a novel role of IGFBP-5 in the induction of epithelial cell adhesion and spreading. This phenomenon could limit the progression of fibrosis. This is further evidence of IGFBP-5 playing a protective role. In addition, this may activate stellate cells to create scar tissue in the progression of fibrosis and thereby further preserve the tissue. Thus, menadione and other toxins investigated in this thesis may act to damage the liver by decreasing IGFBP-5 secretion which could potentially aid in hepatocyte survival.

7.2 Future work

The work featured could be aided by a more sophisticated culture system to avoid the rapid onset of dedifferentiation. Simple sandwich cultures with collagen or Matrigel or more advanced 3D culture systems have been shown to maintain hepatic phenotype for longer culture periods.

Co-cultures of hepatocytes and stellate cells would also be an advantage for a model of fibrosis, as well as NAFLD. Adding stellate cells would add a level of complexity to the in vitro model as they are involved in the progression of liver fibrosis, through the over production of ECM upon activation and the prelease of growth factors and cytokines. A source of quiescent (non-activated) stellate cells would be critical for the success of a fibrosis model. Using activated stellate cells would limit research, particularly if a stimulus was being investigated. In this thesis, it was noted that LX2 cells were already partially activated (Sokolovic et al., 2010).

Evidence in this thesis does not necessarily highlight IGFBP-5 as a useful biomarker for the detection of liver disease, however, there may be use for it in combination with other biomarkers. Unfortunately, after initial positive results with the in vitro NALFD model data, the human patient study did not yield positive results, but published literature, cited 8 times since publication, has indicated its ability to differentiate patients with different stages of NAFLD (Colak et al., 2012).

References

- ADALI, G., YORULMAZ, E., OZKANLI, S., ULASOGLU, C., BAYRAKTAR, B., ORHUN, A., COLAK, Y. & TUNCER, I. 2013. Serum concentrations of insulin-like growth factor-binding protein 5 in Crohn's disease. *World journal of gastroenterology,* 19**,** 9049-9056.
- ADAMS, L. A., ANGULO, P. & LINDOR, K. D. 2005. Nonalcoholic fatty liver disease. *CMAJ,* 172**,** 899-905.
- ADAMS, L. A., WATERS, O. R., KNUIMAN, M. W., ELLIOTT, R. R. & OLYNYK, J. K. 2009. NAFLD as a Risk Factor for the Development of Diabetes and the Metabolic Syndrome: An Eleven-Year Follow-up Study. *Am J Gastroenterol,* 104**,** 861-867.
- ALLAN, G. J., TONNER, E., BARBER, M. C., TRAVERS, M. T., SHAND, J. H., VERNON, R. G., KELLY, P. A., BINART, N. & FLINT, D. J. 2002. Growth hormone, acting in part through the insulin-like growth factor axis, rescues developmental, but not metabolic, activity in the mammary gland of mice expressing a single allele of the prolactin receptor. *Endocrinology,* 143**,** 4310-9.
- ANDERSON, K., YIN, L., MACDONALD, C. & GRANT, M. H. 1996. Immortalized hepatocytes as in vitro model systems for toxicity testing: the comparative toxicity of menadione in immortalized cells, primary cultures of hepatocytes and HTC hepatoma cells. *Toxicology in Vitro,* 10**,** 721-727.
- ARAI, T., PARKER, A., BUSBY, W., JR. & CLEMMONS, D. R. 1994. Heparin, heparan sulfate, and dermatan sulfate regulate formation of the insulin-like growth factor-I and insulin-like growth factor-binding protein complexes. *J. Biol. Chem.,* 269**,** 20388-20393.
- ASAHINA, K., TSAI, S. Y., LI, P., ISHII, M., MAXSON, R. E., SUCOV, H. M. & TSUKAMOTO, H. 2009. Mesenchymal origin of hepatic stellate cells, submesothelial cells, and perivascular mesenchymal cells during mouse liver development. *Hepatology,* 49**,** 998-1011.
- ASHAMISS, F., WIERZBICKI, Z., CHRZANOWSKA, A., SCIBIOR, D., PACHOLCZYK, M., KOSIERADZKI, M., LAGIEWSKA, B., POREMBSKA, Z. & ROWINSKI, W. 2004. Clinical significance of arginase after liver transplantation. *Annals of Transplantation,* 9**,** 58-60.
- BADR, M. Z., GANEY, P. E., YOSHIHARA, H., KAUFFMAN, F. C. & THURMAN, R. G. 1989. Hepatotoxicity of menadione predominates in oxygen-rich zones of the liver lobule. *Journal of Pharmacology and Experimental Therapeutics,* 248**,** 1317-1322.
- BARTEL, D. P. 2004. MicroRNAs: genomics, biogenesis, mechanism, and function. *Cell,* 116**,** 281-297.
- BATALLER, R. & BRENNER, D. A. 2005. Liver Fibrosis. *The Journal of Clinical Investigation,* 115**,** 209-218.
- BEATTIE, J., ALLAN, G. J., LOCHRIE, J. D. & FLINT, D. J. 2006. Insulin-like growth factor-binding protein-5 (IGFBP-5): a critical member of the IGF axis. *Biochem J,* 395**,** 1-19.
- BEDOGNI, G., MIGLIOLI, L., MASUTTI, F., TIRIBELLI, C., MARCHESINI, G. & BELLENTANI, S. 2005. Prevalence of and risk factors

for nonalcoholic fatty liver disease: The Dionysos nutrition and liver study. *Hepatology,* 42**,** 44-52.

- BHATIA, S. N., BALIS, U. J., YARMUSH, M. L. & TONER, M. 1999. Effect of cell–cell interactions in preservation of cellular phenotype: cocultivation of hepatocytes and nonparenchymal cells. *The FASEB Journal,* 13**,** 1883-1900.
- BLECHACZ, B. & GORES, G. J. 2008. Tumor-specific marker genes for intrahepatic cholangiocarcinoma: Utility and mechanistic insight. *Journal of Hepatology,* 49**,** 160-162.
- BOERS, W., AARRASS, S., LINTHORST, C., PINZANI, M., ELFERINK, R. O. & BOSMA, P. 2006. Transcriptional Profiling Reveals Novel Markers of Liver Fibrogenesis. *Journal of Biological Chemistry,* 281**,** 16289-16295.
- BORENFREUND, E. & PUERNER, J. A. 1985. Toxicity determined in vitro by morphological alterations and neutral red absorption. *Toxicology Letters,* 24**,** 119-124.
- BOSETTI, C., LEVI, F., LUCCHINI, F., ZATONSKI, W. A., NEGRI, E. & LA VECCHIA, C. 2007. Worldwide mortality from cirrhosis: An update to 2002. *Journal of hepatology,* 46**,** 827-839.
- BRAET, F. & WISSE, E. 2002. Structural and functional aspects of liver sinusoidal endothelial cell fenestrae: a review. *Comparative Hepatology C7 - 1,* 1**,** 1-17.
- BULLOCK, C. 1990. The biochemistry of alcohol metabolism — A brief review. *Biochemical Education,* 18**,** 62-66.
- CAHILL, A., CUNNINGHAM, C. C., ADACHI, M., ISHII, H., BAILEY, S. M., FROMENTY, B. & DAVIES, A. 2002. Effects of Alcohol and Oxidative Stress on Liver Pathology: The Role of the Mitochondrion. *Alcoholism: Clinical and Experimental Research,* 26**,** 907-915.
- CAIN, K. & FREATHY, C. 2001. Liver toxicity and apoptosis: role of TGF-[beta]1, cytochrome c and the apoptosome. *Toxicology Letters,* 120**,** 307-315.
- CARO, A. A. & CEDERBAUM, A. I. 2004. OXIDATIVE STRESS, TOXICOLOGY, AND PHARMACOLOGY OF CYP2E1*. *Annual Review of Pharmacology and Toxicology,* 44**,** 27-42.
- CHEN, G.-F., RONIS, M. J. J., THOMAS, P. E., FLINT, D. J. & BADGER, T. M. 1997. Hormonal Regulation of Microsomal Cytochrome P450 2C11 in Rat Liver and Kidney. *Journal of Pharmacology and Experimental Therapeutics,* 283**,** 1486-1494.
- CHOVAN, J. P., RING, S. C., YU, E. & BALDINO, J. P. 2007. Cytochrome P450 probe substrate metabolism kinetics in Sprague Dawley rats. *Xenobiotica,* 37**,** 459-473.
- COBBOLD, J., MORIN, S. & TAYLOR-ROBINSON, S. 2007. Transient elastography for the assessment of chronic liver disease: ready for the clinic? *World Journal of Gastroenterology,* 13**,** 4791-4797.
- COLACINO, J. M. 1996. Mechanisms for the anti-hepatitis B virus activity and mitochondrial toxicity of fialuridine (FIAU). *Antiviral Research,* 29**,** 125-139.
- COLAK, Y., SENATES, E., OZTURK, O., YILMAZ, Y., ZEMHERI, E., YILMAZ ENC, F., ULASOGLU, C., AKSARAY, S., BOZBEYOGLU, S. G., KIZILTAS, S., KURDAS, O. O. & TUNCER, I. 2012. Serum concentrations

of human insulin-like growth factor-1 and levels of insulin-like growth factor-binding protein-5 in patients with nonalcoholic fatty liver disease: association with liver histology. *European Journal of Gastroenterology & Hepatology,* 24**,** 255-261.

- COLAKOGLU, O., TASKIRAN, B., COLAKOGLU, G., KIZILDAG, S., ARI OZCAN, F. & UNSAL, B. 2007. Serum insulin like growth factor-1 (IGF-1) and insulin like growth factor binding protein-3 (IGFBP-3) levels in liver cirrhosis. *The Turkish Journal of Gastroenterology,* 18**,** 245-249.
- CONDE DE LA ROSA, L., SCHOEMAKER, M. H., VRENKEN, T. E., BUIST-HOMAN, M., HAVINGA, R., JANSEN, P. L. M. & MOSHAGE, H. 2006. Superoxide anions and hydrogen peroxide induce hepatocyte death by different mechanisms: Involvement of JNK and ERK MAP kinases. *Journal of Hepatology,* 44**,** 918-929.
- DANIEL, V. 1993. Glutathione S-Transferases: Gene Structure and Regulation of Expression. *Critical Reviews in Biochemistry and Molecular Biology,* 28**,** 173-207.
- DE LEEUW, M., BROUWER, A. & KNOOK, D. L. 1990. Sinusoidal endothelial cells of the liver: Fine structure and function in relation to age. *Journal of Electron Microscopy Technique,* 14**,** 218-236.
- DE MINICIS, S., SEKI, E., UCHINAMI, H., KLUWE, J., ZHANG, Y., BRENNER, D. A. & SCHWABE, R. F. 2007. Gene Expression Profiles During Hepatic Stellate Cell Activation in Culture and In Vivo. *Gastroenterology,* 132**,** 1937-1946.
- DE SERRES, F. & BLANCO, I. 2014. Role of alpha-1 antitrypsin in human health and disease. *J Intern Med.*
- DI MONTE, D., BELLOMO, G., THOR, H., NICOTERA, P. & ORRENIUS, S. 1984a. Menadione-induced cytotoxicity is associated with protein thiol oxidation and alteration in intracellular Ca2+ homeostasis. *Archives of Biochemistry and Biophysics,* 235**,** 343-350.
- DI MONTE, D., ROSS, D., BELLOMO, G., EKLÖW, L. & ORRENIUS, S. 1984b. Alterations in intracellular thiol homeostasis during the metabolism of menadione by isolated rat hepatocytes. *Archives of Biochemistry and Biophysics,* 235**,** 334-342.
- DUFOUR, D. R., LOTT, J. A., NOLTE, F. S., GRETCH, D. R., KOFF, R. S. & SEEFF, L. B. 2000. Diagnosis and Monitoring of Hepatic Injury. II. Recommendations for Use of Laboratory Tests in Screening, Diagnosis, and Monitoring. *Clinical Chemistry,* 46**,** 2050-2068.
- EHRNBORG, C., OHLSSON, C., MOHAN, S., BENGTSSON, B.-A. & ROSÉN, T. 2007. Increased serum concentration of IGFBP-4 and IGFBP-5 in healthy adults during one month's treatment with supraphysiological doses of growth hormone. *Growth Hormone & IGF Research,* 17**,** 234-241.
- ELAUT, G., HENKENS, T., PAPELELEU, P., SNYKERS, S., VINKEN, M., VANHAECKE, T. & ROGIERS, V. 2006. Molecular mechanisms underlying the dedifferentiation process of isolated hepatocytes and their cultures. *Current Drug Metabolism,* 7**,** 629-660.
- FEGHALI-BOSTWICK, C. A. 2005. IGF-I: mediator of fibrosis or carcinogenesis? *Am J Physiol Lung Cell Mol Physiol,* 288**,** L803-804.

- FEGHALI, C. A. & WRIGHT, T. M. 1999. Identification of multiple, differentially expressed messenger RNAs in dermal fibroblasts from patients with systemic sclerosis. *Arthritis Rheum,* 42**,** 1451-7.
- FERNANDEZ, M., TREPO, E., DEGRE, D., GUSTOT, T., VERSET, L., DEMETTER, P., DEVIERE, J., ADLER, M. & MORENO, C. 2015. Transient elastography using Fibroscan is the most reliable noninvasive method for the diagnosis of advanced fibrosis and cirrhosis in alcoholic liver disease. *Eur J Gastroenterol Hepatol*.
- FERRÉ, P. & FOUFELLE, F. 2010. Hepatic steatosis: a role for de novo lipogenesis and the transcription factor SREBP-1c. *Diabetes, Obesity and Metabolism,* 12**,** 83-92.
- FERRI, D., MORO, L., MASTRODONATO, M., CAPUANO, F., MARRA, E., LIQUORI, G. E. & GRECO, M. 2005. Ultrastructural zonal heterogeneity of hepatocytes and mitochondria within the hepatic acinus during liver regeneration after partial hepatectomy. *Biology of the Cell,* 97**,** 277-288.
- FILIPPI, C., KEATCH, S. A., RANGAR, D., NELSON, L. J., HAYES, P. C. & PLEVRIS, J. N. 2004. Improvement of C3A cell metabolism for usage in bioartificial liver support systems. *Journal of Hepatology,* 41**,** 599-605.
- FIRTH, S. M. & BAXTER, R. C. 2002. Cellular Actions of the Insulin-Like Growth Factor Binding Proteins. *Endocr Rev,* 23**,** 824-854.
- FRIEDMAN, S. L. 2003. Liver fibrosis -- from bench to bedside. *J Hepatol,* 38 Suppl 1**,** S38-53.
- FRIEDRICH-RUST, M., ONG, M., MARTENS, S., SARRAZIN, C., BOJUNGA, J., ZEUZEM, S. & HERRMANN, E. 2008. Performance of Transient Elastography for the Staging of Liver Fibrosis: A Meta-Analysis. *Gastroenterology,* 134**,** 960-974.e8.
- GALLI, A., SVEGLIATI-BARONI, G., CENI, E., MILANI, S., RIDOLFI, F., SALZANO, R., TAROCCHI, M., GRAPPONE, C., PELLEGRINI, G., BENEDETTI, A., SURRENTI, C. & CASINI, A. 2005. Oxidative stress stimulates proliferation and invasiveness of hepatic stellate cells via a MMP2-mediated mechanism. *Hepatology,* 41**,** 1074-1084.
- GAO, S., SEKER, E., CASALI, M., WANG, F., BALE, S. S., PRICE, G. M. & YARMUSH, M. L. C. P. C. N. 2012. Ex vivo gene delivery to hepatocytes: techniques, challenges, and underlying mechanisms. *Ann Biomed Eng,* 40**,** 1851-61.
- GARDMO, C., KOTOKORPI, P., HELANDER, H. & MODE, A. 2005. Transfection of adult primary rat hepatocytes in culture. *Biochem Pharmacol,* 69**,** 1805-13.
- GEERTS, A. 2001. History, heterogeneity, developmental biology, and functions of quiescent hepatic stellate cells. *Semin Liver Dis,* 21**,** 311-35.
- GERETS, H., TILMANT, K., GERIN, B., CHANTEUX, H., DEPELCHIN, B., DHALLIUN, S. & ATIENZAR, F. 2012. Characterization of primary human hepatocytes, HepG2 cells, and HepaRG cells at the mRNA level and CYP activity in response to inducers and their predictivity for the detection of human hepatotoxins. *Cell Biology and Toxicology,* 28**,** 69-87.
- GIBONEY, P. T. 2005. Mildly elevated liver transaminase levels in the asymptomatic patient. *American Family Physician,* 15**,** 1105-1110.

- GINOT, F., DECAUX, J. F., COGNET, M., BERBAR, T., LEVRAT, F., KAHN, A. & WEBER, A. 1989. Transfection of hepatic genes into adult rat hepatocytes in primary culture and their tissue-specific expression. *Eur J Biochem,* 180**,** 289-94.
- GODOY, P., HEWITT, N., ALBRECHT, U., ANDERSEN, M., ANSARI, N., BHATTACHARYA, S., BODE, J., BOLLEYN, J., BORNER, C., BOTTGER, J., BRAEUNING, A., BUDINSKY, R., BURKHARDT, B., CAMERON, N., CAMUSSI, G., CHO, C.-S., CHOI, Y.-J., CRAIG ROWLANDS, J., DAHMEN, U., DAMM, G., DIRSCH, O., DONATO, M., DONG, J., DOOLEY, S., DRASDO, D., EAKINS, R., FERREIRA, K., FONSATO, V., FRACZEK, J., GEBHARDT, R., GIBSON, A., GLANEMANN, M., GOLDRING, C. P., GOMEZ-LECHON, M. J., GROOTHUIS, G. M., GUSTAVSSON, L., GUYOT, C., HALLIFAX, D., HAMMAD, S., HAYWARD, A., HÃUSSINGER, D., HELLERBRAND, C., HEWITT, P., HOEHME, S., HOLZHÃTTER, H.-G., HOUSTON, J. B., HRACH, J., ITO, K., JAESCHKE, H., KEITEL, V., KELM, J., KEVIN PARK, B., KORDES, C., KULLAK-UBLICK, G., LECLUYSE, E., LU, P., LUEBKE-WHEELER, J., LUTZ, A., MALTMAN, D., MATZ-SOJA, M., MCMULLEN, P., MERFORT, I., MESSNER, S., MEYER, C., MWINYI, J., NAISBITT, D., NUSSLER, A., OLINGA, P., PAMPALONI, F., PI, J., PLUTA, L., PRZYBORSKI, S., RAMACHANDRAN, A., ROGIERS, V., ROWE, C., SCHELCHER, C., SCHMICH, K., SCHWARZ, M., SINGH, B., STELZER, E. K., STIEGER, B., STOBER, R., SUGIYAMA, Y., TETTA, C., THASLER, W., VANHAECKE, T., VINKEN, M., WEISS, T., WIDERA, A., WOODS, C., XU, J., YARBOROUGH, K. & HENGSTLER, J. 2013. Recent advances in 2D and 3D in vitro systems using primary hepatocytes, alternative hepatocyte sources and non-parenchymal liver cells and their use in investigating mechanisms of hepatotoxicity, cell signaling and ADME. *Archives of Toxicology,* 87**,** 1315-1530.
- GOVERNMENT, S. 2008. Changing Scotland's relationship with alcohol: a discussion paper on our strategic approach
- GRANT, M. H., MELVIN, M. A. L., SHAW, P., MELVIN, W. T. & BURKE, M. D. 1985. Studies on the maintenance of cytochromes P-450 and b5, monooxygenases and cytochrome reductases in primary cultures of rat hepatocytes. *FEBS Letters,* 190**,** 99-103.
- GUO, L., DIAL, S., SHI, L., BRANHAM, W., LIU, J., FANG, J.-L., GREEN, B., DENG, H., KAPUT, J. & NING, B. 2010. Similarities and Differences in the Expression of Drug-Metabolizing Enzymes between Human Hepatic Cell Lines and Primary Human Hepatocytes. *Drug Metabolism and Disposition,* 39**,** 528-538.
- GUO, W., CHOI, J. K., KIRKLAND, J. L., CORKEY, B. E. & HAMILTON, J. A. 2000. Esterification of free fatty acids in adipocytes: a comparison between octanoate and oleate. *Biochem. J.,* 349**,** 463-471.
- GUTIERREZ-RUIZ, M., QUIROZ, L. G., HERNANDEZ, E., BUCIO, L., SOUZA, V., LLORENTE, L. & KERSHENOBICH, D. 2001. Cytokine response and oxidative stress produced by ethanol, acetaldehyde and endotoxin treatment in HepG2 cells. *The Israel Medical Association,* 3**,** 131-136.

- HAN, D., HANAWA, N., SABERI, B. & KAPLOWITZ, N. 2006. Hydrogen peroxide and redox modulation sensitize primary mouse hepatocytes to TNF-induced apoptosis. *Free Radical Biology and Medicine,* 41**,** 627-639.
- HATAYAMA, I., YAMADA, Y., TANAKA, K., ICHIHARA, A. & SATO, K. 1991. Induction of glutathione S-transferase P-form in primary cultured rat hepatocytes by epidermal growth factor and insulin. *Cancer Science,* 82**,** 807-814.
- HAUTEKEETE, M. L. & GEERTS, A. 1997. The hepatic stellate (Ito) cell: its role in human liver disease. *Virchows Arch,* 430**,** 195-207.
- HELLERBRAND, C., STEFANOVIC, B., GIORDANO, F., BURCHARDT, E. R. & BRENNER, D. A. 1999. The role of TGFb in initiating hepatic stellate cell activation in vivo. *Journal of Hepatology,* 30**,** 77-87.
- HOEBE, K. H. N., WITKAMP, R. F., FINK-GREMMELS, J., VAN MIERT, A. S. J. P. A. M. & MONSHOUWER, M. 2001. *Direct cell-to-cell contact between Kupffer cells and hepatocytes augments endotoxin-induced hepatic injury*.
- HORNBY, R. J., STARKEY LEWIS, P., DEAR, J., GOLDRING, C. & PARK, B. K. 2014. MicroRNAs as potential circulating biomarkers of drug-induced liver injury: key current and future issues for translation to humans. *Expert Review of Clinical Pharmacology,* 7**,** 349-362.
- HWA, V., OH, Y. & ROSENFELD, R. G. 1999. The Insulin-Like Growth Factor-Binding Protein (IGFBP) Superfamily. *Endocr Rev,* 20**,** 761-787.
- INAGAKI, Y. & OKAZAKI, I. 2007. Emerging insights into Transforming growth factor {beta} Smad signal in hepatic fibrogenesis. *Gut,* 56**,** 284-292.
- IP, S., YANG, H., SUN, H. & CHE, C. 2002. Dihydroisotanshinone I protects against menadione-induced toxicity in a primary culture of rat hepatocytes. *Planta Medica,* 68**,** 1077-1081.
- IWAKAMI, S., MISU, H., TAKEDA, T., SUGIMORI, M., MATSUGO, S., KANEKO, S. & TAKAMURA, T. 2011. Concentration-dependent Dual Effects of Hydrogen Peroxide on Insulin Signal Transduction in H4IIEC Hepatocytes. *PLoS ONE,* 6**,** e27401.
- JEHLE, P., SCHULTEN, K., SCHULZ, W., JEHLE, D., STRACKE, S., MANFRAS, B., BOEHM, B., BAYLINK, D. & MOHAN, S. 2003. Serum levels of insulin-like growth factor (IGF)-I and IGF binding protein (IGFBP)-1 to -6 and their relationship to bone metabolism in osteoporosis patients. *European Journal of Internal Medicine,* 14**,** 32-38.
- JEHLE, P. M., JEHLE, D. R., MOHAN, S. & BOHM, B. O. 1998. Serum levels of insulin-like growth factor system components and relationship to bone metabolism in Type 1 and Type 2 diabetes mellitus patients. *Journal of Endocrinology,* 159**,** 297-306.
- JOPLING, C. L. 2008. Regulation of hepatitis C virus by microRNA-122. *Biochemical Society Transactions,* 36**,** 1220-1223.
- KALUS, W., ZWECKSTETTER, M., RENNER, C., SANCHEZ, Y., GEORGESCU, J., GROL, M., DEMUTH, D., SCHUMACHER, R., DONY, C., LANG, K. & HOLAK, T. 1998. Structure of the IGF-binding domain of the insulin-like growth factor-binding protein-5 (IGFBP-5): implications for IGF and IGF-I receptor interactions. *The EMBO Journal,* 17**,** 6558-6572.

- KANNAN, K. & JAIN, S. K. 2000. Oxidative stress and apoptosis. *Pathophysiology,* 7**,** 153-163.
- KELLY, J. H. 1994. Containing cell line that produces albumin an alphafetoprotein. Google Patents.
- KERN, A., BADER, A., PICHLMAYR, R. & SEWING, K. F. 1997. Drug metabolism in hepatocyte sandwich cultures of rats and humans. *Biochemical Pharmacology,* 54**,** 761-772.
- KETTERER, B. 1988. Protective role of glutathione and glutathione transferases in mutagenesis and carcinogenesis. *Mutation Research/Fundamental and Molecular Mechanisms of Mutagenesis,* 202**,** 343-361.
- KIA, R., KELLY, L., SISON-YOUNG, R. L. C., ZHANG, F., PRIDGEON, C. S., HESLOP, J. A., METCALFE, P., KITTERINGHAM, N. R., BAXTER, M., HARRISON, S., HANLEY, N. A., BURKE, Z. D., STORM, M. P., WELHAM, M. J., TOSH, D., KÜPPERS-MUNTHER, B., EDSBAGGE, J., STARKEY LEWIS, P. J., BONNER, F., HARPUR, E., SIDAWAY, J., BOWES, J., FENWICK, S. W., MALIK, H., GOLDRING, C. E. P. & PARK, B. K. 2015. MicroRNA-122: A Novel Hepatocyte-Enriched in vitro Marker of Drug-Induced Cellular Toxicity. *Toxicological Sciences,* 144**,** 173-185.
- KIM, C. H. & YOUNOSSI, Z. M. 2008. Nonalcoholic fatty liver disease: A manifestation of the metabolic syndrome. *Cleveland Clinic Journal of Medicine,* 75**,** 721-728.
- KIM, K. S., SEU, Y. B., BAEK, S.-H., KIM, M. J., KIM, K. J., KIM, J. H. & KIM, J.-R. 2007. Induction of Cellular Senescence by Insulin-like Growth Factor Binding Protein-5 through a p53-dependent Mechanism. *Molecular Biology of the Cell,* 18**,** 4543-4552.
- KNOCKAERT, L., DESCATOIRE, V., VADROT, N., FROMENTY, B. & ROBIN, M.-A. 2011. Mitochondrial CYP2E1 is sufficient to mediate oxidative stress and cytotoxicity induced by ethanol and acetaminophen. *Toxicology in Vitro,* 25**,** 475-484.
- KRAWCZYK, M., BONFRATE, L. & PORTINCASA, P. 2010. Nonalcoholic fatty liver disease. *Best Practice & Research Clinical Gastroenterology,* 24**,** 695-708.
- LEASK, A. 2007. TGF{beta}, cardiac fibroblasts, and the fibrotic response. *Cardiovasc Res,* 74**,** 207-212.
- LEASK, A. & ABRAHAM, D. J. 2004. TGF-{beta} signaling and the fibrotic response. *FASEB J.,* 18**,** 816-827.
- LECLERCQ, I. & HORSMANS, Y. 2008. Nonalcoholic fatty liver disease: the potential role of nutritional management. *Current opinion in clinical nutrition and metabolic care,* 11**,** 766-773.
- LECLUYSE, E. L., WITEK, R. P., ANDERSEN, M. E. & POWERS, M. J. 2012. Organotypic liver culture models: Meeting current challenges in toxicity testing. *Critical Reviews in Toxicology,* 0**,** 1-48.
- LEWIS, J. & MOHANTY, S. 2010. Nonalcoholic Fatty Liver Disease: A Review and Update. *Digestive Diseases and Sciences,* 55**,** 560-578.

- LI, X., CAO, X., LI, X., ZHANG, W. & FENG, Y. 2007. Expression level of insulin-like growth factor binding protein 5 mRNA is a prognostic factor for breast cancer. *Cancer Science,* 98**,** 1592-1596.
- LIEBER, C. S. 1997. Ethanol metabolism, cirrhosis and alcoholism. *Clinica Chimica Acta,* 257**,** 59-84.
- LIU, X.-J., XIE, Q., ZHU, Y.-F., CHEN, C. & LING, N. 2001. Identification of a Nonpeptide Ligand That Releases Bioactive Insulin-like Growth Factor-I from Its Binding Protein Complex. *Journal of Biological Chemistry,* 276**,** 32419-32422.
- LOCK, E. A. & BONVENTRE, J. V. 2008. Biomarkers in translation; past, present and future. *Toxicology,* 245**,** 163-166.
- LOCKMAN, K. A., BAREN, J. P., PEMBERTON, C. J., BAGHDADI, H., BURGESS, K. E., PLEVRIS-PAPAIOANNOU, N., LEE, P., HOWIE, F., BECKETT, G., PRYDE, A., JAAP, A. J., HAYES, P. C., FILIPPI, C. & PLEVRIS, J. N. 2012. Oxidative stress rather than triglyceride accumulation is a determinant of mitochondrial dysfunction in in vitro models of hepatic cellular steatosis. *Liver International*.
- LONGO, V. D. & FINCH, C. E. 2003. Evolutionary Medicine: From Dwarf Model Systems to Healthy Centenarians? *Science,* 299**,** 1342-1346.
- LOOMBA, R. & SANYAL, A. J. 2013. The global NAFLD epidemic. *Nat Rev Gastroenterol Hepatol,* 10**,** 686-690.
- LOWRY, O. H., ROSEBROUGH, N. J., FARR, A. L. & RANDALL, R. J. 1951. Protein Measurement with the Folin Phenol Reagent. *The Journal of Biological Chemistry,* 193**,** 265-275.
- LUDWIG, J., VIGGIANO, T., MCGILL, D. & OH, B. 1980. Nonalcoholic steatohepatitis: Mayo Clinic experiences with a hitherto unnamed disease. *Mayo Clinic Proceedings,* 55**,** 434-438.
- LUTTRINGER, O., THEIL, F.-P., LAVE, T., WERNLI-KURATLI, K., GUENTERT, T. W. & DE SAIZIEU, A. 2002. Influence of isolation procedure, extracellular matrix and dexamethasone on the regulation of membrane transporters gene expression in rat hepatocytes. *Biochemical Pharmacology,* 64**,** 1637-1650.
- MANNERVIK, B., HELENA DANIELSON, U. & KETTERER, B. 1988. Glutathione Transferases Structure and Catalytic Activity. *Critical Reviews in Biochemistry and Molecular Biology,* 23**,** 283-337.
- MARCH, S., HUI, E. E., UNDERHILL, G. H., KHETANI, S. & BHATIA, S. N. 2009. Microenvironmental regulation of the sinusoidal endothelial cell phenotype in vitro. *Hepatology,* 50**,** 920-928.
- MARTINI, F., OBER, W., GARRISON, C., WELCH, K. & HUTCHINGS, R. 2007. *Fundamentals of anatomy & physiology,* San Francisco, Benjamin Cummings.
- MEIJER, D. F., MOL, W. M., MÜLLER, M. & KURZ, G. 1990. Carrier-mediated transport in the hepatic distribution and elimination of drugs, with special reference to the category of organic cations. *Journal of Pharmacokinetics and Biopharmaceutics,* 18**,** 35-70.

- MELLO, T., CENI, E., SURRENTI, C. & GALLI, A. 2008. Alcohol induced hepatic fibrosis: Role of acetaldehyde. *Molecular Aspects of Medicine,* 29**,** 17-21.
- MICHALOPOULOS, G. K. 2014. Advances in liver regeneration. *Expert Review of Gastroenterology and Hepatology,* 1.
- MOLDEUS, P., HOGBERG, J. & ORRENIUS, S. 1978. *Isolation and use of liver cells*.
- MOREIRA, R. K. 2007. Hepatic stellate cells and liver fibrosis. *Arch Pathol Lab Med,* 131**,** 1728-34.
- MORRISON, H., JERNSTRÖM, B., NORDENSKJÖLD, M., THOR, H. & ORRENIUS, S. 1984. Induction of dna damage by menadione (2-methyl-1,4-naphthoquinone) in primary cultures of rat hepatocytes. *Biochemical Pharmacology,* 33**,** 1763-1769.
- NAKAMURA, S., TAKAMURA, T., MATSUZAWA-NAGATA, N., TAKAYAMA, H., MISU, H., NODA, H., NABEMOTO, S., KURITA, S., OTA, T., ANDO, H., MIYAMOTO, K.-I. & KANEKO, S. 2009. Palmitate Induces Insulin Resistance in H4IIEC3 Hepatocytes through Reactive Oxygen Species Produced by Mitochondria. *Journal of Biological Chemistry,* 284**,** 14809-14818.
- NANJI, A. A., DANNENBERG, A. J., JOKELAINEN, K. & BASS, N. M. 2004. Alcoholic Liver Injury in the Rat Is Associated with Reduced Expression of Peroxisome Proliferator-α (PPARα)-Regulated Genes and Is Ameliorated by PPARα Activation. *Journal of Pharmacology and Experimental Therapeutics,* 310**,** 417-424.
- NASSIR, F. & IBDAH, J. 2014. Role of Mitochondria in Nonalcoholic Fatty Liver Disease. *International Journal of Molecular Sciences,* 15**,** 8713-8742.
- NEWSHOLME, P., HABER, E. P., HIRABARA, S. M., REBELATO, E. L. O., PROCOPIO, J., MORGAN, D., OLIVEIRA-EMILIO, H. C., CARPINELLI, A. R. & CURI, R. 2007. Diabetes associated cell stress and dysfunction: role of mitochondrial and non-mitochondrial ROS production and activity. *The Journal of Physiology,* 583**,** 9-24.
- NISHINO, R., HONDA, M., YAMASHITA, T., TAKATORI, H., MINATO, H., ZEN, Y., SASAKI, M., TAKAMURA, H., HORIMOTO, K., OHTA, T., NAKANUMA, Y. & KANEKO, S. 2008. Identification of novel candidate tumour marker genes for intrahepatic cholangiocarcinoma. *Journal of Hepatology,* 49**,** 207-216.
- NUTT, D. J., KING, L. A. & PHILLIPS, L. D. 2010. Drug harms in the UK: a multicriteria decision analysis. *The Lancet,* 376**,** 1558-1565.
- OZER, J., RATNER, M., SHAW, M., BAILEY, W. & SCHOMAKER, S. 2008. The current state of serum biomarkers of hepatotoxicity. *Toxicology,* 245**,** 194-205.
- PADDA, M. S., SANCHEZ, M., AKHTAR, A. J. & BOYER, J. L. 2011. Drug-induced cholestasis. *Hepatology,* 53**,** 1377-1387.
- PADGHAM, C. R. W., BOYLE, C. C., WANG, X. J., RALEIGH, S. M., WRIGHT, M. C. & PAINE, A. J. 1993. Alteration of Transcription Factor mRNAs during the Isolation and Culture of Rat Hepatocytes Suggests the

Activation of a Proliferative Mode Underlies Their Dedifferentiation. *Biochemical and Biophysical Research Communications,* 197**,** 599-605.

- PAINE, A. J., HOCKIN, L. J. & ALLEN, C. M. 1982. Long term maintenance and induction of cytochrome P-450 in rat liver cell culture. *Biochemical Pharmacology,* 31**,** 1175-1178.
- PERKS, C. M., VERNON, E. G., ROSENDAHL, A. H., TONGE, D. & HOLLY, J. M. P. 2007. IGF-II and IGFBP-2 differentially regulate PTEN in human breast cancer cells. *Oncogene,* 26**,** 5966-5972.
- PESSAYRE, D. 2007. Role of mitochondria in non-alcoholic fatty liver disease. *Journal of Gastroenterology and Hepatology,* 22**,** S20-S27.
- PESSAYRE, D. & FROMENTY, B. 2005. NASH: a mitochondrial disease. *Journal of hepatology,* 42**,** 928-940.
- PETTA, S., MAIDA, M., MACALUSO, F. S., MARCO, V. D., CAMMÀ, C., CABIBI, D. & CRAXÌ, A. 2015. The severity of steatosis influences liver stiffness measurement in patients with nonalcoholic fatty liver disease. *Hepatology***,** n/a-n/a.
- PETTERSSON, J., HINDORF, U., PERSSON, P., BENGTSSON, T., MALMQVIST, U., WERKSTRÖM, V. & EKELUND, M. 2008. Muscular exercise can cause highly pathological liver function tests in healthy men. *British Journal of Clinical Pharmacology,* 65**,** 253-259.
- PILEWSKI, J. M., LIU, L., HENRY, A. C., KNAUER, A. V. & FEGHALI-BOSTWICK, C. A. 2005. Insulin-Like Growth Factor Binding Proteins 3 and 5 Are Overexpressed in Idiopathic Pulmonary Fibrosis and Contribute to Extracellular Matrix Deposition. *Am J Pathol,* 166**,** 399-407.
- POLI, G. 2000. Pathogenesis of liver fibrosis: role of oxidative stress. *Mol Aspects Med,* 21**,** 49-98.
- PURKINS, L., LOVE, E. R., EVE, M. D., WOOLDRIDGE, C. L., COWAN, C., SMART, T. S., JOHNSON, P. J. & RAPEPORT, W. G. 2004. The influence of diet upon liver function tests and serum lipids in healthy male volunteers resident in a Phase I unit. *British Journal of Clinical Pharmacology,* 57**,** 199-208.
- RENAUD, S. & DE LORGERIL, M. 1992. Wine, alcohol, platelets, and the French paradox for coronary heart disease. *The Lancet,* 339**,** 1523-1526.
- ROBERTS, R. A., GANEY, P. E., JU, C., KAMENDULIS, L. M., RUSYN, I. & KLAUNIG, J. E. 2007. Role of the Kupffer Cell in Mediating Hepatic Toxicity and Carcinogenesis. *Toxicological Sciences,* 96**,** 2-15.
- ROGIERS, V., VANDENBERGHE, Y., CALLAERTS, A., VERLEYE, G., CORNET, M., MERTENS, K., SONCK, W. & VERCRUYSSE, A. 1990. Phase I and phase II xenobiotic biotransformation in cultures and co-cultures of adult rat hepatocytes. *Biochemical Pharmacology,* 40**,** 1701-1706.
- SANDHU, H. & MADDOCK, H. 2014. Molecular basis of cancer-therapy-induced cardiotoxicity: introducing microRNA biomarkers for early assessment of subclinical myocardial injury. *Clinical Science,* 126**,** 377-400.
- SANDRIN, L., FOURQUET, B., HASQUENOPH, J.-M., YON, S., FOURNIER, C., MAL, F., CHRISTIDIS, C., ZIOL, M., POULET, B., KAZEMI, F., BEAUGRAND, M. & PALAU, R. 2003. Transient elastography:

a new noninvasive method for assessment of hepatic fibrosis. *Ultrasound in medicine & biology,* 29**,** 1705-1713.

- SCHNEIDER, M. R., WOLF, E., HOEFLICH, A. & LAHM, H. 2002. IGF-binding protein-5: flexible player in the IGF system and effector on its own. *Journal of Endocrinology,* 172**,** 423-440.
- SCHUG, M., HEISE, T., BAUER, A., STORM, D., BLASZKEWICZ, M., BEDAWY, E., BRULPORT, M., GEPPERT, B., HERMES, M., FÃLLMANN, W., RAPP, K., MACCOUX, L., SCHORMANN, W., APPEL, K. E., OBEREMM, A., GUNDERT-REMY, U. & HENGSTLER, J. G. 2008. Primary rat hepatocytes as in vitro system for gene expression studies: comparison of sandwich, Matrigel and 2D cultures. *Archives of Toxicology,* 82**,** 923-931.
- SCOTLAND, N. H. 2010. Monitoring and Evaluating Scotland's Alcohol Strategy; Analysis of alcohol sales data, 2005-2009.
- SETSHEDI, M., WANDS, J. & MONTE, S. D. L. 2010. Acetaldehyde adducts in alcoholic liver disease. *Oxidative Medicine and Cellular Longevity,* 3**,** 178-185.
- SHAND, J. H., BEATTIE, J., SONG, H., PHILLIPS, K., KELLY, S. M., FLINT, D. J. & ALLAN, G. J. 2003. Specific Amino Acid Substitutions Determine the Differential Contribution of the N- and C-terminal Domains of Insulin-like Growth Factor (IGF)-binding Protein-5 in Binding IGF-I. *Journal of Biological Chemistry,* 278**,** 17859-17866.
- SHERON, N., HAWKEY, C. & GILMORE, I. 2011. Projections of alcohol deaths?a wake-up call. *The Lancet,* 377**,** 1297-1299.
- SHIFENG, H., DANNI, W., PU, C., PING, Y., JU, C. & LIPING, Z. 2013. Circulating Liver-Specific miR-122 as a Novel Potential Biomarker for Diagnosis of Cholestatic Liver Injury. *PLoS ONE,* 8**,** e73133.
- SIES, H. 2014. Role of Metabolic H2O2 Generation: Redox Signalling and Oxidative Stress. *Journal of Biological Chemistry,* 289**,** 8735-8741.
- SOARS, M. G., MCGINNITY, D. F., GRIME, K. & RILEY, R. J. 2007. The pivotal role of hepatocytes in drug discovery. *Chemico-Biological Interactions,* 168**,** 2-15.
- SOKOLOVIC, A., MONTENEGRO-MIRANDA, P., WAART, D. D., CAPPAI, R., DUIJST, S., SOKOLOVIC, M. & BOSMA, P. 2012. Overexpression of insulin like growth factor binding protein 5 reduces liver fibrosis in chronic cholangiopathy. *Biochimica et Biophysica Acta (BBA) - Molecular Basis of Disease,* 1822**,** 996-1003.
- SOKOLOVIC, A., SOKOLOVIC, M., BOERS, W., ELFERINK, R. & BOSMA, P. 2010. Insulin-like growth factor binding protein 5 enhances survival of LX2 human hepatic stellate cells. *Fibrogenesis & Tissue Repair,* 3**,** 3.
- SOLDATOW, V., LECLUYSE, E., GRIFFITH, L. & RUSYN, I. 2013. In vitro models for liver toxicity testing. *Toxicology research,* 2**,** 23-39.
- STARKE, P. E. & FARBER, J. L. 1985. Endogenous defenses against the cytotoxicity of hydrogen peroxide in cultured rat hepatocytes. *Journal of Biological Chemistry,* 260**,** 86-92.

- STARKEY LEWIS, P. J., DEAR, J., PLATT, V., SIMPSON, K. J., CRAIG, D. G. N., ANTOINE, D. J., FRENCH, N. S., DHAUN, N., WEBB, D. J., COSTELLO, E. M., NEOPTOLEMOS, J. P., MOGGS, J., GOLDRING, C. E. & PARK, B. K. 2011. Circulating microRNAs as potential markers of human drug-induced liver injury. *Hepatology,* 54**,** 1767-1776.
- STARKEY LEWIS, P. J., MERZ, M., COUTTET, P., GRENET, O., DEAR, J., ANTOINE, D. J., GOLDRING, C., PARK, B. K. & MOGGS, J. G. 2012. Serum microRNA Biomarkers for Drug-Induced Liver Injury. *Clin Pharmacol Ther,* 92**,** 291-293.
- STEFAN G. HÜBSCHER, A. J. S. 2005. Another Notch to be added to the list of hepatocellular growth regulatory factors? *Hepatology,* 41**,** 439-442.
- SU, T. H., KAO, J. H. & LIU, C. J. 2014. Molecular mechanism and treatment of viral hepatitis-related liver fibrosis. *Int J Mol Sci,* 15**,** 10578-604.
- SUN, Y., COTGREAVE, I. A., LINDEKE, B. & MOLDÉUS, P. 1990. The Protective Effect of Sulfite on Menadione- and Diquat-Induced Cytotoxicity in Isolated Rat Hepatocytes. *Pharmacology & Toxicology,* 66**,** 393-398.
- SURESHBABU, A., OKAJIMA, H., YAMANAKA, D., SHASTRI, S., TONNER, E., RAE, C., SZYMANOWSKA, M., SHAND, J. H., TAKAHASHI, S.-I., BEATTIE, J., ALLAN, G. J. & FLINT, D. J. 2009. IGFBP-5 induces epithelial and fibroblast responses consistent with the fibrotic response. *Biochemical Society Transactions,* 037**,** 882-885.
- SURESHBABU, A., OKAJIMA, H., YAMANAKA, D., TONNER, E., SHASTRI, S., MAYCOCK, J., SZYMANOWSKA, M., SHAND, J., TAKAHASHI, S.-I., BEATTIE, J., ALLAN, G. & FLINT, D. 2012. IGFBP5 induces cell adhesion, increases cell survival and inhibits cell migration in MCF-7 human breast cancer cells. *Journal of Cell Science,* 125**,** 1693-1705.
- SVEGLIATI-BARONI, G., RIDOLFI, F., DI SARIO, A., SACCOMANNO, S., BENDIA, E., BENEDETTI, A. & GREENWEL, P. 2001. Intracellular signaling pathways involved in acetaldehyde-induced collagen and fibronectin gene expression in human hepatic stellate cells. *Hepatology,* 33**,** 1130-1140.
- SWALES, N. J., JOHNSON, T. & CALDWELL, J. 1996. Cryopreservation of rat and mouse hepatocytes. II. Assessment of metabolic capacity using testosterone metabolism. *Drug Metabolism and Disposition,* 24**,** 1224-1230.
- SYSA, P., POTTER, J., LIU, F. & MEZEY, E. 2009. Transforming growth factor-beta1 up-regulation of human alpha(1)(I) collagen is mediated by Sp1 and Smad2 transacting factors. *DNA and cell biology,* 28**,** 425-434.
- TARANTINO, G., SAVASTANO, S. & A, A. C. 2010. Hepatic steatosis, low-grade chronic inflammation and hormone/growth factor/adipokine imbalance. *World Journal of Gastroenterology,* 16**,** 4773-4783.
- TAUB, R. 2004. Liver regeneration: from myth to mechanism. *Nat Rev Mol Cell Biol,* 5**,** 836-847.
- TEE, L., GILMORE, K. S., MEYER, D. J., KETTERER, B., VANDENBERGHE, Y. & YEOH, G. C. 1992. Expression of glutathione S-transferase during rat liver development. *The Biochemical Journal,* 282**,** 209-218.
- THOR, H., SMITH, M. T., HARTZELL, P., BELLOMO, G., JEWELL, S. A. & ORRENIUS, S. 1982. The metabolism of menadione (2-methyl-1,4-

naphthoquinone) by isolated hepatocytes. A study of the implications of oxidative stress in intact cells. *J. Biol. Chem.*, 257**,** 12419-12425.

- TILG, H. & MOSCHEN, A. R. 2008. Insulin resistance, inflammation, and non-alcoholic fatty liver disease. *Trends in Endocrinology & Metabolism,* 19**,** 371-379.
- ULINSKI, T., MOHAN, S., KIEPE, D., BLUM, W., WINGEN, A., MEHLS, O. & TONSHOFF, B. 2000. Serum insulin-like growth factor binding protein (IGFBP)-4 and IGFBP-5 in children with chronic renal failure: relationship to growth and glomerular filtration rate. The European Study Group for Nutritional Treatment of Chronic Renal Failure in Childhood. German Study Group for Growth Hormone Treatment in Chronic Renal Failure. *Pediatric nephrology,* 14**,** 589-597.
- VANDEN HEUVEL, J. P. 1999. Peroxisome Proliferator–Activated Receptors: A Critical Link among Fatty Acids, Gene Expression and Carcinogenesis. *The Journal of Nutrition,* 129**,** 575.
- VANDENBERGHE, Y., GLAISE, D., MEYER, D. J., GUILLOUZO, A. & KETTERER, B. 1988. Glutathione transferase isoenzymes in cultured rat hepatocytes. *Biochemical Pharmacology,* 37**,** 2482-2485.
- VIÑA, J., ESTRELA, J. M., GUERRI, C. & ROMERO, F. J. 1980. Effect of ethanol on glutathione concentration in isolated hepatocytes. *Journal of Biochemistry,* 188**,** 549-552.
- WANG, K., ZHANG, S., MARZOLF, B., TROISCH, P., BRIGHTMAN, A., HU, Z., HOOD, L. E. & GALAS, D. J. 2009. Circulating microRNAs, potential biomarkers for drug-induced liver injury. *Proceedings of the National Academy of Sciences,* 106**,** 4402-4407.
- WHO 2009. Global Burden of Disease Project, World Health Organisation.
- WILKENING, S., STAHL, F. & BADER, A. 2003. COMPARISON OF PRIMARY HUMAN HEPATOCYTES AND HEPATOMA CELL LINE HEPG2 WITH REGARD TO THEIR BIOTRANSFORMATION PROPERTIES. *Drug Metabolism and Disposition,* 31**,** 1035-1042.
- WORTELBOER, H., DE KRUIF, C. A., VAN IERSEL, A. A., FALKE, H. E., NOORDHOEK, J. & BLAAUBOER, B. J. 1990. The isoenzyme pattern of cytochrome P450 in rat hepatocytes in primary culture, comparing different enzyme activities in microsomal incubations and in intact monolayers. *Biochemical Pharmacology,* 40**,** 2525-2534.
- XIE, G., WANG, L., WANG, X., WANG, L. & DELEVE, L. D. 2010. *Isolation of periportal, midlobular, and centrilobular rat liver sinusoidal endothelial cells enables study of zonated drug toxicity*.
- XU, L., HUI, A. Y., ALBANIS, E., ARTHUR, M. J., O'BYRNE, S. M., BLANER, W. S., MUKHERJEE, P., FRIEDMAN, S. L. & ENG, F. J. 2005. Human hepatic stellate cell lines, LX-1 and LX-2: new tools for analysis of hepatic fibrosis. *Gut,* 54**,** 142-151.
- YANG, S.-S., HUANG, C.-C., CHEN, J.-R., CHIU, C.-L., SHIEH, M.-J. & YANG, C.-C. 2005. Effects of ethanol on antiaxidant capacity in isolated rat hepatocytes. *World Journal of Gastroenterology,* 11**,** 7272-7276.
- YASUOKA, H., JUKIC, D. M., ZHOU, Z., CHOI, A. M. & FEGHALI-BOSTWICK, C. A. 2006. Insulin-like growth factor binding protein 5 induces

skin fibrosis: A novel murine model for dermal fibrosis. *Arthritis Rheum,* 54**,** 3001-10.

- YASUOKA, H., YAMAGUCHI, Y. & FEGHALI-BOSTWICK, C. A. C. P. 2009. The pro-fibrotic factor IGFBP-5 induces lung fibroblast and mononuclear cell migration. *Am J Respir Cell Mol Biol,* 41**,** 179-88.
- YASUOKA, H., ZHOU, Z., PILEWSKI, J. M., OURY, T. D., CHOI, A. M. & FEGHALI-BOSTWICK, C. A. C. P. 2006a. Insulin-like growth factor-binding protein-5 induces pulmonary fibrosis and triggers mononuclear cellular infiltration. *Am J Pathol,* 169**,** 1633-42.
- YU, H.-S., OYAMA, T., ISSE, T., KITAGAWA, K., PHAM, T.-T.-P., TANAKA, M. & KAWAMOTO, T. 2010. Formation of acetaldehyde-derived DNA adducts due to alcohol exposure. *Chemico-Biological Interactions,* 188**,** 367-375.
- YUTAKA, I., KIYOSHI, H., MIWA, K., YUN YU, H., SACHIE, N., REIICHI, H., TADASHI, M., JOHBU, I., TOSHIYUKI, M., TORU, K., GOSHI, S., ICHIRO, K. & ISAO, O. 2008. Hepatocyte Growth Factor Suppresses Profibrogenic Signal Transduction via Nuclear Export of Smad3 With Galectin-7. *Gastroenterology,* 134**,** 1180-1190.
- ZHANG, W., KUDO, H., KAWAI, K., FUJISAKA, S., USUI, I., SUGIYAMA, T., TSUKADA, K., CHEN, N. & TAKAHARA, T. 2010. Tumor necrosis factor-[alpha] accelerates apoptosis of steatotic hepatocytes from a murine model of non-alcoholic fatty liver disease. *Biochemical and Biophysical Research Communications,* 391**,** 1731-1736.

Appendix i

Production of recombinant wild type IGFBP-5 and IGFBP-5 adenovirus

Rat IGFBP-5 cDNA, without the signal peptide encoding sequence, was cloned into the pGEX 6P-1 vector (Amersham Pharmacia Biotech, USA) between BamHI and EcoRI in the multiple cloning site so that the proteins would have a N-terminal glutathione S-transferase (GST) tag. The proteins were expressed in the Origami B (DE3) pLys strain of Escherichia coli (Novagen, USA) and following cell lysis the GST-IGFBP-5 fusion proteins were extracted from the soluble fraction only and underwent subsequent rounds of purification. The IGFBP-5 protein was isolated using a glutathione-Sepharose column for removal of the GST tag with PreScission protease (Amersham Pharmacia Biotech, USA). The untagged IGFBP-5 was then purified using an IGF-1 affinity column.

IGFBP-5 adenovirus was produced as follows; briefly, wild type IGFBP-5 was cloned between the EcoR1 and HindIII sites of the shuttle plasmid pDC516 (Admax, Microbix Biosystems Inc, Canada) containing murine cytomegalovirus immediate early gene promoter (MCMVPr). The shuttle plasmids were then co-transfected with the adenoviral genomic plasmid (pBHGtrtΔE1,3FLP) into HEK293 cells to employ FLP-mediated site-specific recombination between two plasmids, resulting in recombinant, non-replicative, adenovirus (Ad-IGFBP-5). All procedures used were as per the manufacturers' recommendations and their Ad Vector Construction Manual (MicroBix Biosystems Inc, Canada). Adenoviral stocks were generated commercially and a null vector (Lock and Bonventre) was purchased from the same source (Welgen Incorporation, USA).

Appendix ii

RIPA buffer preparation

Final concentration	Reagent	Stock Concentration		Dilution of stock
50 mM	Tris-HCl, pH 7.4	250 mM	30.285 g/l	1/5
150 mM	NaCl	7.5 mM	43.83 g/l	1/5
0.5 mM	EGTA, pH 7.4	50 mM in H2O	19.22 mg/ml	1/100
0.5 mM	EDTA, pH 7.4	50 mM in H2O	18.61 mg/ml	1/100
1 % v/v	Igepal CA-630	10 % v/v in H2O	1 ml/10 ml	1/10
0.25 % w/v	Na-deoxycholate	10 % w/v in H2O	1 g/10 ml	1/40